10-28-2022 11:00 AM

Western diet-like culture conditions and oxidative stress on a cell model of non-alcoholic fatty liver disease

Celina M. Valvano, *The University of Western Ontario*

Supervisor: Kelly, Gregory M., *The University of Western Ontario*
Co-Supervisor: Regnault, Timothy RH., *The University of Western Ontario*
A thesis submitted in partial fulfillment of the requirements for the Master of Science degree in Biology
© Celina M. Valvano 2022

Recommended Citation

Abstract

Non-alcoholic fatty liver disease (NAFLD) is a major health burden in the Western world, as the Western diet (WD) appears to be the driving force of this disease. However, the individual contributions of the diet and the impacts of their individual metabolism are currently ill-defined. This study used HepG2 cells to understand the impact of the individual components of WD in early NAFLD development under basal insulin levels. Specifically, nutrient-induced changes in reactive oxygen species (ROS) and signaling pathways, such as sterol regulatory element binding proteins (SREBPs), were examined to identify the root cause of steatosis development. High-fat and WD-exposed cells were associated with triglyceride and lipid droplet accumulation, paired with changes in *SREBPs* and lipid processing genes. These cells displayed hallmarks of lipotoxicity, such as decreased cell number and increased ROS. Together, this work unravels the maladaptive phenotypes associated with WD consumption, as these events may be critical in the onset of NAFLD pathogenesis.

Keywords

Non-alcoholic fatty liver disease (NAFLD), Western Diet (WD), Oxidative Stress, Reactive Oxygen Species (ROS), Sterol Regulatory Element Binding Protein (SREBP), HepG2

Summary for Lay Audience

The Western world is currently burdened with the rising rates of metabolic diseases, as many individuals continue to engage in unhealthy eating practices. One such pattern, characterized by excessive saturated fat and sugar consumption, is the Western diet (WD). This diet has been linked to the worsening of metabolic health, leading to the development of diseases such as type II diabetes mellitus and obesity. The liver is especially susceptible to the ongoing consumption of the WD, as it overwhelms the processes that breakdown fats and sugars. Excessive nutrient intake can disrupt these processes, leading to the accumulation and storage of fats (steatosis) – the hallmark of non-alcoholic fatty liver disease (NAFLD). NAFLD involves a spectrum of liver defects that are characterized by steatosis and inflammation. Over time, these events may lead to fibrosis, cirrhosis, cancer, and eventually death. While the mechanisms of this disease have been heavily studied in obese individuals who present with various metabolic abnormalities, people with lean NAFLD are currently underrepresented and the disease is misunderstood. Using a cell model, the goal of this study was to understand the consequences of WD-like consumption and individual nutrients on the mechanisms of steatosis development in early stages of NAFLD. This was not a model of obese NAFLD as cells were not exposed to certain complications associated with obesity, such as inflammation or high concentrations of insulin. Cells with high-fat and WD treatment displayed lipid accumulation and storage, followed by changes in the expression of genes that regulate lipid metabolism. Moreover, these treatments displayed decreases in cell number with accumulation of harmful products in the cells. Taken together, this work reveals that while the quantity of calories one consumes is alarming, the type of calories is equally concerning as certain nutrient components may disrupt normal liver functioning, resulting in hepatic steatosis and NAFLD. These findings are significant in that it investigates the direct effects of dietary components in dysregulated metabolic functioning in an otherwise healthy model, revealing key events in early steatosis development and furthering our understanding of NAFLD.

Co-Authorship Statement

All studies in this thesis were performed by Celina M. Valvano, with notable contributions from the individuals below.

Dr. GM Kelly	Supervisor throughout research project, provided financial support, aided in project design/data interpretation, edited manuscript, provided advice and support.
Dr. TRH Regnault	Co-supervisor throughout research project, provided financial support, aided in project design/data interpretation, edited manuscript, provided advice and support.
Dr. NM Borradaile	Provided HepG2 cells, experimental protocols, offered guidance and support throughout the development of this project.
RB Wilson	Performed lipid mass/triglyceride experiments, provided training, guidance, and support through the development of this project.
CG Sawyez	Performed lipid mass/triglyceride experiments.
Dr. DH Betts	Member of advisory committee who provided advice and support.
Dr. J Karagiannis	Member of advisory committee who provided advice and support.

Acknowledgments

This thesis is dedicated to all patients with non-alcoholic fatty liver disease. May this be one step in the right direction to broaden our understanding of this disease.

To my supervisor, Dr. Gregory Kelly, thank you for being a constant beacon of support and for being so welcoming. My experience as both your undergraduate and graduate student has been one that I will never forget. I cannot thank you enough for believing in me and for providing me with the opportunity to grow both as a person and a researcher.

To my co-supervisor, Dr. Timothy Regnault, thank you for your guidance and support throughout this project, and for taking me on as your student. It was through our discussions that you ignited my passion to continue studying metabolic diseases. Thank you for your constant reassurance and advice, and for teaching me how to think critically and creatively as a researcher.

Thank you to Dr. Nica Borradaile and Rachel Wilson for always being available to discuss my research and guide me in the right direction. You both played a large role in shaping my project, and I am grateful for the constant support and kindness you have shown me. To my advisory committee, Dr. Dean Betts and Dr. Jim Karagiannis, thank you for your time and guidance throughout my project, and for challenging me to be a better researcher.

Thank you to all past and current members of both the Kelly and Regnault labs for your advice and support throughout my time as a graduate student. Whether it was to listen to me present, discuss research topics, or to help me with an experiment, your support did not go unnoticed.

To the Favotto family, I cannot even begin to explain how much you mean to me. This thank you is not enough for everything you have done and continue to do for me. Knowing that you are all in my corner cheering me on in everything that I do, and that I always have you to lean on (and vent to) is something that I will always cherish.

I would also like to thank the Valvano family. I cannot put into words how thankful I am for the endless love, encouragement, and support you have shown me throughout my life. You have all

taught me that no obstacle is strong enough to tear us down. To my Zia Rosa and Zia Lena, thank you for always being there for me, whether it be a text or a phone call away. Thank you for seeing me as a strong woman when I could not see it myself, and for reminding me that I can do anything that I set my mind to.

To my brother Antonio, thank you for being the best roommate I could ask for. Thank you for listening to me during my ups and downs, and for being a shoulder to cry on. I will continue to emulate your confidence and work-ethic in everything that I do. To my mother Maria, there truly is no greater mother than you. Thank you for continually showing me what it means to be a strong woman. Thank you for your unconditional love and encouragement, and for dropping everything and anything to be there for me when I needed you most.

Lastly, I would like to thank my father Vince – my greatest teacher. You continue to amaze me every day with the amount of strength and resiliency you embody. Thank you for setting an example for me and teaching me how important it is to be kind, humble, and hard-working. You are the main reason why I pushed myself to continue this degree and I am forever grateful.

Table of Contents

List of Tables

List of Figures

Appendix C

List of Appendices

List of Abbreviations

ABTS   Azino-di-(3-ethylbenzathiazoline sulphonate)

ACACA   Acetyl-CoA carboxylase alpha

ACACB   Acetyl-CoA carboxylase beta

ACADVL   Very long chain acyl-CoA dehydrogenase

ACC1   Acetyl-CoA carboxylase 1

ACSL5   Long chain acyl-CoA synthetase 5

ACTB   Actin beta

AKT   Protein kinase B

AMP   Adenosine monophosphate

ANOVA   One-way analysis of variance

ATP   Adenosine triphosphate

BSA   Bovine serum albumin

BMI   Body mass index

cAMP   Cyclic adenosine monophosphate

cDNA   Complementary deoxyribonucleic acid

$CHCl_3$ Trichloromethane

CREB3L3   cAMP responsive element-binding protein 3-like 3

COPII   Coat protein complex II

Cq	Quantitation cycle
DCF	2'7'-dichlorofluorescin
DCFDA	2',7'-dichlorofluorescin diacetate
DMSO	Dimethyl sulfoxide
DNA	Deoxyribonucleic acid
DNL	*De novo* lipogenesis
ER	Endoplasmic reticulum
ERK1/2	Extracellular signal-regulated kinase ½
ETC	Electron transport chain
Ex/Em	Fluorescence excitation/emission
FASN	Fatty acid synthase
FBS	Fetal bovine serum
FFA	Free fatty acid
F1P	Fructose-1-phosphate
F-1,6-BP	Fructose-1,6-bisphosphate
F6P	Fructose-6-phosphate
GA-3-P	Glyceraldehyde-3-phosphate
GLUT2	Glucose transporter 2
G6P	Glucose-6-phosphate
G6PD	Glucose-6-phosphate dehydrogenase

HCC	Hepatocellular carcinoma
HDL	High-density lipoprotein
HepG2	Human hepatocellular carcinoma cells/cell line
HFCS	High-fructose corn syrup
HMGCR	3-hydroxy-3-methylglutaryl-CoA reductase
H_2O	Water
H_2O_2	Hydrogen peroxide
IRS1	Insulin receptor substrate 1
INSIG1/2	Insulin induced gene protein 1/2
KHK-C	Ketohexokinase isoform C
KRAS	Kirsten rat sarcoma viral oncogene homolog
LDL	Low-density lipoprotein
LDLR	Low-density lipoprotein receptor
LIRKO	Liver insulin receptor knock-out mice
LXRα	Liver X receptor alpha
MAFLD	Metabolic dysfunction-associated fatty liver disease
MAPK	Mitogen-activated protein kinase
MEK1/2	Mitogen-activated protein kinase/extracellular signal-regulated kinase 1/2
MetS	Metabolic syndrome
MitoSOX™	Mitochondrial superoxide indicator

mL	Millilitre
mM	Millimolar
mmol/L	Millimoles per litre
mRNA	Messenger ribonucleic acid
MTT	3-(4,5-dimethylthiazol-2-yl)-2,5-diphenyl-2H-tetrazolium bromide
mTORC1	Mammalian target of rapamycin complex 1
MUFA	Monounsaturated fatty acid
NADPH	Nicotinamide adenine dinucleotide phosphate
NAFLD	Non-alcoholic fatty liver disease
NASH	Non-alcoholic steatohepatitis
NaOH	Sodium hydroxide
NEFA	Non-esterified fatty acid
nm	Nanometer
nM	Nanomolar
n-SREBP	Nuclear sterol regulatory element binding protein
OA	Oleic acid
OXPHOS	Oxidative phosphorylation
PA	Palmitic acid
PA/OA	Palmitic/oleic acid
PBS	Phosphate buffered saline

PFK	Phosphofructokinase
PI3K	Phosphoinositide 3-kinase
PLIN2	Perilipin 2
PSMB6	Proteasome 20S subunit beta 6
PUFA	Polyunsaturated fatty acid
qRT-PCR	Quantitative reverse transcription polymerase chain reaction
RAF	Rapidly accelerated fibrosarcoma kinase
RAS	Rat sarcoma virus GTPase
RNA	Ribonucleic acid
ROS	Reactive oxygen species
RPLP0	Ribosomal protein lateral stalk subunit P0
SCD1	Stearoyl-coenzyme A desaturase 1
SFA	Saturated fatty acid
SCAP	Sterol regulatory element binding protein cleavage activating protein
SREBP	Sterol regulatory element binding protein
SREBP-1a	Sterol regulatory element binding protein 1a
SREBP-1c	Sterol regulatory element binding protein 1c
SREBP-2	Sterol regulatory element binding protein 2
SEM	Standard error of the mean
S1P	Site 1 protease

S2P	Site 2 protease
S6K	Ribosomal S6 kinase
Tm	Melting temperature
TNFα	Tumor necrosis factor alpha
TSC1/2	Tuberous sclerosis protein 1/2
T2DM	Type II diabetes mellitus
UPR	Unfolded protein response
VAT	Visceral adipose tissue
VLDL	Very low-density lipoprotein
WD	Western diet
μg	Microgram
μL	Microliter
ΔOD	Delta optical density

Chapter 1: Literature Review

1.1 Western Diet and its Impact on Health

1.1.1 Western Diet

There is growing awareness that over the course of six to eight generations, especially in the last two decades[1], there has been a shift in global dietary patterns that has negatively influenced the health and well-being of individuals. Dietary patterns describe the complex relationship between diet and health, and how certain nutrients alone or combined can contribute to overall health[2]. A dietary pattern is defined as the quantity or proportion, variety, and combination of different foods and beverages that are routinely consumed by an individual[3]. Food intake and dietary patterns vary among individuals around the world, allowing for the study of various nutrient combinations on health. While biological determinants such as appetite and hunger play a large role in one's food choices, other factors such as food access and availability, income, culture, stress, and the attitudes, beliefs, and knowledge one holds about food can influence what they consume.

Alongside these different lifestyles, the Western dietary pattern has emerged and is currently believed to play a substantial role in the recently observed decline in individual health, along with the onset of "civilization diseases" (obesity, type II diabetes mellitus, dyslipidemia, cardiovascular diseases, hypertension, etc.)[1,4]. The Western diet (WD) is characterized by the overindulgence of refined sugars, saturated fats, salt, processed meats, and refined grains, leaving individuals in a constant post-prandial state[5]. With the Agricultural Revolution ~10,000 years ago, and even more so with the Industrial Revolution 250 years ago, these events caused profound environmental changes in diet and lifestyle – changes that happened too quickly for the human genome to adapt to[1,4]. While this diet was established in North America over the past two centuries, it seems as though nutrient transformations are occurring more rapidly in developing countries due to the increased availability and affordability of these foods, coupled with globalization and economic growth[6]. With the rise of obesity to epidemic proportions[7] – a consequence of the convergence to a WD – it is not uncommon to find millions of people in Western civilizations attempting to lose weight at any given time of the year.

In a healthy diet, such as the Mediterranean diet, macronutrients (*i.e.,* carbohydrates, lipids, proteins) are consumed in appropriate amounts to provide and support the body with its daily energetic and physiological needs. In regard to the calorically-rich WD, the excessive quantity and proportion of macronutrients consumed by individuals is concerning[5]. Equally alarming is the unfavourable quality of nutrients that are being consumed, as data from 1908–1989 in the United States revealed that total calories consumed from carbohydrates decreased from 57% to 35%, with total calories available from fats increasing from 32% to 45%, providing insight on modern macronutrient intake trends[5,8].

Although the amount of carbohydrates consumed in the WD is decreasing, the kilocalorie intake of simple sugars such as fructose and glucose are increasing, along with foods high in glycemic index. These foods are known to have a direct effect on the harmful metabolic properties associated with the WD[5]. Fructose consumption in particular has increased significantly over the past 400 years (~10% of caloric intake in the United States[9,10]) and this increase is strongly correlated with non-alcoholic fatty liver disease (NAFLD) and hypertension[9], as well as type II diabetes mellitus (T2DM). Paired with the low consumption of fruits and vegetables, beans, and whole grains, the lack of these high-quality carbohydrates in the WD prevents individuals from consuming essential sources of vitamins and minerals needed for proper cellular and organ functioning.

Also crucial to various biological and cellular functions are fatty acids. Diet is one of the two main sources of lipids in an organism, and the type of lipids circulating within an organism are strongly influenced by food intake. Saturated fatty acids (SFAs) in particular are known to be deleterious to metabolic health[11], and the quantity and quality in which they are consumed directly influence the magnitude of chronic inflammation present in metabolic diseases[5]. In fact, many studies have found that the consumption of a SFA-rich diet, such as the WD, is positively correlated with the presence of hepatic steatosis, T2DM, and obesity[11]. Additionally, these dietary fats can disrupt immune system functioning by altering the cell membranes of immune cells[12]. Common dietary SFAs, such as palmitic, stearic, lauric, and myristic acid have proven to be the most inflammatory[12], which together with its influence on the production of low-density lipoprotein (LDL) cholesterol, can contribute to the formation of atherosclerotic plaques and consequently, cellular damage[4,13].

While an excess of SFAs in the diet cause negative side effects in terms of health outcomes, monounsaturated fatty acids (MUFAs) and polyunsaturated fatty acids (PUFAs) tend to have the opposite effect. Specifically, omega-3 PUFAs, such as α-linolenic, docosahexaenoic, and eicosapentaenoic acid can have beneficial effects on metabolic health as they are anti-inflammatory in nature and promote antioxidant activity[11]. Through these mechanisms, PUFAs can regulate and improve metabolic health in the nervous system and circulatory system, as well as glucose tolerance, and skeletal muscle metabolism[14]. Regarding MUFAs like oleic acid, these are also known to promote metabolic health and can prevent the development of thrombosis and atherosclerosis through improvements in the gut microbiome[11,15,16]. Compared to the WD, dietary patterns such as the Mediterranean diet, which is characterized by the high consumption of olive oil, fish, whole grains, and fruits and vegetables, have a higher amount of MUFAs consumed (60%) compared to SFAs (20%) (WD: 36% MUFAs, 33% SFAs)[11,17]. Increased MUFA consumption has also been positively correlated with lower incidences of metabolic syndrome (MetS) and obesity, resulting in decreased chronic inflammation and mortality[11,18,19]. Additionally, diets with high MUFA content have been associated with improvements in circulating lipid and blood glucose profiles, as well as with lowering blood pressure[11,20–22]. As such, these diets can promote cardiovascular health and contribute to beneficial changes in the gut microbiome that improve general metabolic health[11,15,16].

Overall, the WD can exert negative impacts on the metabolic health and well-being of individuals. While a total increase in caloric intake contributes to the many mechanisms involved in WD consumption, the type of calories and nutrients one consumes may be of greater importance as each nutrient component can affect metabolic processes in different ways. Individuals should be made aware of the harmful consequences the WD poses to their health and their organs, as modifications and improvements in diet can alleviate the heavy burden it places on the development of chronic diseases[23].

1.1.2 Western Diet and the Liver

As the central hub of metabolic and physiological processes, the liver is an important organ in the human body that interacts with nearly every other organ system[24]. Among its main functions, the liver plays a large role in the metabolism of macronutrients through which it provides the body with the energy it needs to drive physiological processes. A growing body of

evidence has revealed that lifestyle factors such as diet, in particular total caloric intake and specific nutrient intake[25], play a large role in dysregulating metabolic processes within the liver and lead to the development of metabolic diseases such as NAFLD – an umbrella term for a disease spectrum that is characterized by increased fat accumulation in the liver.

There are controversial results when it comes to reporting the exact cause of fatty liver in regard to diet. Previous studies have reported that an increased intake of SFAs and total fats causes the deposition of lipids, while others state that diets high in total carbohydrates and sugars are to blame[25]. Consistent among these studies is that in general, an excess of nutrients can lead to hepatic fat accumulation; however, isocaloric diets may trigger different responses in the liver as the "type" of calories consumed may be of greater importance[23].

With adherence to the Western dietary pattern, this places patients at a greater risk of developing a fatty liver as it disrupts metabolic pathways involved in fatty acid and glucose metabolism. In regard to dietary fat content, it has been found that when compared to MUFAs and PUFAs, which can decrease liver triglyceride levels[26], SFAs can increase liver fat and exacerbate insulin resistance[25–27]. Additionally, human subjects with fatty livers tend to have higher concentrations of SFAs and MUFAs in total plasma and hepatic lipids compared to healthy individuals[26,28,29]. The high intake of SFAs typical of the WD is detrimental to liver functioning as these fatty acids are known to cause lipotoxic effects which include mitochondrial dysfunction, endoplasmic reticulum (ER) stress, and oxidative stress[26,30,31]. Further, SFAs may upregulate lipogenic genes which act to promote triglyceride synthesis[26,32].

Another component of the WD that is strongly associated with liver-related pathologies is the increased intake of fructose, particularly from sweetened beverages like soft drinks[33]. Fructose consumption can come in the form of sucrose (table sugar: 50% fructose, 50% glucose) or as high fructose corn syrup (HFCS: 55% fructose, 45% glucose). It has been implicated in liver pathologies as it can cause hepatic steatosis in animal models following its administration[33–36]. Interestingly, in rat models of NAFLD, liver fat accumulation is achieved when animals are administered diets high in sucrose, even though they are under a calorically restricted regimen[33,35]. Additionally, individuals with NAFLD have been found to consume fructose-containing soft drinks in higher amounts than their healthy counterparts, causing an increased

expression of hepatic fructose-metabolizing enzymes[33,37]. This ultimately leads to mitochondrial oxidative stress, along with fat accumulation[33,38–40].

Given the impact of Western dietary components on the liver, this further emphasizes the importance of the type of nutrients one consumes. Overall, the habitual consumption of excess nutrients in the WD can negatively impact the liver through the alteration and dysfunction of metabolic processes.

1.1.3 Metabolism of Fatty Acids in the Liver

One of the main functions of the liver is to maintain and regulate lipid metabolism – a tightly regulated process that relies on the balance between fatty acid uptake and export[41]. When lipid homeostasis is disturbed, this can lead to the development of liver-related pathologies, such as NAFLD. The hepatic free fatty acid (FFA) pool is sourced from *de novo* lipogenesis (DNL), dietary fatty acids, and non-esterified fatty acids (NEFAs) released from adipose tissue in the plasma[42,43]. While these three processes contribute to FFA uptake, their elimination occurs through β-oxidation in the mitochondria, and to a lesser extent in peroxisomes[44]. They can also be exported from the hepatocyte in the form of very low-density lipoproteins (VLDLs) that are rich in triglycerides[41]. As a result of this balance between FFA uptake/synthesis and export, the liver maintains a steady state of triglyceride content (<5%) as it processes large quantities of FFAs on a daily basis[41,45]. The small amount of triglycerides that remain within the liver are stored in the form of cytoplasmic lipid droplets.

When consuming a Western diet, which is rich in fats, the metabolic capacity of the liver becomes overwhelmed as it cannot accommodate for the overloaded hepatic free fatty acid pool[42,46]. A disequilibrium results between fat production/uptake and degradation – one of the most direct mechanisms involved in the pathogenesis of NAFLD[42]. As fatty acids enter the hepatocyte through fatty acid transporters, these FFAs will be localized to different cellular compartments[47]. Controlled by the sterol regulatory element binding protein (SREBP) family of transcription factors, DNL will convert acetyl-CoA, derived from excess carbohydrates, to new FFAs[47], which can then be stored as triglycerides. β-oxidation will then attempt to reduce increased FFA levels in the mitochondria, however, when overloaded by increased FFA intake, or if the mitochondria are dysfunctional, β-oxidation rates will increase and will be shunted

towards the peroxisomes and cytochromes, effectively generating reactive oxygen species (ROS)[47], inflammation, and liver disease progression[48] (**Fig. 1.1.3-1**). In fact, it has been found that the degree of steatosis is positively correlated with the rate of mitochondrial and peroxisomal β-oxidation, as patients with severe steatosis present with increased rates of β-oxidation in these cellular compartments compared to those with less severe steatosis and non-steatotic controls[49]. Although this is the livers compensatory mechanism to deal with the increased intake of FFAs, this also produces excess ROS, which may overwhelm the antioxidant capacity of the cell and ultimately induce oxidative stress[47].
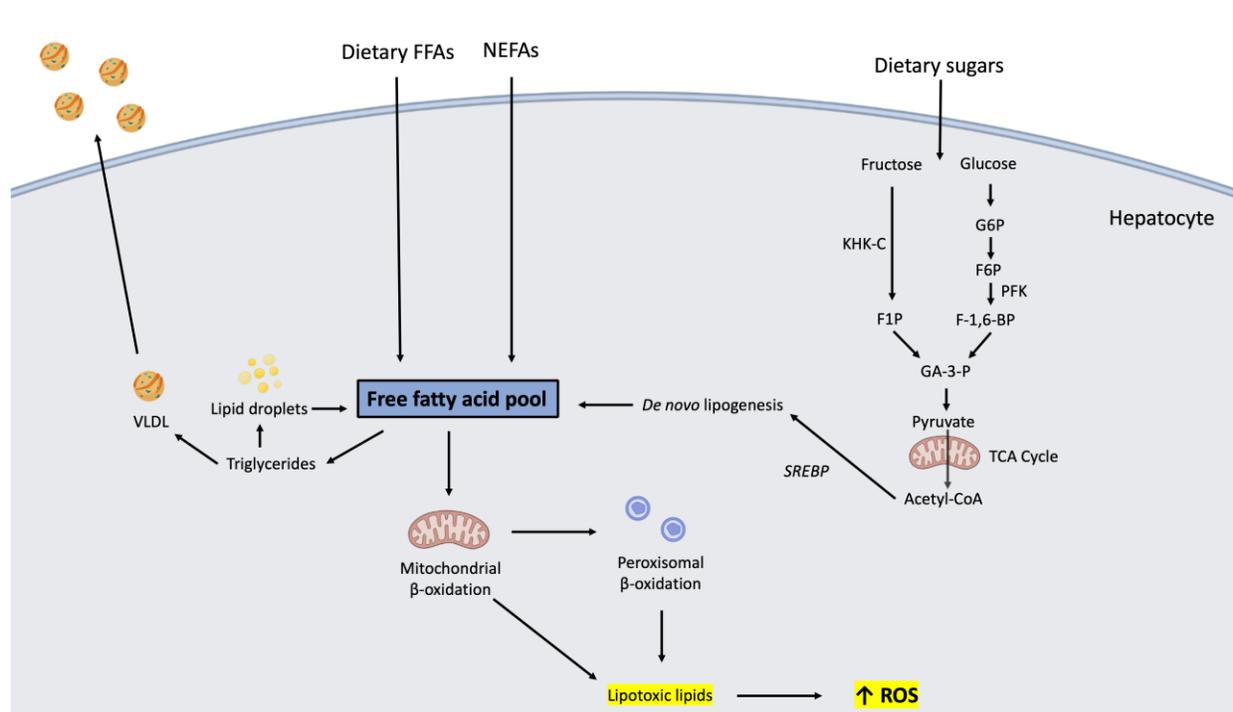
Figure 1.1.3-1. Metabolism of excess fatty acids and sugars in the liver. With WD consumption, the hepatic FFA pool is overloaded by an increased delivery of free fatty acids (FFAs) and non-esterified fatty acids (NEFAs), and dietary sugars which will activate *de novo* lipogenesis. Glucose will be metabolized through glycolysis, forming glucose-6-phosphate (G6P) and fructose-6-phosphate (F6P). F6P will then be phosphorylated by phosphofructokinase (PFK) to form fructose-1,6-bisphosphate (F-1,6-BP). This can then be converted into glyceraldehyde-3-phosphate (GA-3-P), which will then form pyruvate. Conversely, fructose will be rapidly metabolized into fructose-1-phosphate (F1P) by ketohexokinase isoform C (KHK-C). This will eventually be converted into GA-3-P and finally pyruvate. The pyruvate will then be used to fuel

the Citric Acid Cycle (TCA cycle) in the mitochondria, producing acetyl-CoA. This acetyl-CoA will then be used for *de novo* lipogenesis, which is regulated by sterol regulatory element binding proteins (SREBPs). *De novo* lipogenesis will then produce FFAs, further contributing to the FFA pool. The FFAs and NEFAs will directly enter the hepatocytes and can be esterified to form triglycerides, which are stored in lipid droplets; or they are used to form very low-density lipoproteins (VLDLs) which are then transported into the plasma. The large influx of FFAs are also shunted toward mitochondrial β-oxidation in an attempt to catabolize these products. However, the mitochondria eventually become overloaded and/or dysfunctional, and FFAs are then oxidized in peroxisomes, with both processes forming lipotoxic lipid species and culminating in increased reactive oxygen species (ROS) production. Created with BioRender.com and adapted from Chen et al., 2020[42].

1.1.4 Metabolism of Sugars in the Liver

Another important function of the liver is to regulate glucose homeostasis, which is required to maintain individual health, as well as to meet the energy requirements of other organs[50]. While glucose metabolism is more tightly controlled, it is believed that fructose is able to cause liver-related pathologies due to the nature of its metabolism. Firstly, fructose is delivered to the liver in much higher proportions compared to other tissues as it is sent from the small intestine directly to the liver through the portal vein[51,52]. When consumed in low amounts, fructose has been shown to be cleared by the small intestine, where it is converted into glucose and organic acids, then sent to the liver[51]. However, the high intake of this simple sugar overloads the capacity of the small intestine to metabolize fructose, causing it to "spill over" into the liver[51]. Both fructose and glucose from the small intestine are then taken up into hepatocytes by the insulin-independent glucose transporter GLUT2[53]. While glucose is metabolized through glycolysis, fructose will undergo similar steps; however, it bypasses the gating step of glycolysis as it does not need to be phosphorylated by phosphofructokinase (PFK)[51]. Glycolysis begins with phosphorylation of glucose to form glucose-6-phosphate, which is then converted into fructose-6-phosphate (F6P). Phosphofructokinase will then phosphorylate F6P to form fructose-1,6-bisphosphate. Fructose, on the other hand, is phosphorylated at a different position by the high-activity enzyme, ketohexokinase isoform C (KHK-C), to form fructose-1-phosphate[53]. Interestingly, KHK-C is not allosterically regulated, nor does it have a negative feedback

system[53]. This can then be cleaved into three-carbon units without phosphorylation by PFK[51], which is a major rate-limiting step in glycolysis (**Fig. 1.1.3-1**). Due to the rapidity in which fructose is metabolized compared to glucose, it has been proposed that excessive fructose intake can cause a decrease in the ATP:AMP ratio[51], most likely a consequence of uninhibited KHK-C activity[53], resulting in changes in oxidative phosphorylation and mitochondrial dysfunction.

In humans, fructose is rarely consumed alone, but is more commonly consumed with glucose, and together, these two simple sugars can influence fat accumulation in the liver[25]. When excess carbohydrates are consumed, the liver will convert these sugars to glycogen. However, in carbohydrate-rich diets such as the WD, the liver will form fatty acids from the carbohydrates in a process called *de novo* lipogenesis (DNL) using acetyl-CoA derived from the end-product of glycolysis, pyruvate[50]. These fatty acids are then used to form triglycerides and lipid droplets, as well as very low-density lipoproteins (VLDLs) that are transported to white adipose tissue for storage[50,54] (**Fig. 1.1.3-1**). Studies have shown that acute over-feeding of fructose causes significant increases in liver fat content in otherwise healthy individuals[55–58], and it may be due to the ability of fructose to upregulate hepatic DNL, even more so than a high-fat diet[52]. However, when glucose is consumed with fructose, such as in HFCS, it seems that the combination of both sugars is critical for the enhanced activation of hepatic DNL[25,59], as isolated glucose consumption is not incorporated into triglycerides[60]. Since fructose does not require insulin for its metabolism, this makes fructose particularly lipogenic in cases of insulin resistance where it can directly activate sterol regulatory element binding protein 1c (SREBP-1c) – a transcription factor involved in the regulation of DNL[52]. Following activation of SREBP-1c, this results in the transcriptional activation of other lipogenic enzymes such as fatty acid synthase (FASN), acetyl-CoA carboxylase 1 (ACC1), and stearoyl-CoA desaturase 1 (SCD1)[50].

While FFAs contribute to liver fat accumulation, it is evident that the presence of high-sugars in the diet may be of great concern through their activation of DNL. Additionally, in patients with NAFLD, DNL should not be ignored as its marked increase may be the most prominent abnormality present in these patients compared to healthy controls[61,62]. While DNL is upregulated in obese patients who are insulin-resistant, lean patients with NAFLD – a new phenomenon that has emerged – also show signs of DNL activation, although this occurs at lower rates[63–65]. Overall, determining how each individual dietary component contributes to

liver-related pathologies, especially in NAFLD, is of utmost importance as the global population continues to converge to harmful dietary patterns, placing themselves at a greater risk of developing chronic liver diseases.

1.2   Non-Alcoholic Fatty Liver Disease (NAFLD)

1.2.1 Overview of NAFLD

The liver, a complex organ involved in many vital physiological processes, plays a major role in metabolism, including glucose, lipid, and cholesterol homeostasis[66]. In the absence of metabolic homeostasis, sustained chronic inflammation occurs followed by a disruption in systemic metabolic functions[66], and the ability of the liver to resolve inflammation, fueling the progression of metabolic diseases. As tissue homeostasis is disrupted, a series of liver abnormalities result, including hepatic steatosis, fibrosis, cirrhosis, and liver failure, which are key events in the progression of non-alcoholic fatty liver disease[66].

Non-alcoholic fatty liver disease (NAFLD), recently termed metabolic dysfunction-associated fatty liver disease (MAFLD)[67], is an increasing concern and a major health burden in the Western world. NAFLD has become the fastest rising cause of liver disease worldwide, as it is highly associated with the incidence of obesity and type II diabetes mellitus (T2DM)[68,69]. This disease has also been driven by a rise in sedentary lifestyles, coupled with low levels of physical activity and excess caloric intake[67]. As the rates of obesity and metabolic syndrome (MetS) continue to rise, the prevalence of NAFLD has increased steadily alongside it, and has reached a global prevalence of over 25%[70,71]. According to the Canadian Liver Foundation in 2019, NAFLD was found to affect 1 in 5 Canadians from adults to children. With the global population continuing to adhere to a Western dietary pattern, there is an increased risk of developing this disease, as well as the metabolic comorbidities that follow in its wake.

NAFLD is classified by the presence of intracellular fat accumulation in >5% of hepatocytes (steatosis), in the absence of excessive alcohol intake, drugs, or other metabolic conditions[70,72]. It involves a broad spectrum of liver abnormalities, and with each stage the pathogenesis of the disease worsens. It begins with non-inflammatory isolated hepatic steatosis[73], which can be a benign, reversible event, and is characterized by intrahepatic accumulation of triglycerides[69]. This progresses to a more severe form, non-alcoholic steatohepatitis (NASH),

where steatosis, hepatocyte damage and ballooning, chronic inflammation, and varying degrees of fibrosis are observed[69,73]. The disease may advance to cirrhosis and eventually liver failure, and has the potential to lead to hepatocellular carcinoma (HCC), the most common form of liver cancer.

The pathogenesis of NAFLD is still not entirely clear as it is a multifaceted disease involving both genetic and environmental factors[42], as well as complex interactions between diet, obesity, changes in the microbiome, and epigenetics[73]. As such, a new definition has been proposed to better represent the hepatic manifestation of MetS – MAFLD. Since this disease is classified as heterogeneous in its presentation, underlying causes, progression, and outcomes, this definition aims to view the disease as a continuum, rather than one with exclusion criteria[67]. It is possible that different stages of the disease may be present at one time (*e.g.,* hepatic steatosis present with mild NASH). This is beneficial as it helps to identify sub-classes of the disease and will account for the differences in histopathology that are often observed[67]. Further, a multiple-hit hypothesis of disease progression is currently accepted in regard to NAFLD, which proposes that a multitude of factors are acting synergistically, especially in those who are genetically predisposed[73]. In this model, insulin resistance paired with steatosis, increased lipogenesis and impaired fatty acid oxidation, can sensitize the liver to inflammation and cell death, promoting oxidative stress[42]. These pathogenic insults are thought to act in parallel, rather than sequentially, further exacerbating NAFLD pathogenesis. The multiple-hit hypothesis is also beneficial for understanding the different phenotypes that commonly arise in clinical practice, especially in regard to the lean population.

1.2.2 Lean vs. Obese NAFLD

While NAFLD is predominantly associated with obesity, the disease is increasingly being diagnosed in lean and non-obese individuals[74], with 6–20% of NAFLD cases occurring in this population[75]; and this prevalence has been reported to reach as high as 40% in Western countries[67]. Even more concerning is that these patients are asymptomatic and often go undiagnosed for years as the disease is discovered incidentally[76]. Although research on lean NAFLD is currently scarce, many studies have stated that these patients share a similar metabolic milieu to that of their obese counterparts[76,77]. These metabolic abnormalities may include, but are not limited to, dyslipidemia, insulin resistance, and high blood pressure[78]. In the

absence of these comorbidities, it has also been found that lean or non-obese NAFLD patients are at an increased risk for their development, along with incident T2DM, cardiovascular disease, and all-cause mortality compared to obese patients without NAFLD or MetS[75,78–82].

In North America, the lean patient is defined as an individual with a body mass index (BMI) $\leq$25 kg/m^2, with the BMI of non-obese overweight patients ranging from 25–30 kg/m^2, and a BMI $\geq$30 kg/m^2 characterizing obese patients[83]. Although useful, BMI as an indicator of NAFLD is often inappropriate for lean patients as it fails to identify body fat composition and differences in visceral adiposity among patients[76] – a factor that plays a large role in the development of NAFLD. Importantly, lean NAFLD individuals tend to have a lower body weight and waist circumference compared to obese patients; however, they may present with increased adiposity in the abdomen[76]. Lean patients have also displayed increased visceral adipose tissue (VAT) compared to healthy controls[84–86]. Another limitation to the use of BMI as an indicator of NAFLD is that different cut-offs have been established for different cultures, which may lead to a misinterpretation of the literature on lean NAFLD. Due to the difficulty of screening lean individuals for NAFLD, it may be beneficial to measure waist circumference routinely. Physicians may also be aware of the fact that lean NAFLD is more common in younger patients who are male[79], and who have lower levels of fasting glucose, blood pressure, and glycated hemoglobin (HbA1c) compared to their obese counterparts; although when compared to healthy controls, these markers are increased along with the presence of dyslipidemia[76,87,88].

While there are differences between lean/non-obese NAFLD individuals and obese NAFLD subjects, in general, the pathogenesis of the disease in both populations is relatively similar (**Fig. 1.2.2-1**). A hallmark of disease development in both groups is the accumulation of free fatty acids in the liver[78], and both groups present with increased triglyceride levels, lower high-density lipoprotein (HDL; "good") cholesterol, and higher low-density lipoprotein (LDL; "bad") cholesterol[84]. Significantly, insulin resistance plays a large role in disease progression in both groups; however, lean NAFLD patients have a higher risk of T2DM than patients who are overweight or obese without the presence of NAFLD[75]; and it is more commonly observed in the lean NAFLD population compared to healthy controls[79]. This increased risk remains in the absence of other metabolic abnormalities[75,89]. Overall, this suggests that lean NAFLD is a major

concern as these individuals are likely to develop metabolic comorbidities, regardless of BMI status.

Lean NAFLD
BMI ≤25 kg/m^2

10-20% of NAFLD cases
↑FFA/triglyceride levels
↑VAT
↑↑Liver-related/all-cause mortality
Higher risk of T2DM
Asymptomatic

Obese NAFLD
BMI ≥30 kg/m^2

80% of NAFLD cases
↑↑FFA/triglyceride levels
↑↑VAT
↑Liver-related/all-cause mortality
Lower risk of T2DM without NAFLD
Complicated by obesity and inflammation
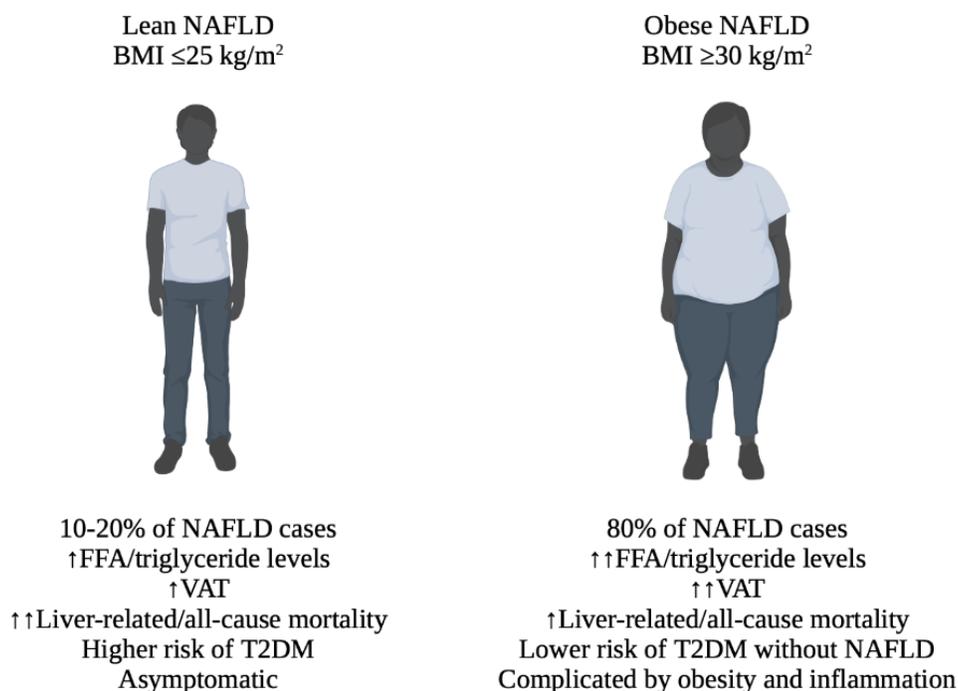
Figure 1.2.2-1. Characteristics of NAFLD in lean vs. obese subjects. The similarities and differences between lean and obese NAFLD. Lean patients are defined as those with a BMI ≤25 kg/m^2, while obese patients have a BMI ≥30 kg/m^2. NAFLD: non-alcoholic fatty liver disease; BMI: body mass index; FFA: free fatty acid; VAT: visceral adipose tissue; T2DM: type II diabetes mellitus. Created with BioRender.com and adapted from Kuchay et al., 2021[78].

1.2.3 Clinical Outcomes and Treatment Options

While obese patients represent the extremes of NAFLD outcomes, lean patients are still at an increased risk for the development of metabolic comorbidities. Strikingly, this population may have even worse outcomes than their obese NAFLD counterparts. Progression to NASH and fibrosis is enhanced in lean individuals, but less significant than the risk posed to obese individuals, as lean NAFLD livers tend to have lower measures of stiffness[90]. Regarding disease progression to cirrhosis and HCC, lean individuals with the presence of diabetes are more likely to progress to these stages[74]. Along with a 50% increase in all-cause mortality, these patients also present with a >2-fold increase in cardiovascular mortality[91]. Significantly, liver-related

mortality is also found to be two times higher in the lean NAFLD population than in their obese counterparts[74] (**Fig. 1.2.2-1**).

There are currently no guidelines or pharmacological interventions available for the treatment of lean NAFLD. As the first course of action, patients are advised to reduce excess body weight, as well as to undergo lifestyle changes[76–79]. Although weight loss has proven to be effective in both obese and non-obese/lean NAFLD patients, body weight is not always the issue in the lean population and may not be the best approach[76]. While histological improvements are observed in tandem with weight loss, oftentimes this does not control the metabolic abnormalities or insulin resistance observed in lean patients[76]. Instead, other lifestyle changes such as increased physical activity, specifically aerobic exercise to target VAT[92–94], or dietary interventions to monitor macronutrient intake, may be more appropriate for these patients. Currently, professional dietary advice is more commonly provided to overweight or obese individuals, suggesting that lean individuals do not require any dietary intervention[23]. This is concerning since low diet quality is known to be an independent predictor of declining metabolic health[23], and may cause exacerbation of NAFLD and metabolic abnormalities, as well as increased risk of complications in the future. Patients should be encouraged to stray from the Western pattern and adhere to a Mediterranean diet paired with decreased consumption of fructose[23,76].

Regarding pharmacological treatment options, some drugs have been studied in the context of obese and diabetic NAFLD patients, but there is currently limited evidence to support a specific treatment regimen in the case of lean NAFLD[76,79]. Some therapeutic agents such as thiazolidinediones (peroxisomal proliferator-activated receptor agonists) and glucagon-like peptide-1 receptor agonists (liraglutide)[78] may be beneficial, as the latter has shown to improve NASH in non-obese patients[95]. These drug classes may be useful in the treatment of lean NAFLD since they target key processes involved in its pathogenesis, such as dysfunctional visceral adiposity and insulin resistance[78]. Since NAFLD is a multi-faceted disease, one treatment option may not be beneficial for every patient, and as such, many factors need to be taken into account to find and implement the best course of action. Further, an emphasis on diet-quality should be at the forefront of treatment options and should be discussed with all patients, regardless of weight.

Overall, there is currently no standard treatment recognized for the effective management of lean NAFLD, except lifestyle modifications and if it reaches cirrhosis, the only available treatment is liver transplantation[69]. As NAFLD is highly associated with metabolic comorbidities, it continues to strain health care systems and the economy, and calls for the attention of physicians, specialists, and health policy makers[96]. This warrants further research, as the pathogenic mechanisms of lean NAFLD are poorly understood[74].

1.3 Signaling Pathways in NAFLD

1.3.1 Sterol Regulatory Element Binding Proteins (SREBPs)

With excessive hepatic lipid accumulation lying at the forefront of NAFLD pathogenesis, steatosis often results from an imbalance between the processes of lipogenesis and lipolysis. These two processes are governed by a family of transcription factors called sterol regulatory element binding proteins (SREBPs)[4,97]. These proteins regulate the transcription of genes involved in cholesterol and fatty acid synthesis in animal cells, as well as phospholipid and triglyceride synthesis, and have been implicated in the progression of NAFLD[97,98]. There are two isoforms, SREBP-1 and SREBP-2, where the former is transcribed into two splicing variants, SREBP-1a and -1c[98,99]. Among the SREBP isoforms, some functional overlap is evident; however, these proteins regulate different metabolic pathways and have specific functions for regulation[98]. Specifically, SREBP-1c and -2 are predominantly expressed in organs such as the liver and adipose tissue[100,101]. Additionally, SREBP-1c displays high expression levels in the adrenal gland, various muscles, and the brain in adult rats and humans[98,99,102], whereas SREBP-1a is expressed in highly proliferative tissues such as the spleen and intestine[102]. Further, the majority of cultured cells have been found to express SREBP-1a and -2[100].

In regard to their function, SREBP-2 is a major regulator of cholesterol biosynthesis, while SREBP-1c regulates fatty acid synthesis and is thought to be a major mediator of insulin action on carbohydrate and lipid metabolism[100,101]. Interestingly, the SREBP-1a isoform can activate both cholesterol and fatty acid synthesis pathways[103], providing the precursors for membrane synthesis, and is a stronger activator of these pathways due to its longer transactivation domain[100]. As such, SREBP-1a has the ability to activate transcription of all

SREBP target genes, with SREBP-1c preferentially activating genes involved in fatty acid synthesis and SREBP-2 activating genes involved in cholesterol synthesis[104].

Activation of SREBPs are regulated by proteins from the insulin-induced gene protein (INSIG) family. INSIGs are important in the regulation of lipid metabolism and are defined as oxysterol-binding proteins[103,105]. In humans, there are two INSIG proteins, INSIG1 and INSIG2, that both bind to SREBP cleavage-activating protein (SCAP) in a sterol-dependent manner[106]. INSIG2 is ubiquitously expressed in human tissues, whereas INSIG1 is highly expressed in the liver. Significantly, INSIG1 regulates the expression of SREBP target genes in HepG2 cells and is a target of nuclear-SREBPs (n-SREBPs) as its mRNA levels rise and fall with n-SREBP levels[103,106]. Through their binding activities, both proteins influence lipogenesis, cholesterol metabolism, and glucose homeostasis[103].

In general, SREBP isoforms are directly regulated by sterols, steroids, and SCAP[103]. Inactive SREBPs are synthesized on the endoplasmic reticulum (ER) membrane where they immediately form a complex with SCAP. INSIG1/2 will bind to SCAP when sterols are abundant, retaining the INSIG/SCAP/SREBP complex in the ER membrane[103]. When sterols are depleted, SCAP will dissociate from INSIG1/2 and carry SREBP to the Golgi apparatus. Here, SREBP is cleaved, released into the cytoplasm, and translocates to the nucleus to induce transcription of its target genes[105] (**Fig. 1.3.1-1**). These target genes include fatty acid synthase (*FASN*), acetyl-CoA carboxylase 1 (*ACC1*), LDL receptor (*LDLR*), stearoyl-CoA desaturase 1 (*SCD1*), and 3-hydroxy-3-methyl-glutaryl-coenzyme A reductase (*HMGCR*) – all of which are involved in lipogenesis and cholesterol synthesis.

While SREBP-1a and -2 expression increase with low sterol availability, in rodents, SREBP-1c expression appears to be regulated by nutritional changes[99], specifically by changes in insulin levels[107]. SREBP-1c expression decreases in fasting rodents, but upon refeeding with a carbohydrate-rich diet, SREBP-1c levels increase markedly[99]. Experiments on isolated rat hepatocytes demonstrated that SREBP-1c transcription is induced by a rise in insulin, with a subsequent increase in both its ER membrane-bound precursor and its nuclear form to act as a transcription factor[99,108]. SREBP-1c transcription is also activated by Liver X Receptor (LXR) α, a nuclear hormone receptor that is activated in the presence of oxysterols. Here, SREBP-1c can

act as a transcription factor involved in cholesterol efflux and clearance[99]. When fed a diet high in cholesterol, rodent cells selectively increase their levels of SREBP-1c mRNA and nuclear protein, followed by the expression of lipogenic target genes, and a subsequent increase in lipogenesis[99,109–111]. The mechanism through which insulin induces SREBP-1c activation is thought to be linked with LXRα, where insulin has been shown to increase *LXRα* mRNA levels[112]. As such, it has been suggested that SREBP-1c is involved in insulin resistance, and has been closely associated with NAFLD as it is known to be a key regulator for mediating the signaling of insulin and glucose to lipogenesis[113]. However, both SREBP-1 isoforms can exhibit insulin-independent stimulation through pathways caused by hyperglycemia[114–116], however, these pathways are less understood.

Additionally, it is thought that the presence of obesity and T2DM, which is often associated with NAFLD, may be attributable to SREBP-1c overactivation[114]. In human NAFLD livers, expression of SREBP-1c and its target genes are increased[107,117–119]; an effect that was also observed in animal models of hepatic steatosis and obesity[118,120,121]. Many mouse models of diet-induced obesity, as well as leptin-deficient *ob/ob* and *db/db* mice, have established SREBP-1c in the liver to be a marker and possible therapeutic target for hepatic steatosis[114,122]. The regulation of SREBP-1c in the context of lean NAFLD may be similar to that in obese NAFLD; however, its mechanism of action remains undescribed.

The function of SREBPs in the liver have been characterized *in vivo* through the use of transgenic and knockout mice that lack or overexpress components of the SREBP pathway[123,124]. Transgenic mice overexpressing nuclear SREBP-1a displayed the most dramatic phenotype as they developed extensive fatty livers filled with both triglycerides and cholesterol esters[125]. Additionally, microarray data revealed that these mice had a 26-fold increase in fatty acid synthesis gene expression, with a 5-fold increase in cholesterol biosynthesis genes[123], which accounted for the accumulation of triglycerides. Compared to overexpressed nuclear SREBP-1c, these mice presented with fatty livers enriched with triglycerides and no increases in cholesterol content[124]. Overexpressed nuclear SREBP-2 was found to cause increases in all cholesterol biosynthetic enzymes, with a smaller effect on activation of fatty acid synthesis genes[126]. In regard to SREBP global knockouts or deficiencies in SREBP processing genes such as SCAP, these mouse models can recover from hepatosteatosis in the presence of obesity[114]. However,

deficiencies or partial knockouts of SREBP-1c moderately improve steatosis, suggesting that other factors are involved in hepatic lipogenesis during NAFLD development[114,127,128].
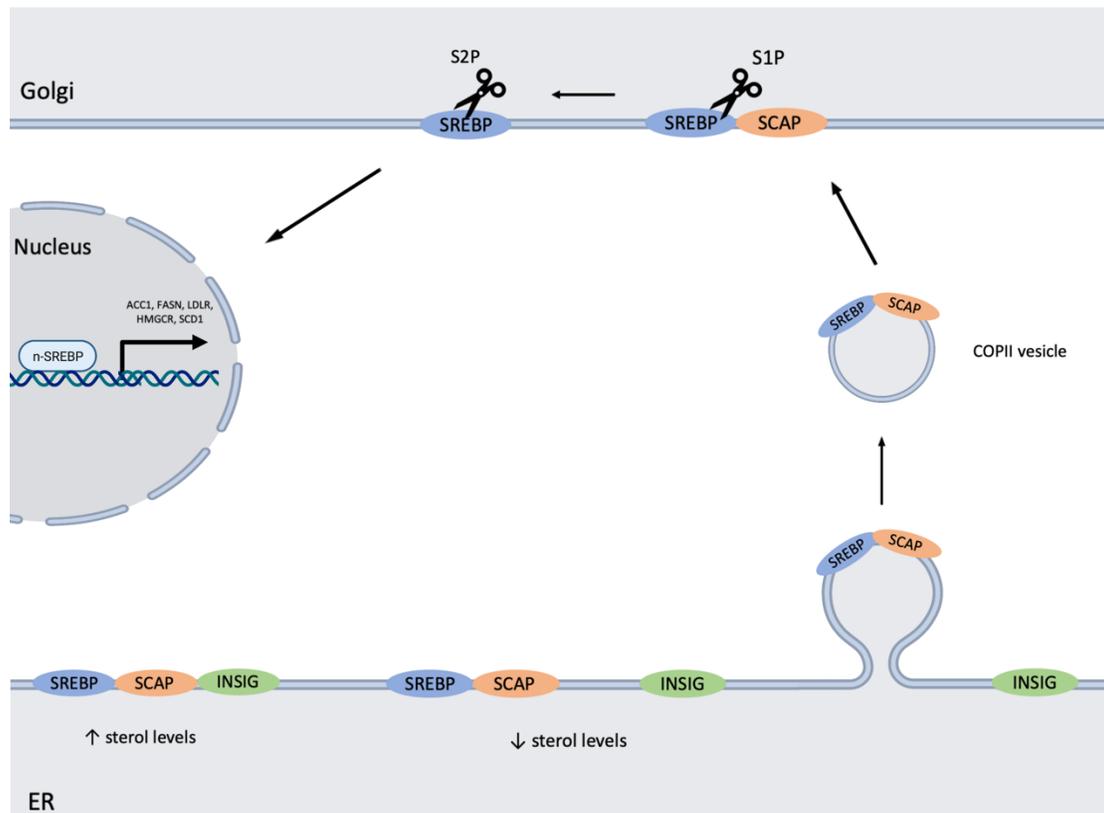
Figure 1.3.1-1. Activation and proteolytic processing of SREBPs. In the endoplasmic reticulum (ER), inactive SREBPs are processed and immediately bind to SCAP to form a complex. When intracellular sterol levels are high, INSIG will bind to SCAP, retaining the SREBP/SCAP/INSIG complex in the ER membrane. When sterol levels are low, the SREBP/SCAP complex will dissociate from INSIG and will be moved to the Golgi apparatus in COPII vesicles. Once in the Golgi, SREBP will be cleaved by site 1 and site 2 proteases, forming the mature form of SREBP that will be translocated to the nucleus (n-SREBP). Here, n-SREBP will bind to the sterol response element to induce transcription of its target genes (*ACC1, FASN, LDLR, HMGCR, SCD1*). SREBP: sterol regulatory element binding protein; SCAP: SREBP cleavage activating protein; INSIG: insulin induced gene protein; COPII: coat protein complex II; S1P: site 1 protease; S2P: site 2 protease; n-SREBP: nuclear SREBP; ACC1: acetyl CoA carboxylase 1; FASN: fatty acid synthase; LDLR: low-density lipoprotein receptor; HMGCR: HMG-CoA

reductase; SCD1: stearoyl-CoA desaturase 1. Created with Biorender.com and adapted from Espenshade & Hughes, 2007[129].

1.3.2 Nutrient-Induced Regulation of SREBPs

In contrast to SREBP-1a and -2 which are activated in response to sterols, SREBP-1c may be of more concern since it is regulated by nutrient conditions, and may have many implications in metabolic disorders that are influenced by dietary intake. In cell culture and *in vivo*, it has been established that while carbohydrate meals activate SREBP-1c, glucose does not cause activation of this gene; rather, insulin spikes following glucose consumption is the main inducer of this isoform[107,130–132]. This results in activation of lipogenic pathways, which have also been found to be strongly activated by dietary fructose intake[107]. Studies using rodent primary hepatocytes have shown that SREBP-1c expression is activated by fructose-rich diets[133–135], as fructose can slightly increase plasma insulin concentrations[133,134], although it does not stimulate insulin secretion from the pancreas[136].

Additionally, the type of fatty acids that one consumes may also be important during SREBP-1c activation, as the effects of these potent regulators differ depending on their saturation[107]. Unsaturated fatty acids, such as MUFAs and PUFAs, can inhibit hepatic lipogenesis by their direct action on SREBP-1c and -1a isoforms, which can occur both post-transcriptionally and post-translationally[137,138]. Unsaturated fatty acids can increase RNA decay of SREBP-1, degrade mature n-SREBP-1, or most commonly, inhibit its proteolytic processing[139]. In contrast to SREBP-2, unsaturated fatty acids are less effective than sterols in regard to their inhibitory action[140]. While the action of unsaturated fatty acids on SREBPs are well understood, the mechanisms through which saturated fatty acids may act on this gene are still unclear. While palmitate has been shown to inhibit SREBP cleavage in *Drosophila*[141], there are controversial results in mammals. It was previously shown that SREBP-1c inhibition increases with the degree of FFA unsaturation, with palmitate having no effect[140]; but it was later proven that diets high in saturated fats can increase SREBP-1c expression, along with its target genes[107].

Overall, the effect of individual dietary components on the activation of all SREBPs should be investigated further, both in the context of high and low insulin concentrations to understand its mechanism of action during times of nutrient excess, especially in lean NAFLD.

1.3.3 Selective Insulin Resistance

Although SREBP-1c is dependent on insulin for its activation, it is interesting that it is highly expressed in patients with metabolic syndromes such as T2DM, which is characterized by insulin resistance. While SREBP-1c can act on many different pathways, the activation of this isoform by insulin involves phosphoinositide 3-kinase (PI3K), as well as the mitogen activated protein kinase (MAPK) pathway (**Fig. 1.3.3-1**). Both of these pathways begin with the activation of insulin receptor substrate 1/2 (IRS1/2) and result in the activation of mammalian target of rapamycin complex 1 (mTORC1). Through this increased mTORC1 activation, this can activate ribosomal S6 kinase (S6K), which will act to enhance the proteolytic processing of SREBP-1c[142]. Additionally, mTORC1 activation will cause inhibition of lipin-1, a known inhibitor of SREBP-1c, resulting in enhanced n-SREBP-1c activity as a transcriptional activator[142,143] (**Fig. 1.3.3-1**). Several explanations can be put forth as to how these pathways become dysregulated in pathological conditions, and while it is understood how SREBPs are activated under different nutrient conditions, few studies have investigated the influence of individual nutrient components on these pathways in lean NAFLD specifically, both in the presence and absence of insulin.

In insulin resistant states, it has been theorized that lipogenesis can be driven by insulin-independent pathways[143]. This state has been termed as selective hepatic insulin resistance where insulin fails to suppress gluconeogenesis, while continually activating lipogenesis in situations of hyperinsulinemia[143,144]. In this context, it is thought that SREBP-1c remains sensitive to its activation by insulin[143,144], most likely through its ability to inhibit INSIG (**Fig. 1.3.3-1**). As a result, n-SREBP-1c accumulates and accentuates fatty acid synthesis, causing an accumulation of triglycerides in the liver. Additionally, IRS1/2 is also important in the regulation of carbohydrate and lipid metabolism, and can be phosphorylated under basal conditions by insulin-independent kinases, or in response to lipid and inflammatory mediators that are often elevated in metabolic diseases[145,146]. Although this effect is exacerbated in hyperinsulinemic states, it is suggested that excessive nutrients may also play a role in the activation of IRS1/2 under basal

insulin levels, resulting in activation of the PI3K and MAPK pathways. While common in metabolic diseases, this dysregulation has been attributed to hyperinsulinemia, as well as insulin-independent feedback pathways as lipids can "hijack" the insulin-regulated phosphorylation of IRS1/2[147].

This phenomenon has been studied in liver insulin receptor knock-out mice (LIRKO) and it was found that without insulin, there is no activation of SREBP-1c, resulting in less VLDL secretion and oftentimes, these animals do not present with hypertriglyceridemia[148]. This is similar to insulin resistant states in NAFLD where a marked decrease in VLDL secretion is observed[149]. Although SREBP-1c cannot be maximally activated as when insulin is present, LIRKO mice studies have demonstrated that it can still be activated, as long as there is a sufficient amount of carbohydrates present[116]. Additionally, in mouse livers treated with streptozotocin, an antibiotic that causes mice to be insulin deficient, SREBP-1c and target gene induction still occurred in the presence of excess carbohydrates[115]. This is important to note, especially in the case of the Western diet, as the population is consuming larger amounts of sweetened beverages containing fructose, which may contribute to the induction of SREBPs during selective insulin resistance.

It has also been revealed that following insulin receptor knockdown in *ob/ob* mice models of T2DM, SREBP-1c activation by insulin is prevented[116], suggesting that insulin signaling is more important in the context of obesity. Further, in this condition, SREBP-1c target genes are not induced, thereby lessening the presence of steatosis. While insulin-independent signaling occurs in the context of feeding and can compensate for insulin by SREBP-1c induction, complete activation of this isoform is entirely dependent on insulin and only occurs in obese/T2DM states[116]. These results point to the fact that insulin-independent signaling has a role in the induction of lipogenesis, although to a lesser extent than seen in hyperinsulinemic states.

To better understand the role of insulin-independent or non-hyperinsulinemic signaling on the development of steatotic livers in NAFLD, it will be important to study all SREBP isoforms, along with commonly activated pathways in both obese and lean NAFLD populations. This would be invaluable for the comparison between SREBP mechanisms in early- and end-stage NAFLD.
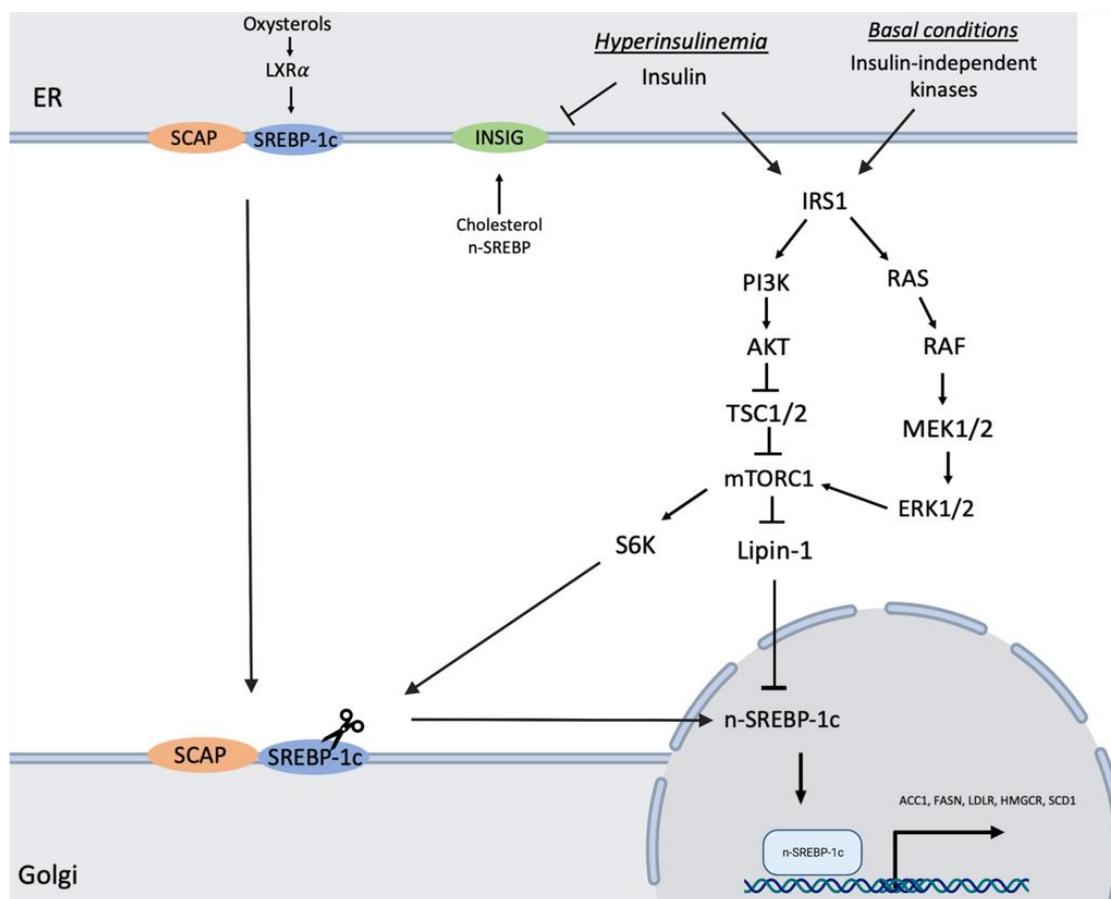
Figure 1.3.3-1. Activation of SREBP-1c and insulin signaling pathways. While SREBP-1c can be activated in response to oxysterol levels through the nuclear receptor LXRα, insulin in hyperinsulinemic conditions can further induce its proteolytic processing. In this context, insulin can cause the phosphorylation of IRS1, which will activate either the PI3K or MAPK pathway. Both pathways eventually lead to increased mTORC1 activation, followed by induction of S6K, which will act to enhance SREBP-1c proteolytic processing. Further, mTORC1 will also inhibit lipin-1 to prevent inhibition of SREBP-1c processing. Under basal conditions, insulin-independent kinases can phosphorylate IRS1, effectively activating insulin signaling pathways and therefore SREBP-1c. Overall, these events lead to increased SREBP-1c activity and target gene expression, causing an increase in lipogenic enzymes. SREBP-1c: sterol regulatory element binding protein 1c; n-SREBP-1c: nuclear SREBP-1c; SCAP: SREBP cleavage activating protein; INSIG: insulin induced gene protein; LXRα: liver X receptor alpha; IRS1: insulin receptor substrate 1; PI3K: phosphoinositide-3-kinase; AKT: protein kinase B; TSC1/2: tuberous sclerosis protein 1/2; mTORC1: mammalian target of rapamycin complex 1; S6K: ribosomal protein S6

kinase; RAS: rat sarcoma virus GTPase; RAF: rapidly accelerated fibrosarcoma kinase; MEK1/2: MAP (mitogen-activated protein) kinase/ERK (extracellular signal-regulated kinase) kinase 1/2; ERK1/2: extracellular signal-regulated kinase. Created with Biorender.com and adapted from Dorotea, Koya, & Ha, 2020[142].

1.3.4 Cholesterol Metabolism

The liver is a major regulator of biological pathways involved in cholesterol metabolism which include cholesterol synthesis, chylomicron uptake, re-uptake from LDL and HDL, release of cholesterol as VLDL, and the production of bile acids[150]. As such, it is important for the liver to regulate plasma cholesterol levels.

In disease states such as NAFLD, the presence of steatosis alone is enough to cause a proatherogenic lipid profile in patients, resulting in the production of proinflammatory markers[151,152]. Emerging evidence has linked alterations in hepatic cholesterol homeostasis and the accumulation of free cholesterol to NAFLD, and to the progression of simple steatosis to NASH[153,154]. In NAFLD animal models, it has been proposed that dysregulation of cholesterol metabolism can contribute to NAFLD[155], and in humans, that NAFLD causes impaired cholesterol metabolism[156]. Additionally, excessive hepatic fat accumulation has been shown to contribute to increased circulating cholesterol levels[157], which tends to precede weight gain and the development of additional metabolic complications[158,159]. Since triglyceride and cholesterol metabolic pathways are tightly linked through SREBPs, it is not surprising that disturbances in liver lipid metabolism play an active role in hypercholesterolemia and increased intracellular cholesterol levels. Therefore, it is important to identify how this may play a role in the pathogenesis of lean NAFLD.

Since cholesterol is an important precursor of bioactive substances and a necessary component of cell membranes, it is of utmost importance that cellular cholesterol levels are maintained in all cell types. Cholesterol homeostasis is dependent on the balance between cholesterol synthesis, elimination, absorption, and storage[154]. Crucial to this process is the LDL receptor (LDLR) as it regulates cholesterol at the cellular level. The LDLR has an intracellular feedback regulation system that senses changes in the levels of LDL cholesterol and its derivatives. Through this system, LDLR can regulate levels of cholesterol uptake, effectively

protecting cells from excessive intracellular cholesterol accumulation[153]. In this way, intra- and extracellular cholesterol are used appropriately to balance cellular and systemic cholesterol levels[154].

The LDLR is also tightly regulated through signaling pathways at the transcriptional and post-transcriptional level. Its expression can be regulated by many different factors which include glucose and its metabolites, cholesterol and its derivatives, inflammatory mediators, hormones, and growth factors[160,161]. The major regulators of LDLR gene transcription are SREBPs[154], with SREBP-2 being the most potent activator of genes involved in cholesterol metabolism[124,162]; however, SREBP-1a also has the ability to activate transcription of LDLR, which becomes activated through the mechanism previously described in response to changing concentrations of intracellular cholesterol (**Fig. 1.3.1-1**). In disease states, cholesterol homeostasis along with LDLR transcription is disturbed[124,160], and it is thought that this can cause lipid-mediated organ damage.

In regard to NAFLD, disrupted hepatic cholesterol homeostasis paired with free cholesterol accumulation is linked to its pathogenesis[154]. Cholesterol has been found to alter the redox status of cells by increasing hepatic reactive oxygen species (ROS) while causing progressive liver damage[28,149]. Recent findings have also shown that patients with insulin resistance have reduced cholesterol absorption, but display an elevation in cholesterol synthesis[163,164]. In chronic inflammatory states, which is commonly observed in NAFLD, inflammatory factors such as Tumor Necrosis Factor α (TNFα) can act to upregulate the LDLR, causing the inappropriate intake of cholesterol into cells[165]. The redistribution of cholesterol from the blood to the tissues, such as the liver, contributes to excessive lipid deposition and further organ damage[154]. Additionally, in NAFLD patients experiencing chronic inflammation, it has been reported that inflammatory cytokines can cause resistance to statins[166] – a class of drugs that help to lower plasma cholesterol levels. While NAFLD patients prescribed statins have shown improved levels of LDL cholesterol, the expression of the receptor remains elevated and is comparable to NAFLD subjects who are not taking these drugs[154]. As such, the dysregulation of the LDLR pathway may be an important factor in the pathogenesis of all forms of NAFLD, especially when coupled with excessive lipid accumulation.

1.3.5 Lipid Droplets

Lipid droplets are dynamic structures found in many cell types that act as energy reservoirs and store lipids in times of energy excess[167]. These organelles consist of a neutral lipid core containing triglycerides and cholesterol esters that are surrounded by a phospholipid monolayer[167,168]. This monolayer is made up of free cholesterol and bound proteins[169], such as perilipins, that aid in lipid droplet structure and formation.

Across cell types, the amount and size of lipid droplets differ. Although they are most abundantly found in white adipose tissue, the liver also possesses a large capacity to store triglycerides in lipid droplets[41]. The lipid core of these droplets differ between hepatic cell types, but in hepatocytes specifically, these cores tend to be enriched with triglycerides[41] – the most abundant neutral lipid in hepatic steatosis[167].

The prominent family of proteins that coat lipid droplets are known as perilipins. In mammals, there are 5 perilipin proteins (perilipins 1–5), and each seem to differ in their function and localization. Perilipins 1, 4, and 5 are more limited in their tissue expression, while perilipins 2 and 3 are ubiquitously expressed[170]. Some perilipins, like perilipin 1 and 2, usually only associate with lipid droplets, however, perilipins 3–5 show no preference in regard to cytoplasmic localization or lipid droplet association as they are stable in both conditions[170]. Additionally, the perilipin 1A isoform, along with perilipins 2 and 5, have a preference for lipid droplet cores enriched with triacylglycerols, which contrast perilipin 4, 1C and 1D isoforms that associate with cholesterol-ester filled lipid droplets[171].

There is currently little understanding between the biology of lipid droplets and how they contribute to NAFLD pathogenesis. As increases in lipogenesis, impaired mitochondrial fatty acid oxidation, and inhibited triglyceride secretion are known to contribute to hepatic steatosis, collectively, these processes exert effects on lipid droplet accumulation in hepatocytes[168], resulting in an increase in perilipin proteins.

The perilipins are the predominant family of lipid droplet proteins found in the liver[41], with perilipin 2 (PLIN2) associating with lipid droplets in hepatocytes and exhibiting the highest expression levels in the liver compared to other perilipin proteins[172,173]. Perilipin 2 is the best-characterized protein in fatty liver diseases, as PLIN2 levels are typically increased during fat

accumulation[169]. Several studies have also found PLIN2 levels to be directly proportional to intracellular lipid levels[174,175]. Interestingly, PLIN2 has been implicated in NAFLD as it has been found to be the highest expressed perilipin protein in the livers of rodent NAFLD models[176], as well as in human NAFLD patients[172]. This protein can also act to promote triglyceride accumulation and inhibit fatty acid oxidation[177,178], and has been correlated with hepatocyte ballooning in NASH through the presence of oxidative stress[179].

The consequence of increased PLIN2 expression in hepatocytes is the intracellular accumulation of lipid droplets that favour adipogenesis[173]. In situations of nutrient excess, it has been suggested that PLIN2 expression is greatly influenced by high fat diets. Mice deficient in PLIN2 displayed a 60% decrease in hepatic triglyceride content and were resistant to diet-induced fatty liver[180], while also being protected from diet-induced obesity[181]. Further, PLIN2 antisense oligonucleotide in both *ob/ob* and diet-induced obese mice resulted in decreased liver steatosis[178]. Together, these results indicate that PLIN2 is important in the development of diet-induced liver steatosis[169]. Additionally, other studies found that knock-outs of PLIN2 could promote VLDL secretion from mice livers[177,182], while those over-expressing PLIN2 in rat hepatocytes demonstrated a decrease in VLDL production and secretion[177], demonstrating the role of PLIN2 in this process. Collectively, the imbalance between lipid droplet production and the secretion of VLDL, aided by PLIN2, may be a contributing factor in the development of steatosis[149,183].

The accumulation of lipid droplets has been associated with detrimental cellular effects such as insulin resistance, mitochondrial dysfunction, and inflammation[184] – all of which are implicated in NAFLD. Specifically, PLIN2 has inflammatory effects, as its expression is increased in states of chronic inflammation, such as foam cell and atherosclerotic plaques[185], non-alcoholic steatotic livers[186], and various cancers. Interestingly, in PLIN2-knockout Western diet-induced obese mice, these animals were unable to improve their insulin resistance and inflammation[181]. Other studies have shown that while ablation of PLIN2 improves steatotic livers in mice, there is still an upregulation of fibrotic genes[187]. This suggests that PLIN2 may be protective and has multiple roles in the progression of NAFLD. This is supported by a study done by Nocetti et al., where they observed higher levels of lipid peroxidation products within the cores of PLIN2-coated lipid droplets of isolated hepatocytes from obese mice[173]. The authors

theorized that while PLIN2 favours accumulation of triacylglycerols and cholesterol esters within the lipid droplets, this action is protective to avoid damage associated with ROS from lipid peroxidation products[173]. However, this protective function could cause the sequestration of unwanted or harmful lipids in cells previously oxidized by other cellular compartments[188].

While the action of PLIN2 may be protective in the context of NAFLD, overall, this results in the accumulation of intracellular lipids, which ultimately contributes to lipotoxicity along with increased ROS and lipid intermediates that can activate signaling cascades involved in hepatic inflammation[173]. Perhaps the action of PLIN2 is like a double-edged sword in that it can protect cells from lipotoxicity to a certain extent, but enhances complications of NAFLD in the process, and may contribute to disease progression. While the effects of PLIN2 in the context of fatty liver diseases have been well-studied in obese animal models, it will be important for future studies to discern the role of PLIN2 in lean NAFLD.

1.3.6 Sources of Reactive Oxygen Species

Oxidative stress occurs when there is an imbalance between the production of reactive oxygen species (ROS) and the ability of cellular antioxidant systems to detoxify these products. It has been recognized that oxidative stress is a central factor involved in the pathogenesis of NAFLD[189], as ROS play an important role in hepatic metabolism[149]; although the underlying mechanisms behind this phenomenon are not clearly understood. In line with the "multiple parallel-hit model" of NAFLD progression, oxidative stress is believed to prime the liver for injury by leading to cellular dysfunction, and is likely the source of hepatic and extrahepatic damage seen in NAFLD[44,149]. In situations of hepatic lipid and carbohydrate overload, lipotoxicity and glucotoxicity can facilitate the overproduction of free radicals, leading to the modification and harmful accumulation of damaged macromolecules in the cell (*i.e.,* DNA, lipids, proteins), resulting in liver injury[42]. The increased production of ROS observed in NAFLD may be a maladaptive response that results in metabolic dysfunction[42,190].

Reactive oxygen species are produced through a sequence of enzymatic and non-enzymatic reactions, and are categorized as free radicals (superoxide, hydroxy radical, nitric oxide, etc.) and non-radicals (hydrogen peroxide, hypochlorous acid, peroxynitrite). Under physiological conditions, ROS concentrations are maintained as they act as signaling molecules

involved in processes such as metabolism, proliferation, cell survival, and differentiation[42]. In various diseases, oftentimes ROS levels begin to accumulate, which can trigger pathological redox signaling and lead to cellular damage[42]. While it is difficult to determine ROS species within the cell, it is not uncommon to find that these ROS are derived from organelles such as the mitochondria, endoplasmic reticulum (ER), or peroxisomes. Additionally, there are non-organelle cytoplasmic sources of ROS that are generated by enzymes such as NADPH oxidases, which can directly catalyze the generation of superoxide or hydrogen peroxide (H_2O_2)[42,191]. While there are many sources of ROS within the cell, mitochondrial and ER sources of ROS will be discussed, as abnormalities in these cellular compartments have been implicated in NAFLD pathogenesis and are the main mechanisms behind the oxidative stress-induced damage to liver structure and hepatic functioning[189].

Mitochondria are known as the major site of fatty acid β-oxidation in cells and have been stated as the most important ROS generators in NAFLD[192–195]. In the presence of increased FFAs and lipid overload, or lipotoxicity, this can cause increases in ROS production with a concomitant decrease in antioxidant systems, as FFAs have been shown to produce significant quantities of ROS in the liver[196]. Mitochondrial function is effected by ROS production which causes deterioration of the electron transport chain (ETC) followed by electron leakage[42,189], as FFAs can interact with the ETC and either increase or decrease superoxide production[197]. Additionally, FFAs can increase membrane fluidity by incorporating into the inner mitochondrial membrane, further promoting electron leakage[198].

During early stages of hepatic fat accumulation in NAFLD, the mitochondria trigger several adaptive mechanisms to prevent oxidative stress and further ROS production[44,199]. One of these compensatory mechanisms is an increase in mitochondrial activity in order to catabolize lipids to prevent from the harmful effects of lipid storage[194]. This early stimulation of β-oxidation reflects the livers attempt to avoid fat accumulation[195]. It has also been proposed that these mechanisms are in place to prevent further oxidative stress and ROS production by separating lipotoxic FFAs into stable triglyceride stores[44,199].

While mitochondria greatly contribute to ROS in the liver, they are not the only source in NAFLD. The ER and oxidative stress have been linked in the progression of NAFLD and are

related to many pathophysiological changes, such as lipogenesis, insulin resistance, and inflammation in animal models of NAFLD and human NAFLD/NASH patients[200,201]. The ER is a potent source of ROS, and maintaining ER homeostasis is important for its proper functioning, as alterations in its production and clearance of H_2O_2 can induce ER stress and exacerbate metabolic dysfunction[200]. Additionally, all ER stress-sensing pathways have been shown to regulate the development of microvesicular steatosis in the liver[202].

In regard to diet, saturated fatty acids (SFAs) have been shown to exhibit a more damaging effect on hepatocytes and the liver as they can disrupt ER homeostasis, which activates the unfolded protein response (UPR) and proinflammatory pathways[44,203], ultimately leading to cell death. ER stress is a mechanism involved in lipotoxicity[204], and under these conditions, misfolded and unfolded proteins begin to accumulate in the ER lumen, activating the UPR in an attempt to restore ER homeostasis[201]. A direct role of lipids in the ER stress response has been supported as lipid saturation of the ER membrane was found to activate the UPR independently of unfolded or misfolded proteins[205]. Additionally, the UPR has been shown to be activated in human NAFLD livers to varying degrees[206], and if prolonged, this response can trigger apoptotic pathways.

Glucotoxicity, along with lipotoxicity, can also contribute to oxidative stress in the context of NAFLD. While lipotoxicity is associated with the harmful effects of increased lipids and lipid derivatives in cells, glucotoxicity is associated with insulin resistance, and is the manifestation of hyperglycemia and the effects of excess carbohydrate intake on cells and tissues[204]. Not only can carbohydrates be converted into triglycerides and FFAs, but they can also form and accumulate hepatotoxic lipids such as ceramides, lysophosphatidyl choline, bile acids, and free cholesterol[204]. Through the induction of ER stress and cell death, glucotoxicity can be injurious to hepatocytes and can alter insulin secretion and action as a result of ROS production[204].

Both glucose and fructose can contribute to oxidative stress in the development of NAFLD and its metabolic comorbidities, such as T2DM. In mice fed a high-glucose diet for 4 weeks, hepatic oxidative stress was induced as a result of increased hepatic FFA accumulation and insulin resistance[207]. Additionally, high fructose diets displayed increases in SFA content

and gluconeogenesis, leading to steatosis[208]; and when combined with a high-fat diet, fructose enhanced liver injury and caused fibrosis, inflammation, ER stress, and apoptosis[204]. This fructose-induced activation of ER stress has also been linked to the activation of SREBP-1c[135,209], with glucose amplifying the effects of FFA-induced ER stress[210]. Overall, the excessive intake of carbohydrates leads to toxic effects within cells that ultimately induces liver toxicity[204]. Closely related to insulin resistance and dysregulated redox signaling, the resultant oxidative stress, ER stress, and inflammation from excessive carbohydrate intake harbours a toxic environment for the liver, culminating in cellular demise.

There has also been evidence of cross-talk between the ER and mitochondria during oxidative stress. As the main site of calcium storage and homeostasis, the ER lumen can be disrupted by SFAs, ultimately effecting calcium stores[44]. This causes calcium leakage from the ER, which can act on mitochondrial membranes through the formation of mitochondrial permeability transition pores[42,44]. This effectively blocks the ETC, causes calcium build up in the mitochondria and release of cytochrome c, culminating in increased ROS production, induction of metabolic disorders, and apoptosis[211–214]. Additionally, when the UPR is activated, cells will increasingly produce ATP-requiring chaperone proteins in order to correctly fold the misfolded proteins[42]. Through the continual activation of this response in NAFLD – a response triggered by the lipotoxic-induced accumulation of misfolded proteins in the ER lumen – increased strain is placed on the mitochondria, which may already be dysfunctional. This can form a vicious cycle that will continue to promote oxidative stress during NAFLD progression. While the sources of ROS in NAFLD are understood, the direct mechanisms of these pathways and how their dysregulation varies depending on disease stage and severity should be studied. Additionally, further research on the role of ROS in all NAFLD populations is warranted as research is currently limited to obese populations.

Overall, the WD is a harmful dietary pattern that can lead to a milieu of metabolic abnormalities, with the excessive consumption of its nutrient components greatly effecting their metabolism within the liver. Through the dysregulation of hepatic lipid and carbohydrate metabolism, this diet is the principal factor contributing to NAFLD progression. Although satisfying, it is evident that this dietary pattern is harmful to metabolic health as it can alter signaling pathways involved in fatty acid and cholesterol synthesis, insulin signaling, and lipid

droplet formation. Additionally, the components of this diet can induce changes in cellular redox signaling, which can contribute to cellular and tissue damage, exacerbating NAFLD progression. Even more alarming is that this disease can go unnoticed for years, and is increasingly being recognized in the lean population. As such, it is important that the whole population is made aware of, and educated on, the deleterious and damaging effects of this diet, regardless of BMI status.

1.4   Rationale, Hypothesis, and Objectives

1.4.1 Rationale

The Western lifestyle, characterized by sedentary behaviour and chronic overeating of harmful nutrients, has contributed to the development of civilization diseases and metabolic dysfunction[1,4,5]. This is inevitable given the association of WD consumption with an increased risk of metabolic diseases such as NAFLD[1], which is now considered as the primary outcome leading to MetS, as well as hyperinsulinemia and T2DM, and eventually cardiovascular diseases[74]. Due to the abundance of SFAs and refined sugars in this diet, these nutrient components effectively dysregulate metabolic processes and cellular signaling pathways, culminating in tissue damage[215–217]. As the central hub of metabolic processes, the liver is especially susceptible to the detrimental effects associated with the habitual consumption of this diet; as not only total caloric intake, but specific nutrient intake, can dysregulate metabolism and lead to the development of NAFLD[25]. While this disease is prevalent in the obese population, adherence to this dietary pattern is becoming increasingly concerning in the lean NAFLD population given that these individuals may present with a metabolic milieu worse than their obese counterparts[76,77,218].

Research has been heavily focused on investigating the impact of the WD on the obese NAFLD population. There has been increasing awareness of the "metabolically healthy" and "metabolically unhealthy" obese patient, classified by the presence or absence of additional metabolic abnormalities such as hypertension, hypertriglyceridemia, or impaired glucose tolerance[23]. This led to the recognition of the "metabolically unhealthy lean" cohort, where it was identified that NAFLD was present in individuals who were classified as non-obese according to their BMI[219]. Since NAFLD has been heavily associated with the WD and obesity, this disease is

currently under-recognized and is often undetected in the lean population[76,219]. This leaves a major gap in the research field as an estimated 6–20% of NAFLD cases fall into the lean category[75], with an even higher prevalence of 40% reported in Western civilizations[67]. This is concerning considering these patients are at an increased risk of developing metabolic comorbidities compared to their obese counterparts[75–82,89]. Since NAFLD is a multi-faceted disease, it is important to study the effects of harmful lifestyles, such as the WD, on both obese and lean NAFLD phenotypes to understand the underlying mechanisms contributing to this disease, as the pathogenic mechanisms of lean NAFLD are poorly understood[74].

Nutrition has been stated as the principal factor governing NAFLD pathogenesis, and evidence points to different dietary components acting to initiate or cause progression of the disease[42]. While it is understood that excessive nutrient intake is detrimental to metabolic health, in the lean population, this may not be the main concern as a healthy daily energy balance is maintained without weight gain. Rather, the emphasis should be placed on the quality of macronutrients consumed[5]. Many convenience foods are rich in oleic and palmitic acid[12], the most abundant fatty acids in the WD[204], along with refined sugars such as glucose and fructose. These nutrients are known to overload hepatic lipid and glucose metabolism, culminating in the production of ROS, inflammation, and organ damage[1]. A major limitation to previous studies is that the majority have investigated the effects of these nutrients in isolation[12]. While it is important to understand how these nutrients act alone, it is equally important to identify how these nutrients work in tandem to alter metabolic signaling, as they would in processed foods.

In the liver specifically, the increased intake of both FFAs and sugars can contribute to the development of steatosis through different mechanisms. Additionally, hepatic lipid levels remain stable after longer periods of treatment[150], therefore it is essential to determine how initial spikes in lipid accumulation trigger changes within cells to recognize warning signs of the disease. While these are heavily studied in the obese phenotype, how each nutrient component, alone and combined, can lead to disease progression in an otherwise healthy individual may illuminate the mechanisms behind early stages of steatosis development before other metabolic abnormalities may complicate the disease. This approach is important for identifying the root cause of diet-induced steatosis in the beginning phases of NAFLD, before additional abnormalities arise, which is more relevant to the lean population.

Prior to weight gain, the WD can lead to the development of insulin resistance due to its propensity to cause hyperinsulinemia and oxidative stress[1]. Many animal models of obese NAFLD have focused on SREBP-1c and insulin signaling as major players in NAFLD pathogenesis; however, less is known about SREBP gene activation and their corresponding pathways in lean NAFLD, especially in response to diet. In line with excessive nutrient intake, all SREBP isoforms exhibit nutrient-induced regulation and often display changes in their expression levels in animal models and human livers with NAFLD[117–121,137–141]. Specifically, SREBP-1c relies on insulin for its maximal activation. However, in pathological conditions such as obesity, and in the presence of a continual post-prandial state, individuals often present with hyperinsulinemia, leading to selective insulin resistance in the liver. In this case, complete induction of SREBP-1c by insulin and insulin signaling has been shown to be more important in the context of obesity[116]. However, in the absence of insulin as in LIRKO mice, SREBP-1c can still be activated as long as sufficient carbohydrates are provided and will activate lipogenic pathways[115]. Collectively, this reveals that under basal insulin levels, insulin signaling may play a dual role in the development of steatosis in NAFLD, and these effects may be more important when studying the lean population where elevated insulin levels may not be present, since most lean NAFLD cases are incidentally detected as they are often asymptomatic[78]. Additionally, all SREBP isoforms should be investigated in the case of nutrient excess under physiological insulin levels to identify the underlying signaling mechanisms in early stages of NAFLD pathogenesis.

Few culture models recapitulate the environment of obese[220] and lean patients. However, majority of cell models are often used for studying the molecular mechanisms involved in NAFLD progression[221]. As such, cell culture models are invaluable for the study of early stages of NAFLD, characterized by the presence of steatosis with the accumulation of triglycerides and no inflammation[72,221,222], which is a hallmark of progression to NASH. Investigating the molecular mechanisms driving early steatosis development may be more applicable to the lean population as hepatic lipid accumulation is an early indicator of metabolic dysfunction[66], and these patients do not present with any abnormalities or symptoms in early stages of this disease[77]. While critical for the lean population, understanding the mechanisms of steatosis development in cell culture is also applicable to all NAFLD subjects as this stage is the initiating factor of the disease in all cases. Further, later stages of NAFLD, such as fibrosis and cirrhosis, seem to develop at slower rates with smaller groups of patients progressing to these stages[221]. Therefore,

investigating steatotic mechanisms may be helpful for identifying the disease before further progression and damage occurs to metabolic health.

Taken together, this study is aimed at identifying the WD-induced signaling pathways and mechanisms governing the early stages of NAFLD as a way to explain mechanisms of action in lean subjects. By discerning the effect of individual nutrient components alone and combined on hepatocytes, the goal of this work is to provide insight on the importance of nutrient quality vs. quantity in the case of early NAFLD and steatosis development. Additionally, both *in vivo* and *in vitro* models are currently lacking in regard to the lean phenotype, and the development of lean NAFLD models is imperative to clarify its pathophysiology[223]. While models have exclusively focused on the obese phenotype, this work uses a human hepatoma-derived cell line (HepG2) which is appropriate to identify the direct effects of nutrient components on liver cells, in the absence of other metabolic comorbidities that often complicate obesity. This includes elevated levels of circulating cytokines, such as interleukin 6 and TNFα that have been shown to be significantly elevated in obese subjects compared to lean controls[224]; and these cytokines were correlated with increased waist circumference and fat mass, as well as decreased pancreatic β-cell function, systemic insulin resistance, and cardiometabolic risk factors[224]. Further, HepG2 cells display unlimited growth potential and maintain a stable phenotype throughout culture time[225]. They are also the most commonly used cell line in hepatotoxicity studies and express many differentiated hepatic functions that are investigated in this study, specifically cholesterol and triglyceride metabolism, and insulin signaling[226].

Given the minimal literature on the mechanisms driving lean NAFLD progression, this preliminary work will provide insight on the role of excessive nutrient intake on NAFLD pathways under basal insulin conditions, which may be more applicable to the lean population, and will provide a snapshot of metabolic dysfunction in the early stages of this disease before metabolic comorbidities arise.

1.4.2 Hypothesis

It is postulated that with exposure to Western diet-like media, HepG2 cells will exhibit steatosis, resulting in a NAFLD phenotype. Moreover, I hypothesize that different nutrient

components in the Western diet will impact SREBP and insulin signaling pathways, lipid processing genes, and cause nutrient-induced changes in reactive oxygen species.

1.4.3 Objectives

The objectives of this work are as follows:

1. To establish an *in vitro* model of non-alcoholic fatty liver disease.

2. To identify the signaling pathways and mechanisms of NAFLD in response to different nutrients under basal insulin levels.

3. To characterize the nutrient-induced effects on reactive oxygen species in early NAFLD.

Chapter 2: Materials and Methods

2.1 Cell Culture

2.1.1 Cell Culture Conditions and Treatments

Human hepatocellular carcinoma cells (HepG2; ATCC HB 8065), a gift from Dr. Nica Borradaile, were cultured in Eagle's Minimal Essential Media (Lonza #12-622F) and supplemented with 10% fetal bovine serum (FBS; Gibco #16141079), 0.125 µg/mL fungizone (Gibco #15290-018), 20 U/mL penicillin and 20 µg/mL streptomycin (Gibco #15140-122), and incubated at 37°C and 5% CO_2. Culture media was replaced every 2 days, and cells were seeded and grown for 3 days prior to treatment and use in each experiment. The passage number of cells ranged from 20–29 passages.

To induce steatosis, cells were treated with a 1 mM mixture of palmitic (Sigma P5585) and oleic (Sigma O1383) acid (PA/OA, 1:1 ratio) – the most abundant free fatty acids (FFAs) in the WD[227]. This concentration was used as it has been reported that regardless of BMI, 1 mM is the peak concentration of FFAs in circulation[228]. These fatty acids were supplemented with growth media and conjugated to fatty acid free bovine serum albumin (BSA; BioShop A6003) in a 2:1 molar ratio as previously described[28,229–231]. This concentration was used to reflect circulating levels of fatty acids found in NAFLD patients[232,233]; however, lipidomic analyses are limited to obese patients[28,29]. Therefore, a 1:1 ratio of PA:OA was used to reflect early NAFLD, as lipotoxic ratios used in previous cell culture models use higher ratios of PA:OA (2:3)[230–232].

Growth media was also supplemented with D-Glucose (Bioshop GLU501.500) at a concentration of 12.5 mM, as Diabetes Canada defines hyperglycemia as blood sugar levels ≥ 11 mmol/L. Of note, EMEM contains 5.5 mM of glucose, which was accounted for when creating the glucose-supplemented and WD media. Additionally, media was supplemented with 15 mM D-Fructose (Sigma F3510-100G) as this concentration has been previously shown to cause changes in lipid accumulation and gene expression[234]. Serum levels of fructose have also been reported to reach 17.2 mM after ingestion of sweetened beverages, like soft drinks, that contain both glucose and fructose[235]. To mimic a WD, a combination of each treatment described above was supplemented into culture media (1 mM PA/OA + 12.5 mM glucose + 15 mM fructose). Fatty acid free BSA was added to each treatment media, including the control. The control media

consisted of EMEM, BSA, and NaOH + cell culture grade water (negative control), which was used to dissolve the FFAs. This negative control was also present in both glucose- and fructose-supplemented media.

All treatments were warmed in a 37°C water bath for 30 minutes prior to treatment. Cells were exposed to each treatment for 6 hours as this duration of treatment with fatty acids has been reported to cause steatosis in HepG2 cells as previously described[231,236], and for analysis of early-stage NAFLD. Additionally, cells need at least 4 hours to store excess calories as fat, which then reaches a peak at 8 hours. As such, the 6 hour treatment regimen was chosen as the intermediate or early NAFLD time point.

2.2   Quantification and Visualization of Lipids

2.2.1 Nile Red Staining and Fluorescence Microscopy

A Nile Red Staining Kit (ab228553) was used to measure steatosis, however, this data was not used in this study (see **Appendix A**). Oil Red O was the selected method of lipid droplet quantification as it has been reported that Nile Red tends to non-specifically label cellular lipid organelles, such as intracellular membranes[237], whereas Oil Red O is more specific to neutral lipid droplet staining.

2.2.2 Oil Red O Staining

Cells were plated in 24-well culture dishes at a density of 75,000 cells and reached approximately 80% confluency. Following treatment, cells were washed 3 times with PBS and fixed with 4% paraformaldehyde (0.25 mL) for 30 minutes, followed by 3 more PBS washes. Oil Red O working solution (60%) was made by adding 3 mL Oil Red O Stock solution (0.5% in isopropanol; Sigma-Aldrich O1391) to 2 mL of PBS and filter sterilized on the day of use[237]. Oil Red O working solution was added to each well (0.25 mL) for 10 minutes, followed by 3 PBS washes, after which the cells were viewed and imaged under a phase contrast microscope (Leica EC3 Camera 2.4). To extract neutral lipids, 4% Nonidet P-40 extraction solution (IGEPAL; Sigma-Aldrich I3021) was used and prepared by adding 2 mL of Nonidet P-40 to 48 mL of isopropanol. This solution was then added to each well for 30 minutes, and later transferred to a

96-well plate where the optical density was measured at 520 nm using the GloMax®-Multi Detection System (Promega).

2.2.3 Lipid Mass and Triglyceride Extraction

Cells were seeded on 6-well plates at 750,000 cells/well and grew for 3 days prior to treatment. Following treatment, cells were washed twice with 2 mL/well of PBS with 0.2 g BSA per 100 mL. This was followed by 3 washes with 2 mL/well of PBS, excluding the BSA. Lipids were then extracted by adding 1 mL/well of a 3:2 (v:v) hexane:isopropanol solvent mixture and incubated for 30 minutes as previously described[231]. To extract proteins, 2 mL/well of 0.1 N NaOH was added to each well for 2 hours, and then incubated for 24 hours at room temperature. Prior to aliquoting the experimental triglyceride samples into 96-well plates, the samples were diluted by adding $CHCl_3$ and $CHCl_3$/1% Triton X-100 to glass tubes, vortexed, and left overnight. These were then evaporated until dry under nitrogen, followed by the addition of 500 µL deionized water. Tubes were vortexed and incubated at 37°C for 15 minutes in a water bath.

The triglyceride assay was performed using WAKO Diagnostics Triglyceride Reagent (#996-02895 and 992-02995). Fifty microlitre (µL) samples were assayed in duplicate using a dilution of 50 µL + 75 µL H_2O/Triton X-100. The first triglyceride reagent (75 µL) was added to all wells and plates were tapped to mix and incubated for 10 minutes. This was repeated with the second reagent (75 µL) and was incubated for an additional 50 minutes at room temperature prior to reading on the GloMax®-Multi Detection System (Promega) at 505 and 700 nm. These values were subtracted and normalized to cell protein levels.

2.3   Gene Expression

2.3.1 Quantitative Reverse Transcription Polymerase Chain Reaction (qRT-PCR)

Cells were grown on 60 mm dishes for 3 days to 80% confluency where they were treated for 6 hours with each media, followed by total RNA isolation and collection using the RNeasy Mini Kit (Qiagen 74104). Following collection, RNA quality was determined using a Nanodrop to ensure the 260/280 ratio fell between 1.8–2.0. RNA integrity was also confirmed by running the samples on a gel to visualize the 5.8S, 18S, and 28S bands. Samples were then reverse transcribed into first strand cDNA using the Applied Biosystems High Capacity cDNA Reverse Transcription Kit (Thermo Fisher Scientific) following the manufacturer's instructions. Primers

were designed for the following genes: *ACACA, ACACB, SCD1, G6PD, TNFα, ACSL5, ACADVL, CREB3L3, PLIN2, ACTB, PSMB6*; while others were drawn from previous studies: *SREBP-1a*[238], *SREBP-1c*[238], *SREBP-2*[239], *FASN*[240], *LDLR*[241], *HMGCR*[242], *LXRα*[243], *IRS1*[244], *PI3K*[245], *KRAS*[246], *RPLP0*[247] (**Table 2.3.1-1**). Temperature optimization and primer efficiency were performed for each primer set, and primers with efficiencies of 90–110% were used[248].

Each reaction was carried out using 400 nM of forward and reverse primer, 8 µL SensiFAST™ SYBR No-ROX Kit (Meridian Bioscience, BIO-98005), and 6 µL of 1:20 cDNA template. The CFX Connect Real-Time PCR Detection System (Bio-Rad Laboratories) was used to analyze and perform the qRT-PCR reactions. Analysis of gene expression was conducted using the comparative Cq method ($[1+ \text{primer efficiency}/100]^{-\Delta Cq}$) to calculate the relative expression of each gene[249]. The relative quantities were then normalized to three constitutively active genes (*RPLP0, ACTB, PSMB6*) using the geometric mean[250]. Expression of these three genes did not vary between the different treatments (see **Appendix B**).

Table 2.3.1-1. List of primers with primer sequences, melting temperatures, efficiencies, and R^2 values used in this study.

Gene	Forward Primer (5'–3')	Reverse Primer (5'–3')	Tm (°C)	Efficiency (%)	R^2
RPLP0	CCCATTCTATCATCAACGGGTACAA	CAGCAAGTGGGAAGGTGTAATCC	56	99.4	0.99
ACTB	GTTGCTATCCAGGCTGTGCT	AGGTAGTCAGTCAGGTCCCG	60	92.7	0.99
PSMB6	CGGGAAGACCTGATGGCGGGA	TCCCGGAGCCTCCAATGGCAAA	60	106.5	0.99
SREBP-1a	CATCGACTACATTCGCTTTCTG	CAGATCCTTCAGAGATTTGCTTT	56	97.5	0.98
SREBP-1c	TGGATTGCACTTTCGAAGACAT	CAGCATAGGGTGGGTCAAATAG	59	98.5	0.99
SREBP-2	GCTGCAACAACAGACGGTAATG	CTGGTATATCAAAGGCTGCTGGAT	56	97.5	0.99
FASN	AAGGACCTGTCTAGGTTTGATGC	CTGGTATATCAAAGGCTGCTGGAT	55	103.1	0.99
ACACA	GATGTGGATGATGGGCTACA	TGAGGCCTTGATCATTACTGG	60	101.7	0.98
LDLR	AGGACGGCTACAGCTACCC	CTCCAGGCAGATGTTCACG	55	99.9	0.99
HMGCR	ATAACACGATGCATAGCCATCCTG	AAAATTGTGAAAAGGCCAGCAATAC	60	99.4	0.99
LXRα	CGCACTACATCTGCCACAGT	TCAGGCGGATCTGTTCTTCT	55	95.2	0.98
IRS1	TATGCCAGCATCAGTTTCCA	TTGCTGAGGTCATTTAGGTCTT	55	95.9	0.99
SCD1	CTTGCTGCAGGACGATATCTCTA	TTCCAAGTAGAGGGGCATCG	61.2	103	0.99
PI3K	AACGAGAACGTGTGCCATTTG	AGAGATTGGCATGCTGTCGAA	55	106.1	0.99
KRAS	TTGACGATACAGCTAATTCAGAATCA	CCTGCTGTGTCGAGAATATCCA	55	99.8	0.99
G6PD	CTACCGCATCGACCACTACC	CCTGTTGGCAAATCTCAGCAC	58	109.4	1.00
TNFα	CTGCTGCCACTGGAACCTAC	TTCTGAAGCGGTGAAGGAGC	59	106.7	0.98
ACSL5	CACCCCAAAAGGCATTGGTG	AGGTCTTCTGGGCTAGGAGG	60	104.5	0.99
ACADVL	CAGGTGTTCCCATACCCGTC	GGGATCGTTCACTTCCTCGAA	60	101.7	0.99
CREB3L3	TTTTGGCCCCAACAAAACCG	GCAGCATCGTTGTGCAAAGT	60	96.4	0.99
PLIN2	ACCTCTCATGGGTAGAGTGGAA	CACCTTGGATGTTGGACAGG	60	96.5	0.99
ACACB	ATTGCCAACAACGGGATTGC	GGGACGTAATGATCCGCCAT	60	101.8	0.99

2.4   Cellular Activity

2.4.1 MTT Assay

Cells were seeded in 96-well plates at 60,000 cells/well and grown for 3 days prior to treatment. Following 6 hours of treatment, cells were incubated with MTT (3-(4,5-dimethylthiazol-2-yl)-2,5-diphenyl-2H-tetrazolium bromide) reagent (2.5 µg/ml; Sigma) for 4 hours at 37°C and 5% CO_2. The MTT was aspirated, and dimethyl sulfoxide (DMSO) was added to each well to solubilize the formazan crystals. Plates were then incubated in the dark at room temperature and placed on a shaker overnight. Absorbance was measured at 560 nm and 750 nm (reference wavelength) using the GloMax®-Multi Detection System (Promega), and these values were subtracted to calculate the difference in optical density (ΔOD) to determine the activity of the cells. These values were then normalized to cell number (cells/mL)[252]. Cells were counted using the DeNovix CellDrop Brightfield Cell Counter, with each treatment plated in duplicate and each well was counted 3 times.

2.5   Reactive Oxygen Species (ROS) Detection

2.5.1 DCFDA Assay and MitoSox™

Total ROS levels were measured using a 2'7'-dicholorfluorescin diacetate (DCFDA) Cellular ROS Assay Kit (ab113851) following the manufacturer's instructions. This assay is based on the ability of ROS products to oxidize DCFDA into 2'7'-dichlorofluorescein (DCF). Briefly, cells were seeded in a 96-well plate with 60,000 cells/well the day before the experiment. The next day, cells were treated with each supplemented media for 6 hours, then washed with 1X buffer and stained with 20 µM DCFDA for 45 minutes at 37°C in the dark. Cells were washed 2 times in 1X buffer, and fluorescence was measured at Ex/Em = 485/535 nm using the GloMax®-Multi Detection System (Promega). Final values were calculated by subtracting blank control readings from the fluorescence readings, which were then normalized to cell number (cells/mL). Cells were counted using the DeNovix CellDrop Brightfield Cell Counter, with each treatment plated in duplicate and each well was counted 3 times.

Mitochondrial ROS was detected using MitoSOX™ Red Mitochondrial Superoxide Indicator (MitoSOX; Thermo Fisher Scientific, M36008). Cells were seeded in a 96-well plate with 60,000 cells/well the day before the experiment. The next day, cells were washed with PBS

and treated with 5 μM MitoSOX™ reagent for 10 minutes, and incubated at 37°C. This was followed by three PBS washes. Fluorescence was then measured at Ex/Em = 510/580 nm using the GloMax®-Multi Detection System (Promega). Final values were calculated by subtracting blank control readings from fluorescence readings, which were then normalized to cell number (cells/mL). Cells were counted as explained above.

2.5.2 Live Cell Fluorescence Microscopy

Cells were seeded in 35 mm glass-bottomed dishes at 200,000 cells. Once 70–80% confluency was reached (~3 days), cells were treated with each media for 6 hours. Following treatment, cells were stained with either DCFDA or MitoSOX™ for 45 minutes and 10 minutes at 37°C, respectively. The cells were then washed with their respective buffers according to the manufacturer's instructions, and were counterstained with Hoescht 33342 (Thermo Fisher Scientific, 62249) by medium exchange (1 μg/mL) for 5 minutes at room temperature. Counterstain was then removed, and cells were left in warm buffer for live cell imaging on the Nikon Eclipse Ti2E Inverted Deconvolution Microscope (Biotron Integrated Microscopy Facility, Western University).

2.5.3 Antioxidant Assay

Total antioxidant capacity of cell lysates was measured using an Antioxidant Assay Kit (Cayman Chemical, 709001). Cells were seeded at 600,000 cells in 60 mm plates and grew for 3 days prior to treatment and harvesting for this experiment. Cell lysates were collected using the assay buffer provided by the kit (5 mM potassium phosphate, pH 7.4, 0.9% sodium chloride, 0.1% glucose). Plates were scraped and pellets were sonicated, followed by a 5X dilution of the lysates using the assay buffer provided. This kit measures the ability of all aqueous- and lipid-soluble antioxidants in the sample (*i.e.,* glutathione, superoxide dismutase, catalase, lipids, vitamins, proteins, uric acid, etc.) to inhibit oxidation of 2,2'-Azino-di-(3-ethylbenzathiazoline sulphonate) (ABTS) to ABTS$^{\bullet+}$ by metmyoglobin. The reaction was initiated by adding 40 μL of 441 μM of hydrogen peroxide to each well, and plates were incubated on a shaker for 5 minutes at room temperature. Absorbance was then measured at 750 nm using the GloMax®-Multi Detection System (Promega). The ability of antioxidants in each sample to cause suppression of absorbance was proportional to their concentration, which was compared to Trolox standards

(see **Appendix C** for standard curve). Antioxidant concentrations were normalized to total cell protein levels and were calculated using the following formula:

$$\text{Antioxidant (mM)} = \left[\frac{(Sample\ average\ absorbance) - (y - intercept)}{slope}\right] x\ Dilution$$

2.6 Statistical Analyses

2.6.1 Statistical Analyses

All data are presented as mean ± SEM from at least four biological replicates. Comparisons between all treatments used a One-Way Analysis of Variance (ANOVA) followed by a Tukey's Honest Significant Difference Test (Graphpad Prism Software, San Diego, California). Normality of all data was confirmed using a Shapiro Wilks Test (Graphpad Prism Software, San Diego, California), and any outliers were removed using a Grubb's Test (α=0.05; Graphpad Prism Software, San Diego, California). For all analyses, statistical significance was assumed when p<0.05.

Chapter 3: Results

3.1 Establishing a cell culture model of NAFLD

3.1.1 Neutral lipid droplet quantification

To establish a model, all treatments were measured to determine the degree to which steatosis, the first stage of NAFLD, could be induced. Steatosis was first measured through Oil Red O staining to indicate the presence of neutral lipid droplet accumulation. The PA/OA treatment displayed a significant increase in Oil Red O absorbance compared to the control treatment ($p<0.05$; PA/OA: 3.579 ± 0.017 nm vs. Control: 3.505 ± 0.019 nm) (**Fig. 3.1.1-1**). There were no significant changes found in Oil Red O absorbance in the PA/OA group compared to both glucose (PA/OA: 3.579 ± 0.017 nm vs. Glucose: 3.522 ± 0.014 nm) and fructose groups (PA/OA: 3.579 ± 0.017 nm vs. Fructose: 3.526 ± 0.007 nm) (**Fig. 3.1.1-1**). Additionally, no significant changes in Oil Red O absorbance were observed between both sugar treatments and the control, as well as between glucose and fructose, as absorbance measures were comparable to each other (Control: 3.505 ± 0.019 nm vs. Glucose: 3.522 ± 0.014 nm vs. Fructose: 3.526 ± 0.007 nm) (**Fig. 3.1.1-1**).

As for the Western diet (WD) treatment, a significant increase in Oil Red O absorbance was observed when compared to the control treatment ($p<0.01$; WD: 3.603 ± 0.014 nm vs. Control: 3.505 ± 0.019 nm) (**Fig. 3.1.1-1**). Additionally, there was a significant increase in absorbance in the WD-treated cells compared to those treated with glucose ($p<0.01$; WD: 3.603 ± 0.014 nm vs. Glucose: 3.522 ± 0.014 nm) and fructose ($p<0.05$; WD: 3.603 ± 0.014 nm vs. Fructose: 3.526 ± 0.007 nm) (**Fig. 3.1.1-1**). Further, an increase in absorbance was observed in the WD treatment compared to the PA/OA treatment; however, this change was not significant (PA/OA: 3.579 ± 0.017 nm vs. WD: 3.603 ± 0.014 nm) (**Fig. 3.1.1-1**). This indicated that there was an accumulation of neutral lipid droplets in cells treated with PA/OA, although more significantly in the WD-treated cells, and as such, the cell model of early NAFLD was established as steatosis was present.

Following staining, cells were imaged and those treated with PA/OA and WD media showed an increase in the amount of stained neutral lipid droplets compared to the control

treatment (**Fig. 3.1.1-2**). Many lipid droplets in the PA/OA treatment appeared to be smaller in size and showed a more dispersed localization, whereas in the WD treatment, the droplets seemed larger and tended to cluster together (**Fig. 3.1.1-2**). In some WD-treated cells, these droplets were accompanied by large swellings, where the droplets were displaced to the periphery of cells, which was not observed in the PA/OA treatment. These swellings were also evident in both high sugar groups (**Fig. 3.1.1-2**).
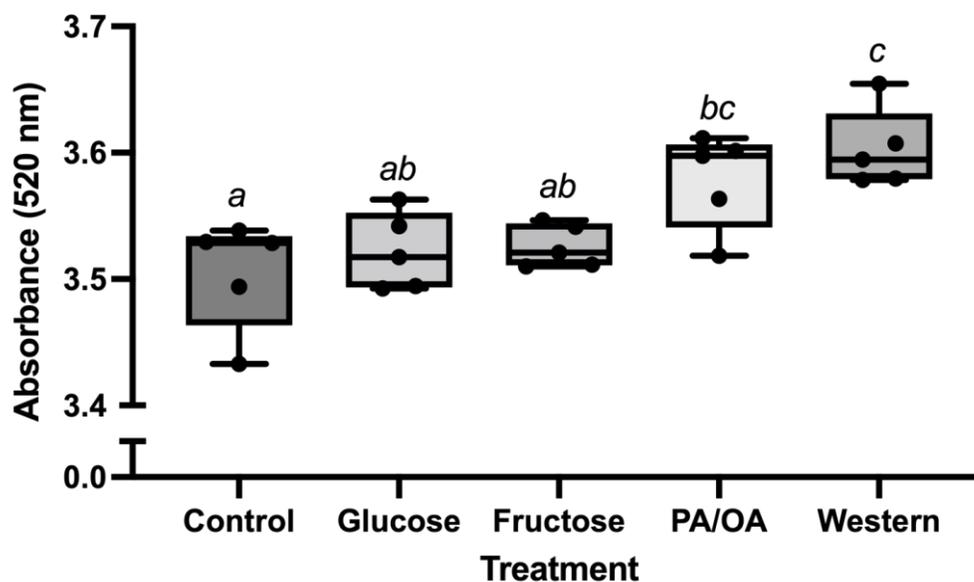
Figure 3.1.1-1. Neutral lipids accumulate in Western diet and high-fat media. Oil Red O absorbance (520 nm) of neutral lipid droplets in cells treated with control, 12.5 mM glucose, 15 mM fructose, 1 mM PA/OA and Western diet (1 mM PA/OA + 12.5 mM glucose + 15 mM fructose) media for 6 hours. Statistical significance was determined using a One-Way ANOVA followed by a Tukey's test. Means followed by the same letter are not significantly different ($p<0.05$) according to Tukey's test. N=5. Box plot legend: median (midline), box (25th–75th percentile), whiskers (extrema).
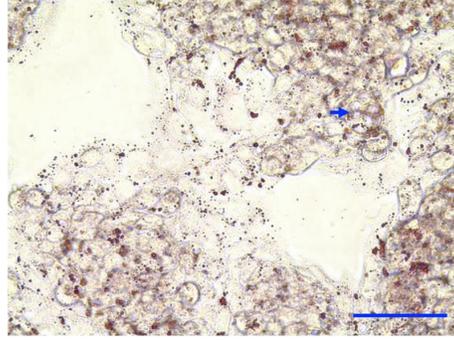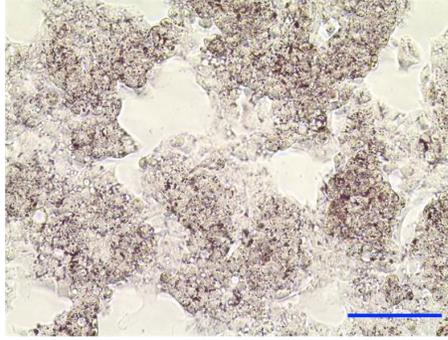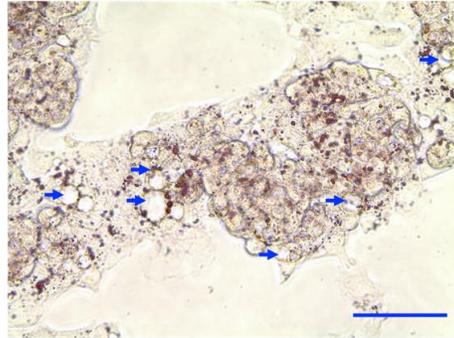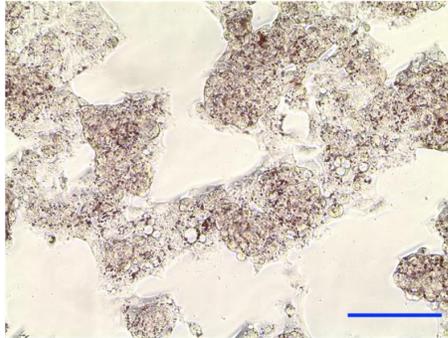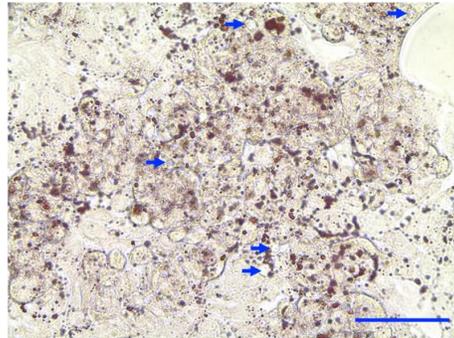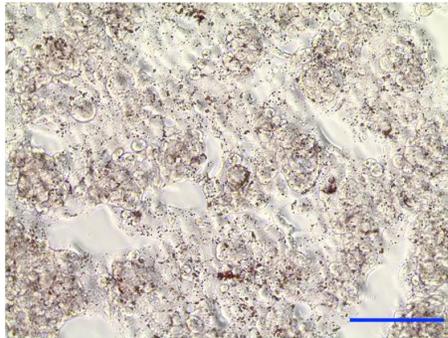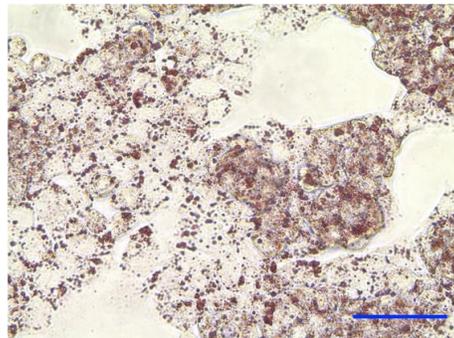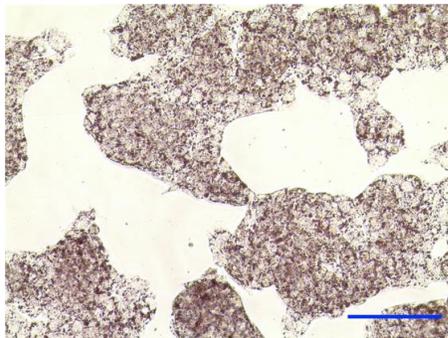
Control
Glucose
Fructose
PA/OA
Western
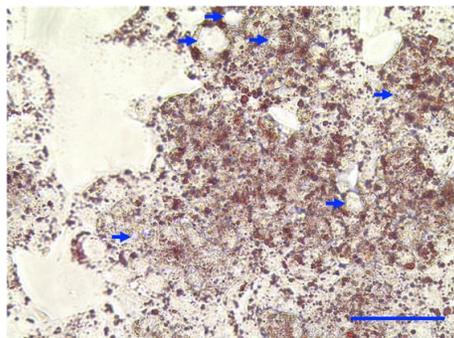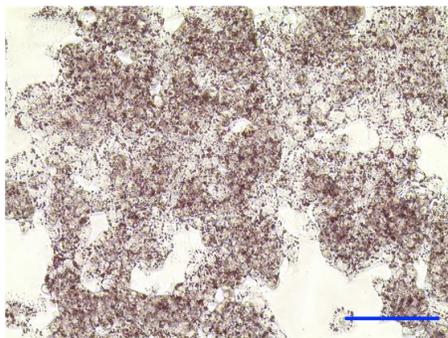
Figure 3.1.1-2. Neutral lipid droplets accumulate, and cellular swellings occur in the Western diet treatment from the high-fat media and high-sugar media, respectively. Representative phase-contrast images of cells stained with Oil Red O after 6 hours of treatment with control, 12.5 mM glucose, 15 mM fructose, 1 mM PA/OA, and Western diet (1 mM PA/OA + 12.5 mM glucose + 15 mM fructose) media at objectives of 20X (left column) and 40X (right column) using a Leica EC3 Camera 2.4. Blue arrows denote areas of intracellular swelling. Scale bar = 100 µm.

3.1.2 Quantification of triglyceride accumulation

Since Oil Red O stains both triglycerides and cholesteryl oleate[253], to get an accurate measure of triglyceride accumulation in the cells, lipids were extracted and normalized to total cell protein levels. There was a significant 2.3-fold increase in triglyceride accumulation observed in the PA/OA treatment when compared to control ($p<0.0001$; PA/OA: 229.0 ± 5.089 µg/mg vs. Control: 98.72 ± 2.760 µg/mg) (**Fig. 3.1.2-1**). This increase was also found to be significantly greater than that of both sugar components ($p<0.0001$; PA/OA: 229.0 ± 5.089 µg/mg vs. Glucose: 100.8 ± 2.208 µg/mg) ($p<0.0001$; PA/OA: 229.0 ± 5.089 µg/mg vs. Fructose: 99.36 ± 1.519 µg/mg) (**Fig. 3.1.2-1**). No significant changes in triglyceride accumulation were observed between both sugar treatments and the control, as well as between glucose and fructose, as lipid mass measures were comparable to each other (Control: 98.72 ± 2.760 µg/mg vs. Fructose: 99.36 ± 1.519 µg/mg vs. Glucose: 100.8 ± 2.208 µg/mg) (**Fig. 3.1.2-1**).

Similarly, the WD treatment displayed a significant increase in triglyceride accumulation compared to control, where a 2.2-fold increase was observed ($p<0.0001$; WD: 220.8 ± 4.246 µg/mg vs. Control: 98.72 ± 2.760 µg/mg) (**Fig. 3.1.2-1**). Triglyceride content in WD-treated cells was also found to be significantly greater than that of both glucose- and fructose-treated cells ($p<0.0001$; WD: 220.8 ± 4.246 µg/mg vs. Glucose: 100.8 ± 2.208 µg/mg) ($p<0.0001$; WD: 220.8 ± 4.246 µg/mg vs. Fructose: 99.36 ± 1.519 µg/mg) (**Fig. 3.1.2-1**). There were no significant changes observed between the PA/OA and WD-treated cells in regard to triglyceride accumulation as measurements were comparable to each other (PA/OA: 229.0 ± 5.089 µg/mg vs. WD: 220.8 ± 4.246 µg/mg) (**Fig. 3.1.2-1**).
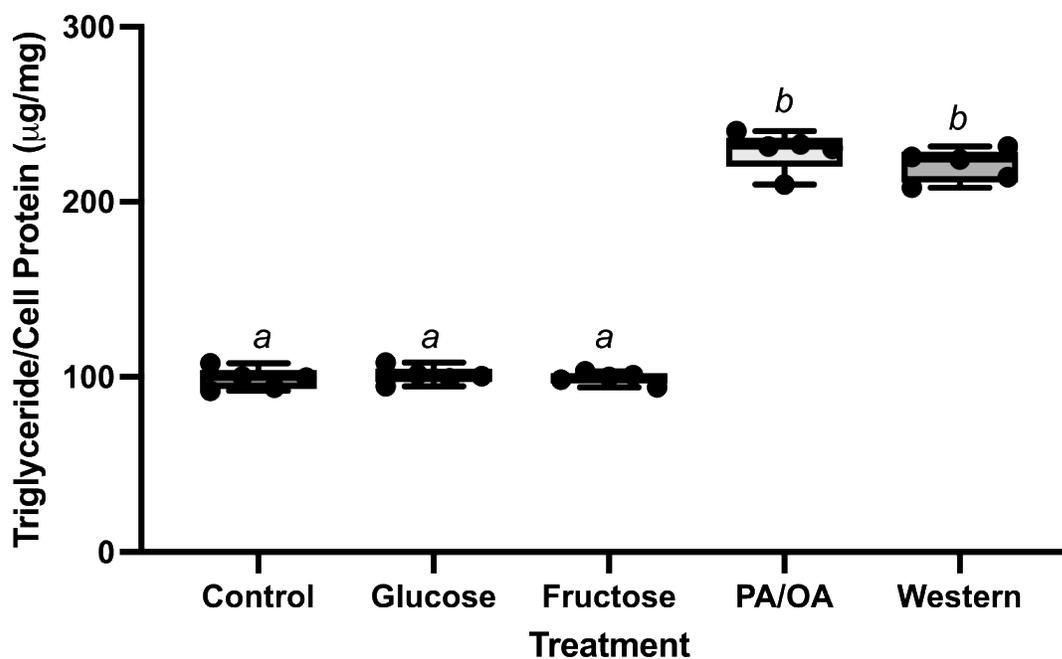
Figure 3.1.2-1. Triglyceride accumulation occurs in high-fat and Western diet media. Lipid mass measurements (μg triglyceride/mg cell protein) in cells treated with control, 12.5 mM glucose, 15 mM fructose, 1 mM PA/OA, and Western diet (1 mM PA/OA + 12.5 mM glucose + 15 mM fructose) media for 6 hours. Statistical significance was determined using a One-Way ANOVA followed by a Tukey's test. Means followed by the same letter are not significantly different ($p<0.05$) according to Tukey's test. N=5. Box plot legend: median (midline), box (25th–75th percentile), whiskers (extrema).

3.2 Changes in gene expression

3.2.1 qRT-PCR analysis of SREBP isoform expression

To determine the effect of different nutrients on transcript expression and cell signaling pathways in NAFLD, qRT-PCR was utilized and relative gene expression was determined. All SREBP isoforms (-1a, -1c, 2), which are known to be involved in the pathogenesis of NAFLD[97,98], were investigated. When cells were treated with high-fat media, there was a significant decrease observed in *SREBP-1a* gene expression compared to control cells ($p<0.05$; PA/OA: 0.617 ± 0.087 vs. Control: 1.000 ± 0.120) and when compared to fructose-treated cells ($p<0.05$; PA/OA: 0.617 ± 0.087 vs. Fructose: 1.099 ± 0.278) (**Fig. 3.2.1-1**). A similar outcome was observed in WD-treated cells as *SREBP-1a* gene expression significantly decreased in comparison to fructose-treated cells ($p<0.05$; WD: 0.676 ± 0.166 vs. Fructose: 1.099 ± 0.278); however, this change was not significant compared to the control (WD: 0.676 ± 0.166 vs. Control: 1.000 ± 0.120) (**Fig. 3.2.1-1**). Compared to the glucose treatment, changes in *SREBP-1a* gene expression were not significant in both PA/OA and WD cells (Glucose: 0.815 ± 0.044 vs. PA/OA: 0.617 ± 0.087 vs. WD: 0.676 ± 0.166) (**Fig. 3.2.1-1**). There were also no significant changes observed between the PA/OA group and the WD group (PA/OA: 0.617 ± 0.087 vs. WD: 0.676 ± 0.166) (**Fig. 3.2.1-1**).

Additionally, there were no significant changes observed in *SREBP-1a* gene expression between fructose and the control treatment as expression levels were comparable to each other (Fructose: 1.099 ± 0.278 vs. Control: 1.000 ± 0.120) (**Fig. 3.2.1-1**). Although *SREBP-1a* gene expression appeared to decrease in cells treated with glucose, this change was also not significant when compared to control and fructose treatments (Glucose: 0.815 ± 0.044 vs. Control: 1.000 ± 0.120 vs. Fructose: 1.099 ± 0.278) (**Fig. 3.2.1-1**).

Regarding the *SREBP-1c* isoform, there were no significant changes in gene expression across all treatment groups (WD: 0.530 ± 0.433 vs. PA/OA: 0.542 ± 0.338 vs. Glucose: 0.826 ± 0.258 vs. Control: 1.000 ± 0.379 vs. Fructose: 1.059 ± 0.465) (**Fig. 3.2.1-2A**). Similarly, the *SREBP-2* isoform displayed no significant changes in gene expression between all treatment

groups (PA/OA: 0.893 ± 0.072 vs. Glucose: 0.967 ± 0.149 vs. Control: 1.000 ± 0.206 vs. WD: 1.043 ± 0.261 vs. Fructose: 1.151 ± 0.385) (**Fig. 3.2.1-2B**).
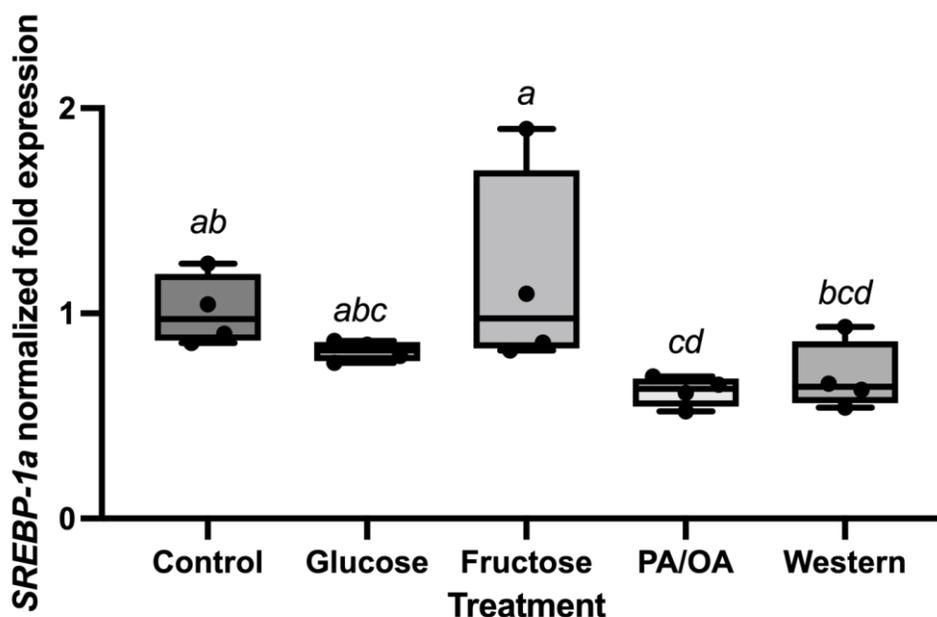
Figure 3.2.1-1. *SREBP-1a* gene expression is decreased in PA/OA- and Western diet-treated cells. Normalized fold expression values from qRT-PCR analysis of *SREBP-1a* when treated with control, 12.5 mM glucose, 15 mM fructose, 1 mM PA/OA, and Western diet (1 mM PA/OA + 12.5 mM glucose + 15 mM fructose) media for 6 hours. Relative quantities were normalized to the expression of *RPLP0*, *ACTB*, and *PSMB6*. Statistical significance was determined using a One-Way ANOVA followed by a Tukey's test. Means followed by the same letter are not significantly different ($p<0.05$) according to Tukey's test. N=4. Box plot legend: median (midline), box (25th–75th percentile), whiskers (extrema).

Figure 3.2.1-2. Gene expression of *SREBP-1c* and *SREBP-2* are unchanged across all treatment groups. Normalized fold expression values from qRT-PCR analysis of (**A**) *SREBP-1c* and (**B**) *SREBP-2* when treated with control, 12.5 mM glucose, 15 mM fructose, 1 mM PA/OA, and Western diet (1 mM PA/OA + 12.5 mM glucose + 15 mM fructose) media for 6 hours. Relative quantities were normalized to the expression of *RPLP0*, *ACTB*, and *PSMB6*. Statistical significance was determined using a One-Way ANOVA followed by a Tukey's test. Means followed by the same letter are not significantly different ($p<0.05$) according to Tukey's test. N=4. Box plot legend: median (midline), box (25th–75th percentile), whiskers (extrema).

3.2.2 qRT-PCR analysis of signaling pathways, inflammation, and target gene expression

Genes known to be involved in the pathogenesis of NAFLD, many of which are direct targets of SREBP isoforms (*FASN, LDLR, ACACA, SCD1, G6PD, HMGCR*) or are involved in their cellular signaling pathways (*LXRα, IRS1, PI3K, KRAS*), as well as inflammatory markers (*TNFα*), were investigated using qRT-PCR. Of note, gene expression of *LDLR* in glucose-treated cells was significantly decreased compared to control cells ($p<0.05$; Glucose: 0.758 ± 0.071 vs. Control: 1.000 ± 0.138) (**Fig. 3.2.2-1**). This change in gene expression, however, was not significant compared to fructose- or PA/OA-treated cells (Glucose: 0.758 ± 0.071 vs. Fructose: 0.944 ± 0.239 vs. PA/OA: 0.944 ± 0.067). Additionally, the expression of *LDLR* significantly decreased 0.66-fold in the glucose treatment group compared to the WD treatment group ($p<0.01$; Glucose: 0.758 ± 0.071 vs. WD: 1.148 ± 0.047) (**Fig. 3.2.2-1**). In the remaining treatment groups, no significant changes were observed in *LDLR* gene expression when compared to control and to each other (Control: 1.000 ± 0.138 vs. PA/OA: 0.944 ± 0.067 vs. Fructose: 0.944 ± 0.239 vs. WD: 1.148 ± 0.047). Additionally, no significant changes in expression were observed in the remainder of genes described above under the differing nutrient conditions (**Fig. 3.2.2-2 & 3.2.2-3**).
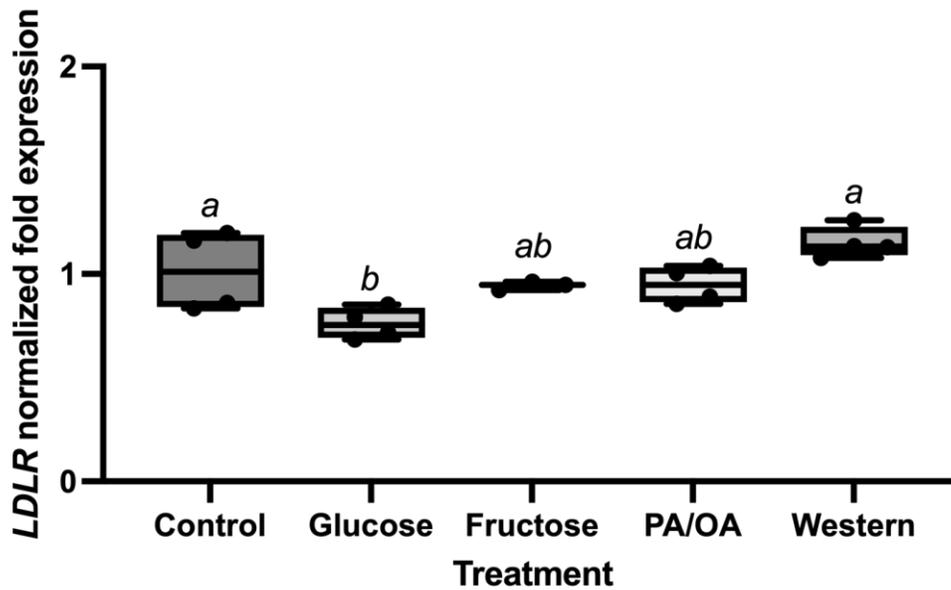
Figure 3.2.2-1. *LDLR* gene expression is decreased in glucose-treated cells. Normalized fold expression values from qRT-PCR analysis of *LDLR* when treated with control, 12.5 mM glucose, 15 mM fructose, 1 mM PA/OA, and Western diet (1 mM PA/OA + 12.5 mM glucose + 15 mM fructose) media for 6 hours. Relative quantities were normalized to the expression of *RPLP0*, *ACTB*, and *PSMB6*. Statistical significance was determined using a One-Way ANOVA followed by a Tukey's test. Means followed by the same letter are not significantly different ($p<0.05$) according to Tukey's test. N=4. Box plot legend: median (midline), box (25th–75th percentile), whiskers (extrema).

Figure 3.2.2-2. Gene expression of SREBP target genes are unchanged across all treatment groups. Normalized fold expression values from qRT-PCR analysis of (**A**) *ACACA*, (**B**) *FASN*, (**C**) *SCD1*, (**D**) *HMGCR*, and (**E**) *G6PD* when treated with control, 12.5 mM glucose, 15 mM fructose, 1 mM PA/OA, and Western diet (1 mM PA/OA + 12.5 mM glucose + 15 mM fructose) media for 6 hours. Relative quantities were normalized to the expression of *RPLP0*, *ACTB*, and *PSMB6*. Statistical significance was determined using a One-Way ANOVA followed by a Tukey's test. Means followed by the same letter are not significantly different ($p<0.05$) according to Tukey's test. N=4. Box plot legend: median (midline), box (25th–75th percentile), whiskers (extrema).
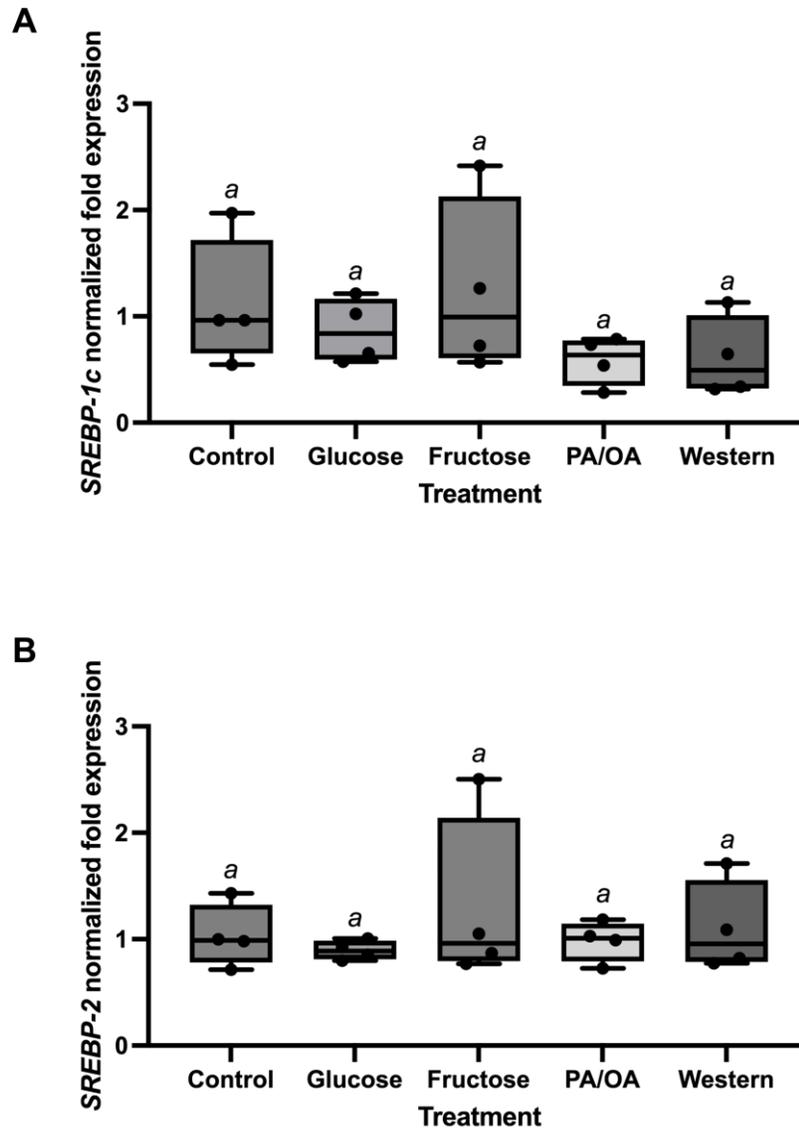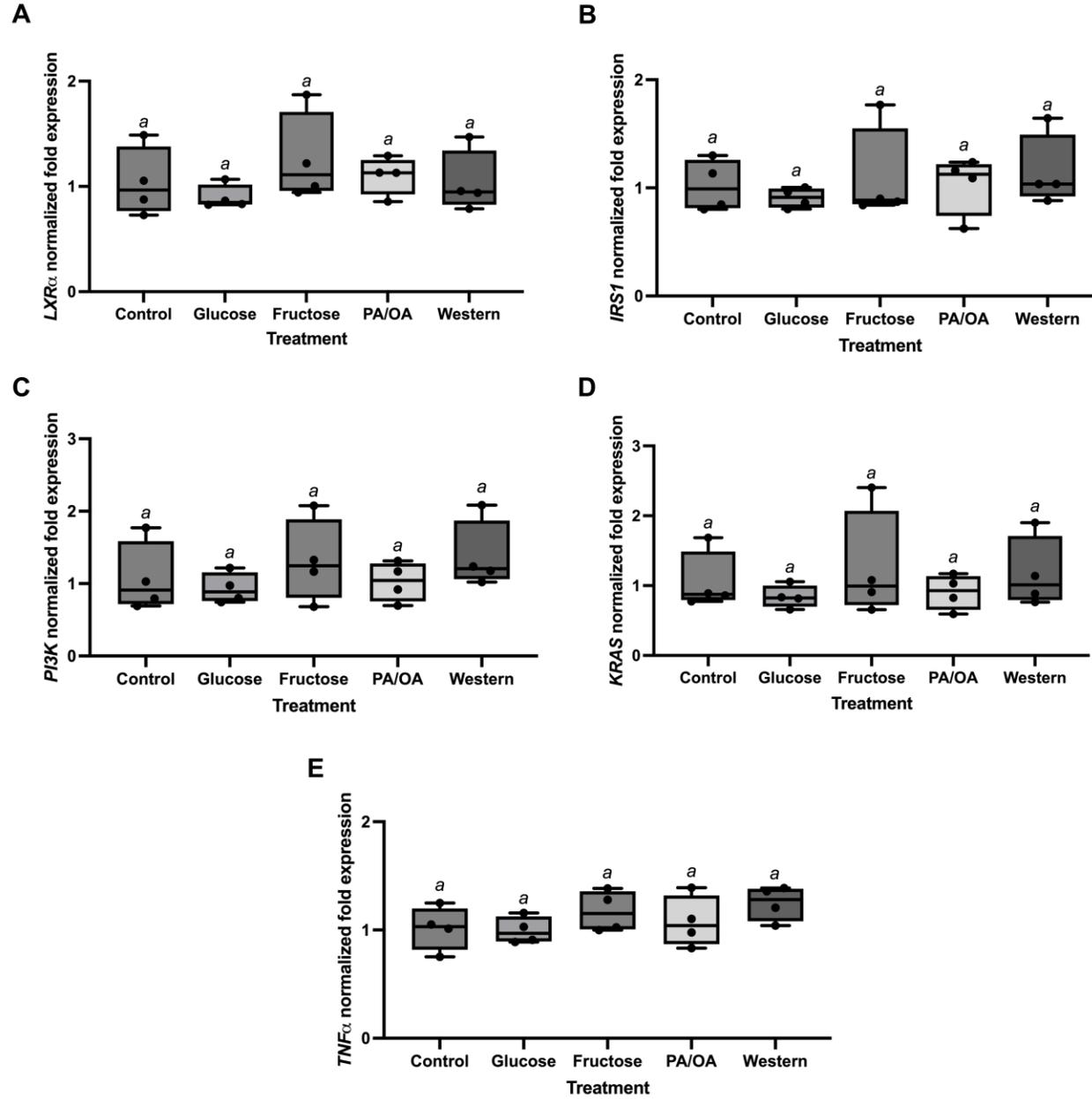
Figure 3.2.2-3. Gene expression of SREBP signaling pathways and inflammatory markers are unchanged across all treatment groups. Normalized fold expression values from qRT-PCR analysis of (**A**) *LXRα*, (**B**) *IRS1*, (**C**) *PI3K*, (**D**) *KRAS*, and (**E**) *TNFα* when treated with control, 12.5 mM glucose, 15 mM fructose, 1 mM PA/OA, and Western diet (1 mM PA/OA + 12.5 mM glucose + 15 mM fructose) media for 6 hours. Relative quantities were normalized to the expression of *RPLP0*, *ACTB*, and *PSMB6*. Statistical significance was determined using a One-Way ANOVA followed by a Tukey's test. Means followed by the same letter are not significantly different ($p<0.05$) according to Tukey's test. N=4. Box plot legend: median (midline), box (25th–75th percentile), whiskers (extrema).

3.2.3 qRT-PCR analysis of lipid processing gene expression

The effect of different nutrients on the expression of several lipid processing genes were analyzed using qRT-PCR. Many genes were considered (*ACADVL, ACACB, ACSL5, CREB3L3, PLIN2*), yet few significant changes in gene expression were observed when cells were exposed to each treatment (**Fig. 3.2.3-1**). However, the expression of *PLIN2* showed significant changes in gene expression, being significantly increased in the PA/OA treatment compared to control, where a ~2.1-fold increase was observed ($p<0.001$; PA/OA: 2.088 ± 0.134 vs. Control: 1.000 ± 0.116) (**Fig. 3.2.3-2**). This increase was also found to be significantly greater than *PLIN2* expression in both glucose- ($p<0.001$; PA/OA: 2.088 ± 0.134 vs. Glucose: 0.933 ± 0.056) and fructose-treated cells ($p<0.001$; PA/OA: 2.088 ± 0.134 vs. Fructose: 1.260 ± 0.238) (**Fig. 3.2.3-2**). Although cells treated with fructose appeared to have a ~1.3-fold increase in expression of *PLIN2*, this change was not significant compared to control or to the glucose treatment (Fructose: 1.260 ± 0.238 vs. Control: 1.000 ± 0.116 vs. Glucose: 0.933 ± 0.238) (**Fig. 3.2.3-2**). Additionally, glucose-treated cells showed no significant changes in *PLIN2* gene expression compared to control (Glucose: 0.933 ± 0.238 vs. Control: 1.000 ± 0.116).

Like the high-fat media, the WD treatment group displayed a significant 2.6-fold increase in *PLIN2* expression compared to control ($p<0.0001$; WD: 2.645 ± 0.059 vs. Control: 1.000 ± 0.116) (**Fig. 3.2.3-2**). This increase was also found to be significantly greater in cells treated with glucose ($p<0.0001$; WD: 2.645 ± 0.059 vs. Glucose: 0.933 ± 0.056) and fructose ($p<0.001$; WD: 2.645 ± 0.059 vs. Fructose: 1.260 ± 0.238) (**Fig. 3.2.3-2**). While there was an increase in the expression of *PLIN2* in the WD condition compared to the PA/OA condition, this change was not significant (WD: 2.645 ± 0.059 vs. PA/OA: 2.088 ± 0.134) (**Fig. 3.2.3-2**).
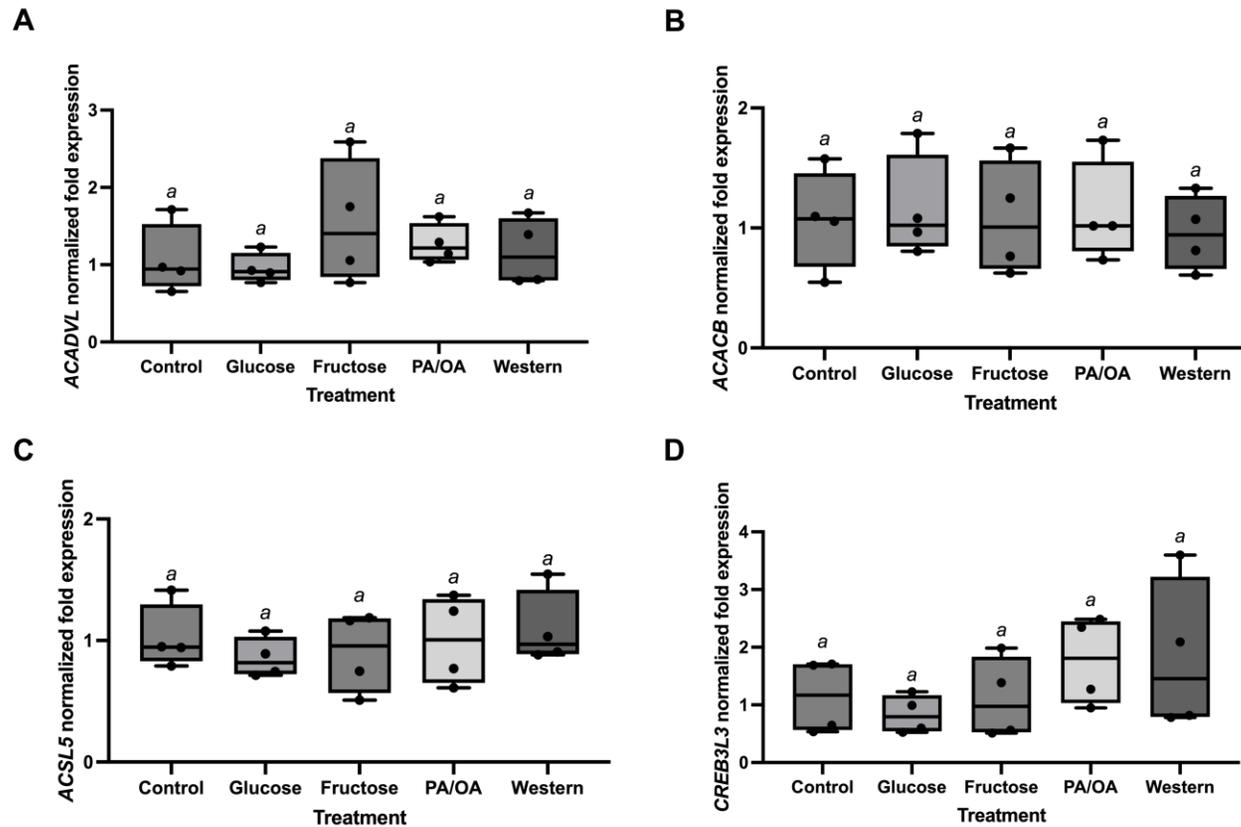
Figure 3.2.3-1. Gene expression of lipid processing genes are unchanged across all treatment groups. Normalized fold expression values from qRT-PCR analysis of (**A**) *ACADVL*, (**B**) *ACACB*, (**C**) *ACSL5*, and (**D**) *CREB3L3* when treated with control, 12.5 mM glucose, 15 mM fructose, 1 mM PA/OA, and Western diet (1 mM PA/OA + 12.5 mM glucose + 15 mM fructose) media for 6 hours. Relative quantities were normalized to the expression of *RPLP0*, *ACTB*, and *PSMB6*. Statistical significance was determined using a One-Way ANOVA followed by a Tukey's test. Means followed by the same letter are not significantly different ($p<0.05$) according to Tukey's test. N=4. Box plot legend: median (midline), box (25th–75th percentile), whiskers (extrema).
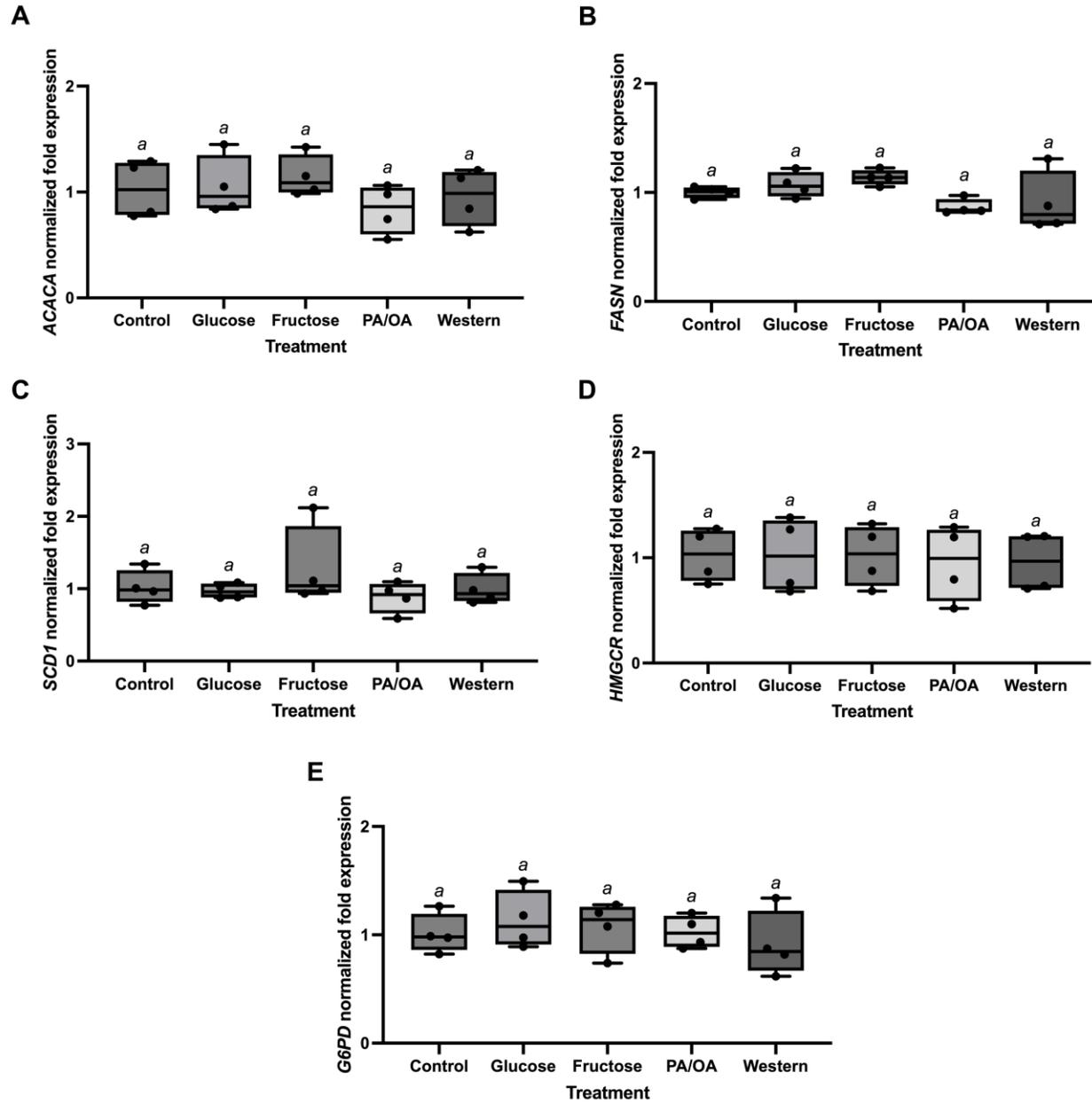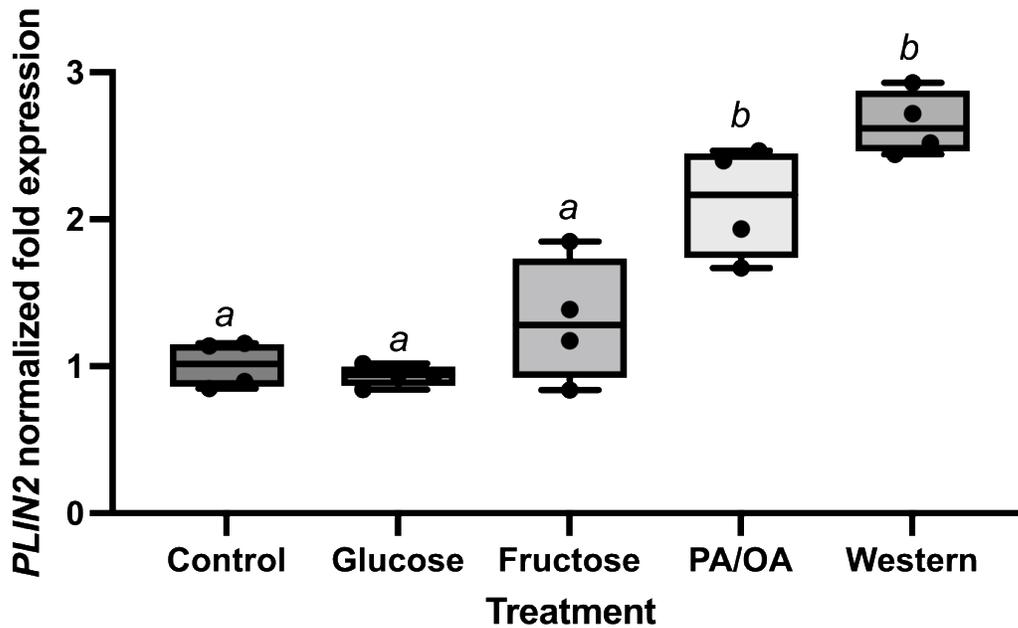
Figure 3.2.3-2. *PLIN2* gene expression is increased in cells treated with high-fat and Western diet media. Normalized fold expression values from qRT-PCR analysis of *PLIN2* when treated with control, 12.5 mM glucose, 15 mM fructose, 1 mM PA/OA, and Western diet (1 mM PA/OA + 12.5 mM glucose + 15 mM fructose) media for 6 hours. Relative quantities were normalized to the expression of *RPLP0*, *ACTB*, and *PSMB6*. Statistical significance was determined using a One-Way ANOVA followed by a Tukey's test. Means followed by the same letter are not significantly different ($p<0.05$) according to Tukey's test. N=4. Box plot legend: median (midline), box (25th–75th percentile), whiskers (extrema).

3.3 Nutrient-induced changes in activity and cell number

3.3.1 MTT assay

To examine the activity of HepG2 cells exposed to different nutrient conditions, an MTT assay was performed and values were measured using a microplate reader and normalized to cell number. This reaction depends on the ability of oxidoreductase enzymes, particularly nicotinamide adenine dinucleotide phosphate (NADPH), to reduce MTT to insoluble formazan crystals, which may indicate metabolic function[252]. It was found that cells treated with PA/OA displayed a significant increase in activity compared to control cells ($p<0.05$; PA/OA: $1.184 \times 10^{-5} \pm 7.185 \times 10^{-7}$ nm/cells/mL vs. Control: $9.827 \times 10^{-6} \pm 4.882 \times 10^{-7}$ nm/cells/mL) (**Fig. 3.3.1-1**). This significant increase in oxidoreductase activity was also observed in PA/OA cells when compared to the activity in both glucose- ($p<0.001$; PA/OA: $1.184 \times 10^{-5} \pm 7.185 \times 10^{-7}$ nm/cells/mL vs. Glucose: $8.675 \times 10^{-6} \pm 3.972 \times 10^{-7}$ nm/cells/mL) and fructose-treated cells ($p<0.001$; PA/OA: $1.184 \times 10^{-5} \pm 7.185 \times 10^{-7}$ nm/cells/mL vs. Fructose: $8.427 \times 10^{-6} \pm 1.442 \times 10^{-7}$ nm/cells/mL) (**Fig. 3.3.1-1**). No significant changes in activity were found in cells treated with glucose or fructose compared to the control and each other (Fructose: $8.427 \times 10^{-6} \pm 1.442 \times 10^{-7}$ nm/cells/mL vs. Glucose: $8.675 \times 10^{-6} \pm 3.972 \times 10^{-7}$ nm/cells/mL vs. Control: $9.827 \times 10^{-6} \pm 4.882 \times 10^{-7}$ nm/cells/mL) (**Fig. 3.3.1-1**).

Regarding the WD-like treatment, there were no significant changes in MTT activity observed when compared to control cells as values were comparable to each other (WD: $1.046 \times 10^{-5} \pm 2.858 \times 10^{-7}$ nm/cells/mL vs. Control: $9.827 \times 10^{-6} \pm 4.882 \times 10^{-7}$ nm/cells/mL) (**Fig. 3.3.1-1**). There was also an increase in activity in the WD group compared to the glucose group, although this change was not significant ($p=0.072$; WD: $1.046 \times 10^{-5} \pm 2.858 \times 10^{-7}$ nm/cells/mL vs. Glucose: $8.675 \times 10^{-6} \pm 3.972 \times 10^{-7}$ nm/cells/mL) (**Fig. 3.3.1-1**). Conversely, when compared to fructose-treated cells, this increase was found to be significantly different ($p<0.05$; WD: $1.046 \times 10^{-5} \pm 2.858 \times 10^{-7}$ nm/cells/mL vs. Fructose: $8.427 \times 10^{-6} \pm 1.442 \times 10^{-7}$ nm/cells/mL) (**Fig. 3.3.1-1**). Additionally, there was a slight increase in reductase activity in the PA/OA treatment group compared to the WD group; however, this was not significant (PA/OA: $1.184 \times 10^{-5} \pm 7.185 \times 10^{-7}$ nm/cells/mL vs. WD: $1.046 \times 10^{-5} \pm 2.858 \times 10^{-7}$ nm/cells/mL) (**Fig. 3.3.1-1**).
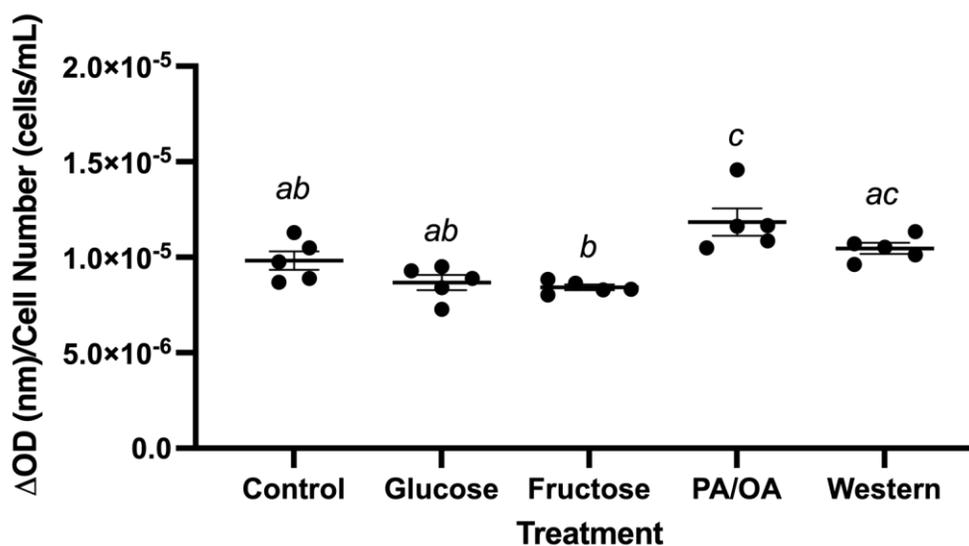
Figure 3.3.1-1. Activity is increased in cells treated with high-fat and Western diet media. Analysis of absorbance (ΔOD=560-750nm) from oxidoreductase activity of the MTT assay reaction in HepG2 cells treated with control, 12.5 mM glucose, 15 mM fructose, 1 mM PA/OA and Western diet (1 mM PA/OA + 12.5 mM glucose + 15 mM fructose) media for 6 hours and normalized to cell number (nm/cells/mL). Values are presented as mean ± SEM. Statistical significance was determined using a One-Way ANOVA followed by a Tukey's test. Means followed by the same letter are not significantly different ($p < 0.05$) according to Tukey's test. N=5.

3.3.2 Cell number

When treated with different nutrient components, significant changes were observed in cell number between the treatment groups. In the PA/OA treatment, there was a significant decrease in cell number compared to the control group ($p<0.05$; PA/OA: $1.032 \times 10^5 \pm 6.462 \times 10^3$ cells/mL vs. Control: $1.276 \times 10^5 \pm 2.455 \times 10^3$ cells/mL) (**Fig. 3.3.2-1**). This decrease in cell number was also significantly different from that of cells treated with glucose ($p<0.001$; PA/OA: $1.032 \times 10^5 \pm 6.462 \times 10^3$ cells/mL vs. Glucose: $1.439 \times 10^5 \pm 6.131 \times 10^3$ cells/mL) and fructose ($p<0.001$; PA/OA: $1.032 \times 10^5 \pm 6.462 \times 10^3$ cells/mL vs. Fructose: $1.438 \times 10^5 \pm 5.420 \times 10^3$ cells/mL) (**Fig. 3.3.2-1**). No significant changes in cell number were observed between the glucose and fructose treatments as the values were comparable; and although cell number appeared to increase in both glucose- and fructose-treated cells compared to control, this change was also not significant (Control: $1.276 \times 10^5 \pm 2.455 \times 10^3$ cells/mL vs. Fructose: $1.438 \times 10^5 \pm 5.420 \times 10^3$ cells/mL vs. Glucose: $1.439 \times 10^5 \pm 6.131 \times 10^3$ cells/mL) (**Fig. 3.3.2-1**).

Similarly, in WD-treated cells, there was a significant decrease in cell number when compared to cells treated with glucose ($p<0.01$; WD: $1.080 \times 10^5 \pm 5.776 \times 10^3$ cells/mL vs. Glucose: $1.439 \times 10^5 \pm 6.131 \times 10^3$ cells/mL) and fructose ($p<0.01$; WD: $1.080 \times 10^5 \pm 5.776 \times 10^3$ cells/mL vs. Fructose: $1.438 \times 10^5 \pm 5.420 \times 10^3$ cells/mL) (**Fig. 3.3.2-1**). While cell number appeared to decrease in the WD treatment compared to the control treatment, this change was not significant (WD: $1.080 \times 10^5 \pm 5.776 \times 10^3$ cells/mL vs. Control: $1.276 \times 10^5 \pm 2.455 \times 10^3$ cells/mL). There was also no significant change observed in cell number between the WD and PA/OA treatment groups as the values were comparable (PA/OA: $1.032 \times 10^5 \pm 6.462 \times 10^3$ cells/mL vs. WD: $1.080 \times 10^5 \pm 5.776 \times 10^3$ cells/mL) (**Fig. 3.3.2-1**).
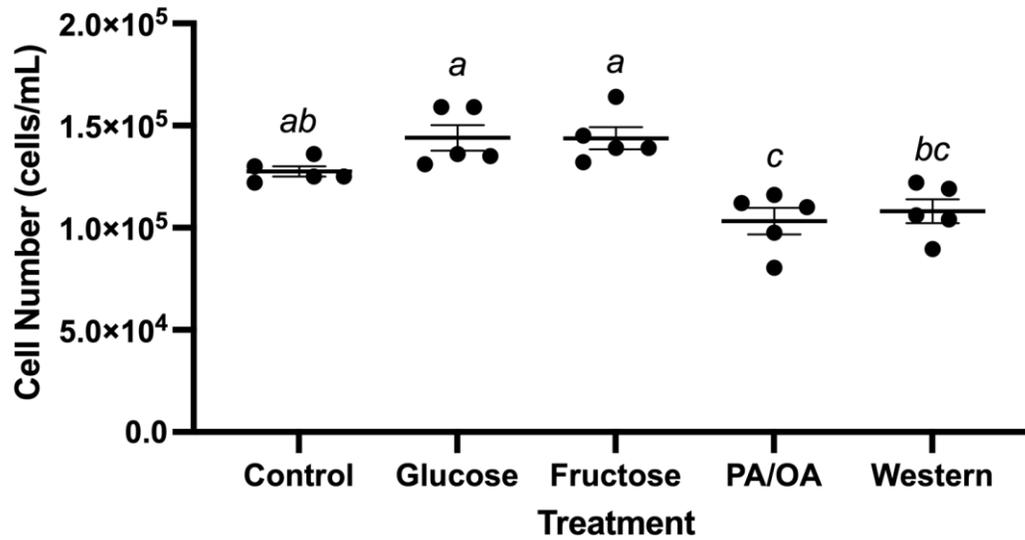
Figure 3.3.2-1. Cell number is decreased in PA/OA- and Western diet-treated cells. Changes in cell number (cell/mL) in HepG2 cells treated for 6 hours with control, 12.5 mM glucose, 15 mM fructose, 1 mM PA/OA, and Western diet (1 mM PA/OA + 12.5 mM glucose + 15 mM fructose) media. Values are presented as mean ± SEM. Statistical significance was determined using a One-Way ANOVA followed by a Tukey's test. Means followed by the same letter are not significantly different ($p < 0.05$) according to Tukey's test. N=5.

3.4 Oxidative stress

3.4.1 Analysis of total antioxidant capacity

To assess if different dietary components influenced cellular antioxidant levels, an antioxidant assay was used to measure total antioxidant capacity. Values were measured using a microplate reader and normalized to total cell protein levels. Antioxidant concentrations were then calculated from the linear regression of the standard curve (See **Chapter 2.1.9** for equation; see **Appendix C** for standard curve). No significant changes in total antioxidant capacity were observed between each treatment group (PA/OA: 3.718 ± 0.028 mM/mg vs. Control: 3.782 ± 0.032 mM/mg vs. Glucose: 3.793 ± 0.039 mM/mg vs. Fructose: 3.823 ± 0.027 mM/mg vs. WD: 3.842 ± 0.029 mM/mg) (**Fig. 3.4.1-1**). Although not significant, the WD group exhibited the largest total antioxidant capacity when compared to the PA/OA treatment, which displayed the lowest total antioxidant capacity (p=0.08; PA/OA: 3.718 ± 0.028 mM/mg vs. WD: 3.842 ± 0.029 mM/mg) (**Fig. 3.4.1-1**).
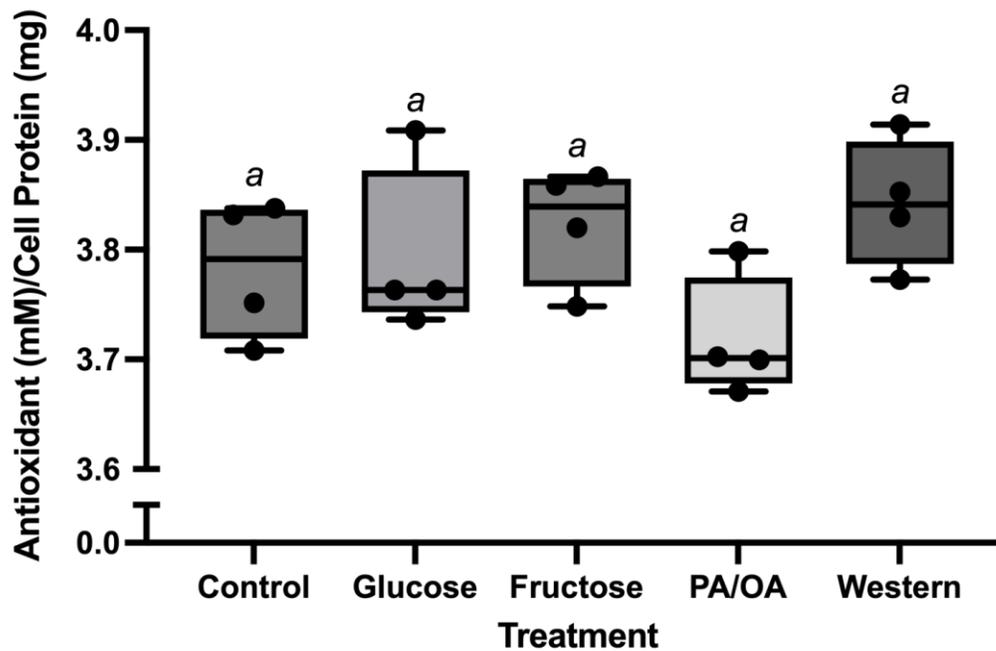
Figure 3.4.1-1. Total antioxidant capacity is unchanged across all treatment groups. Antioxidant capacity normalized to cell protein (mM antioxidant/mg protein) in cells treated with control, 12.5 mM glucose, 15 mM fructose, 1 mM PA/OA, and Western diet (1 mM PA/OA + 12.5 mM glucose + 15 mM fructose) media for 6 hours. Statistical significance was determined using a One-Way ANOVA followed by a Tukey's test. Means followed by the same letter are not significantly different ($p<0.05$) according to Tukey's test. N=4. Box plot legend: median (midline), box (25th–75th percentile), whiskers (extrema).

3.4.2 Analysis of mitochondrial stress

To identify if the major source of ROS was mitochondrial, cells were stained with MitoSOX™. Following staining, fluorescence microscopy was performed to visualize superoxide products within the cells. There seemed to be a decrease in fluorescence observed in the glucose- and fructose-treated cells compared to control, with a slight increase in fluorescence seen in both the PA/OA and WD groups (**Fig. 3.4.2-1**).

To corroborate these results and to determine if there were any changes in superoxide levels, fluorescence values were measured using a microplate reader and normalized to cell number. Compared to the control, there seemed to be a decrease in fluorescence in cells treated with glucose (Glucose: $4.671 \times 10^{-4} \pm 4.470 \times 10^{-5}$ nm/cells/mL vs. Control: $8.535 \times 10^{-4} \pm 1.663 \times 10^{-4}$ nm/cells/mL) and fructose (Fructose: $3.838 \times 10^{-4} \pm 2.513 \times 10^{-4}$ nm/cells/mL vs. Control: $8.535 \times 10^{-4} \pm 1.663 \times 10^{-4}$ nm/cells/mL), however, these changes were not significant (**Fig. 3.4.2-2**). No significant changes in fluorescence were observed between the two sugar groups, and this decrease in fluorescence was also not significant compared to the PA/OA and WD treatments (Fructose: $3.838 \times 10^{-4} \pm 2.513 \times 10^{-4}$ nm/cells/mL vs. Glucose: $4.671 \times 10^{-4} \pm 4.470 \times 10^{-5}$ nm/cells/mL vs. PA/OA: $9.057 \times 10^{-4} \pm 1.911 \times 10^{-4}$ nm/cells/mL vs. WD: $9.058 \times 10^{-4} \pm 1.232 \times 10^{-4}$ nm/cells/mL) (**Fig. 3.4.2-2**). Although there was a 1.06-fold increase of superoxide products in the WD and PA/OA groups compared to control, this increase was not found to be significant, as well as when compared to each other as the values between these two groups were similar (Control: $8.535 \times 10^{-4} \pm 1.663 \times 10^{-4}$ nm/cells/mL vs. PA/OA: $9.057 \times 10^{-4} \pm 1.911 \times 10^{-4}$ nm/cells/mL vs. WD: $9.058 \times 10^{-4} \pm 1.232 \times 10^{-4}$ nm/cells/mL) (**Fig. 3.4.2-2**). Thus, across all treatment groups, no significant changes were observed in mitochondrial ROS.

Control
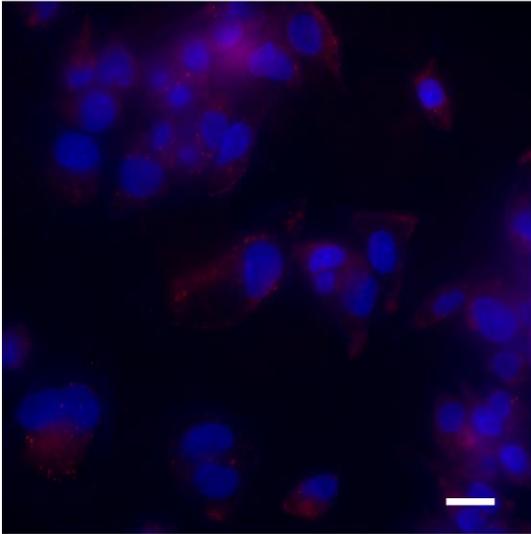
Glucose
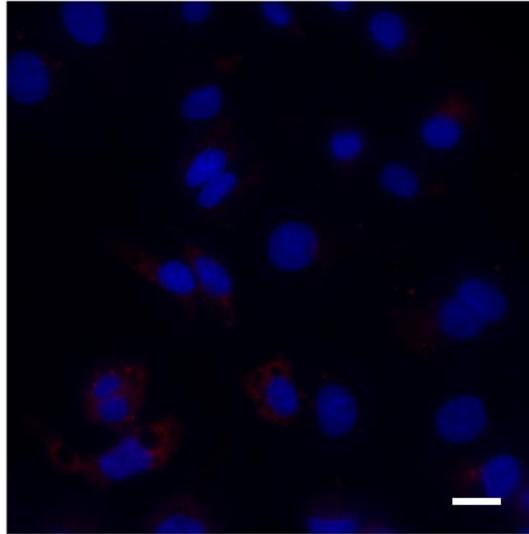
Fructose
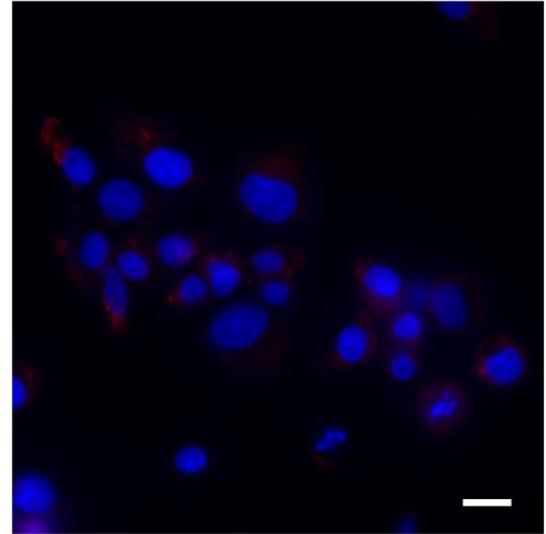
PA/OA
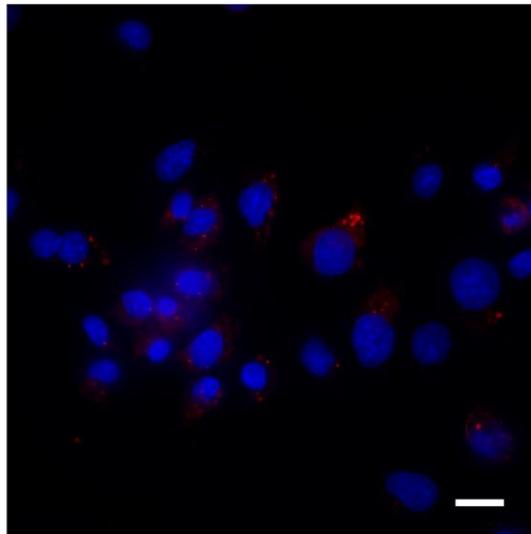
Western
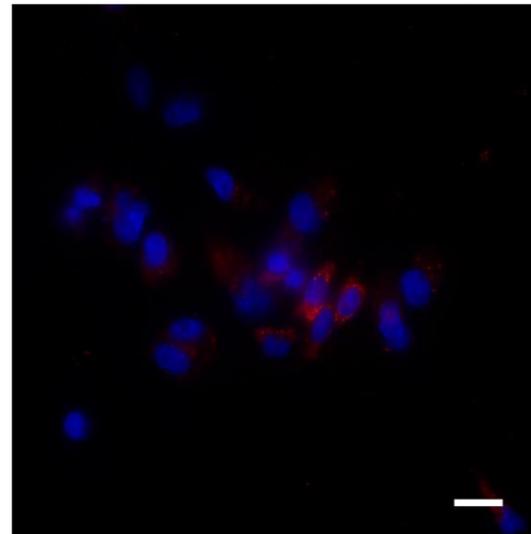
Figure 3.4.2-1. Nutrient-induced mitochondrial superoxide fluorescence. Representative live cell fluorescence microscopy images of stained mitochondrial superoxide using MitoSOX™ in HepG2 cells treated with control, 12.5 mM glucose, 15 mM fructose, 1 mM PA/OA, and Western diet (1 mM PA/OA + 12.5 mM glucose + 15 mM fructose) media for 6 hours. Cells were counterstained with Hoechst 33342 and images were taken at 60X using a Nikon Eclipse Ti2E Inverted Deconvolution Microscope. Scale bar = 20 μm.
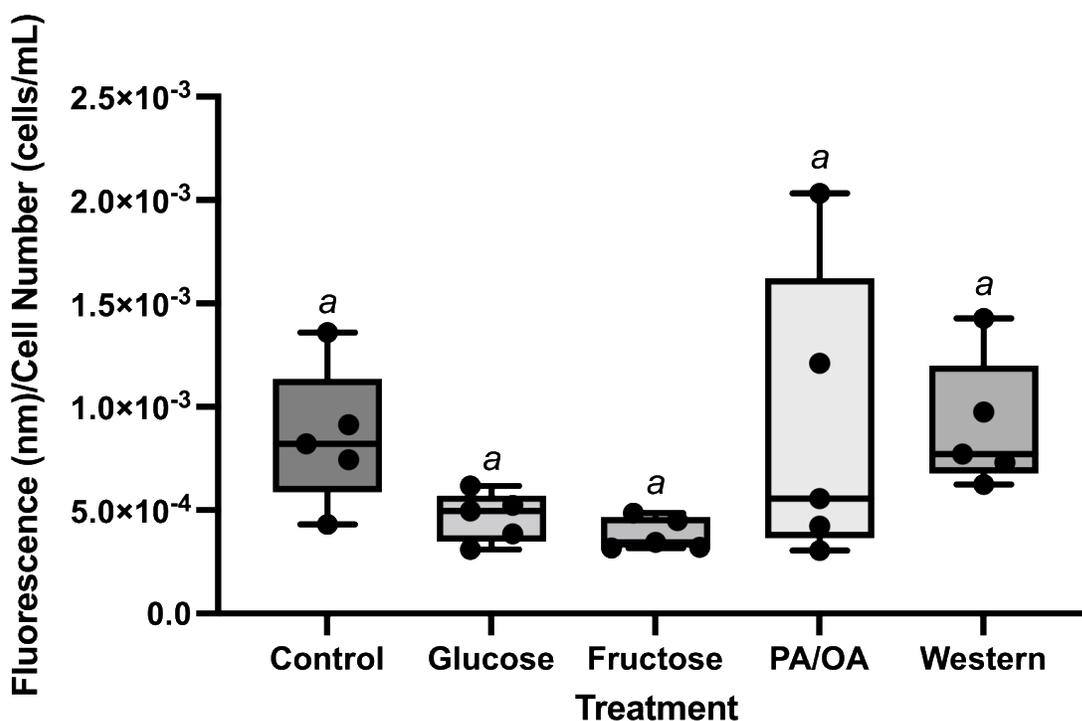
Figure 3.4.2-2. Mitochondrial superoxide levels are unchanged across all treatment groups. Fluorescence of MitoSOX™ normalized to cell number (nm/cells/mL), indicative of mitochondrial superoxide in cells treated with each nutrient condition after 6 hours. Cells were treated with control, 12.5 mM glucose, 15 mM fructose, 1 mM PA/OA and Western diet (1 mM PA/OA + 12.5 mM glucose + 15 mM fructose) media. Statistical significance was determined using a One-Way ANOVA followed by a Tukey's test. Means followed by the same letter are not significantly different ($p<0.05$) according to Tukey's test. N=5. Box plot legend: median (midline), box (25th–75th percentile), whiskers (extrema).

3.4.3 DCFDA assay analysis of total reactive oxygen species

To determine the effect of different nutrient conditions on the oxidative status of the cells, a DCFDA assay was used to analyze measures of total reactive oxygen species (ROS). This assay measures the ability of all ROS (hydroxyl, peroxyl, and other free radicals) to oxidize DCFDA to DCF, resulting in fluorescence. Following live cell imaging, there seemed to be an increase in fluorescence observed in both the PA/OA and WD cells compared to control-, glucose-, and fructose-treated cells (**Fig. 3.4.3-1**); however, upon observation, it was difficult to conclude if the magnitude of this fluorescence was significant. As such, DCFDA fluorescence was measured using a microplate reader and normalized to cell number to corroborate these results.

Cells treated with PA/OA exhibited a significant increase in fluorescence compared to control cells, indicating that there was an increase in the amount of total ROS in these cells ($p<0.05$; PA/OA: 0.096 ± 0.005 nm/cells/mL vs. Control: 0.066 ± 0.006 nm/cells/mL) (**Fig. 3.4.3-2**). Additionally, when compared to both glucose- and fructose-treated cells, the PA/OA treatment displayed a significant increase in ROS products ($p<0.05$; PA/OA: 0.096 ± 0.005 nm/cells/mL vs. Glucose: 0.067 ± 0.003 nm/cells/mL vs. Fructose: 0.065 ± 0.006 nm/cells/mL) (**Fig 3.4.3-2**). There were no significant changes in fluorescence in both sugar groups when compared to control and to each other as the values were similar (Control: 0.066 ± 0.006 nm/cells/mL vs. Glucose: 0.067 ± 0.003 nm/cells/mL vs. Fructose: 0.065 ± 0.006 nm/cells/mL) (**Fig. 3.4.3-2**).

In regard to the WD treatment, there was a significant increase in ROS products observed when compared to control cells ($p<0.05$; WD: 0.099 ± 0.009 nm/cells/mL vs. Control: 0.066 ± 0.006 nm/cells/mL) (**Fig. 3.4.3-2**). This increase was also found to be significant in the WD-treated cells when compared to the glucose treatment ($p<0.05$; WD: 0.099 ± 0.009 nm/cells/mL vs. Glucose: 0.067 ± 0.003 nm/cells/mL), and to the fructose treatment ($p<0.01$; WD: 0.099 ± 0.009 nm/cells/mL vs. Fructose: 0.065 ± 0.006 nm/cells/mL) (**Fig. 3.4.3-2**). There were no significant differences observed between the PA/OA and WD-treated cells in regard to ROS products as values were comparable to each other (PA/OA: 0.096 ± 0.005 nm/cells/mL vs. WD: 0.099 ± 0.009 nm/cells/mL) (**Fig. 3.4.3-2**).

Control
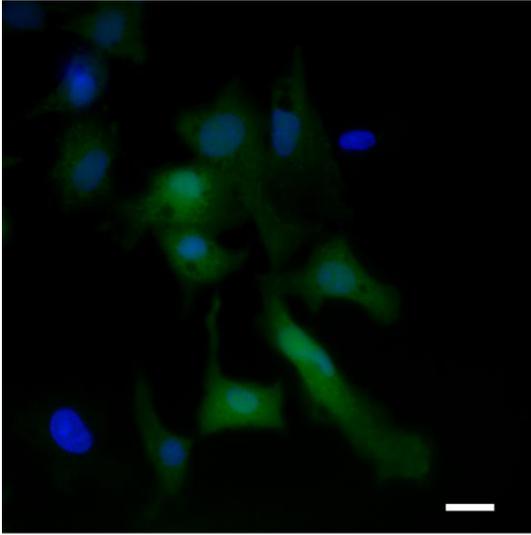
Glucose
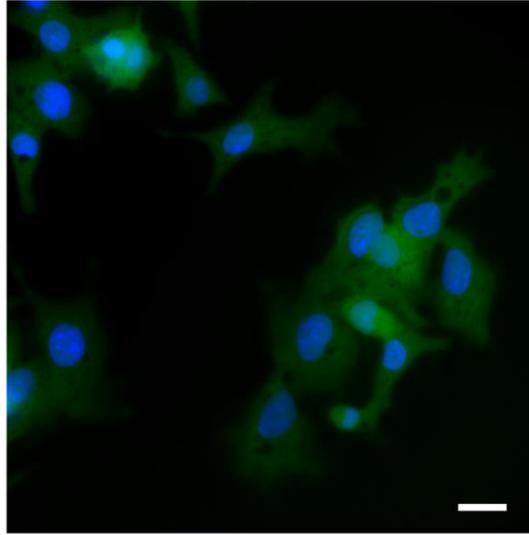
Fructose
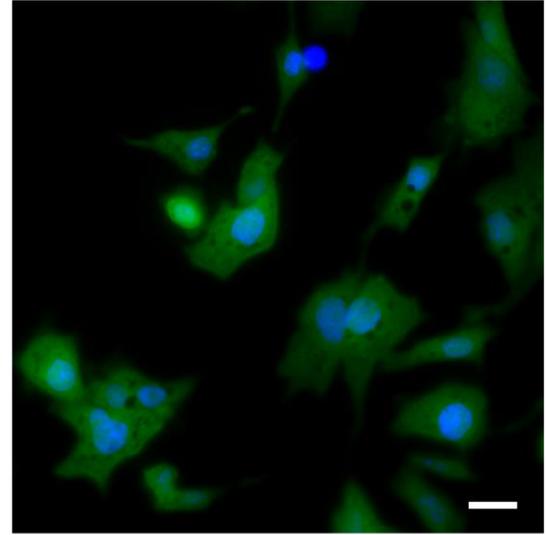
PA/OA
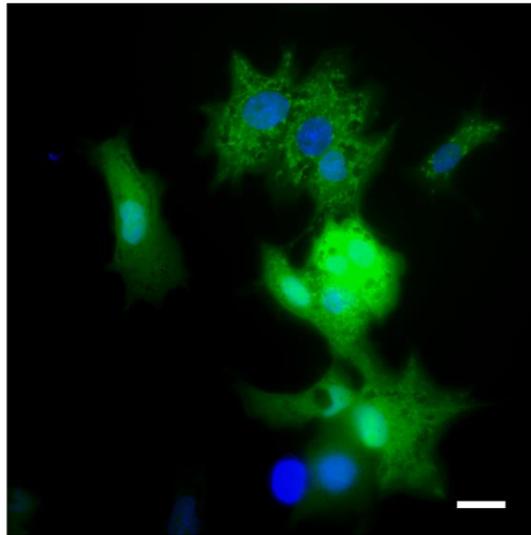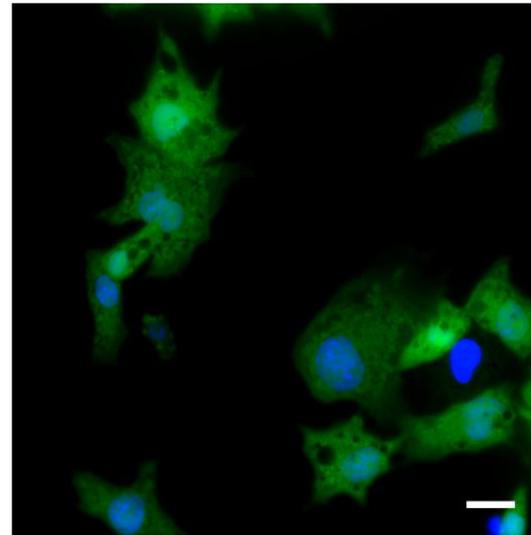
Western

Figure 3.4.3-1. High-fat and Western diet media displayed increased fluorescence of ROS products. Representative fluorescence microscopy images of DCFDA staining of total ROS in HepG2 cells treated with control, 12.5 mM glucose, 15 mM fructose, 1 mM PA/OA, and Western diet (1 mM PA/OA + 12.5 mM glucose + 15 mM fructose) media for 6 hours. Cells were counterstained with Hoechst 33342 and images were taken at 60X using a Nikon Eclipse Ti2E Inverted Deconvolution Microscope. Scale bar = 20 μm.
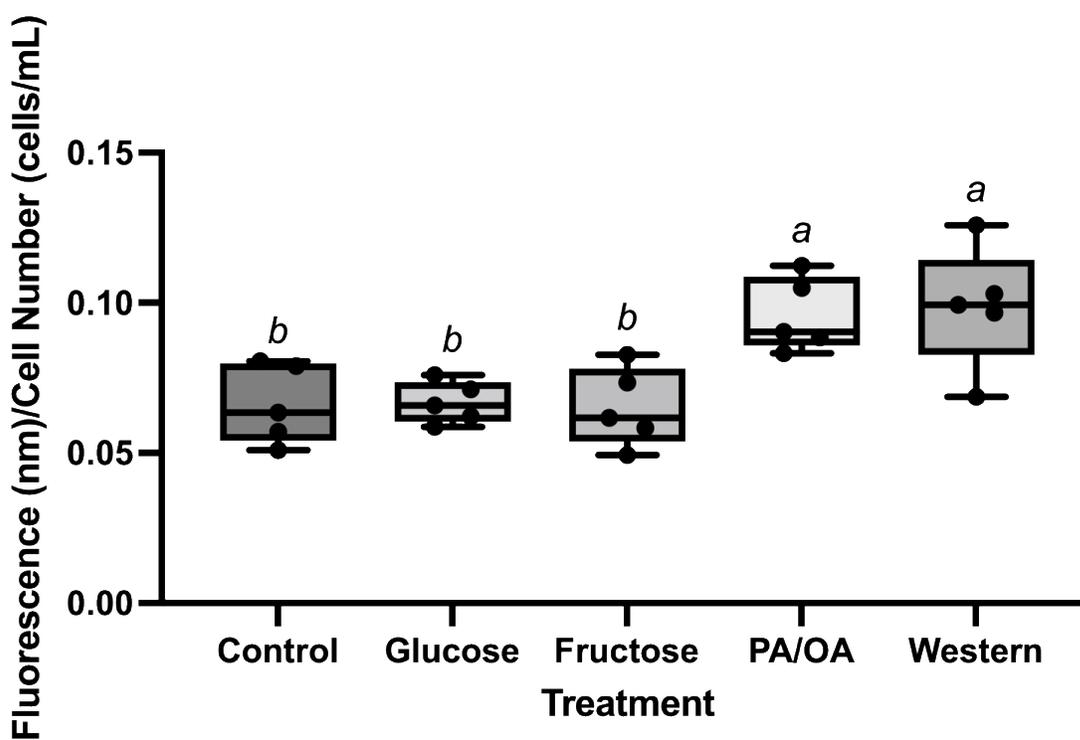
Figure 3.4.3-2. High-fat and Western diet media cause an increase in total ROS products. Fluorescence of DCFDA normalized to cell number (nm/cells/mL), indicative of total ROS products in cells treated with control, 12.5 mM glucose, 15 mM fructose, 1 mM PA/OA and Western diet (1 mM PA/OA + 12.5 mM glucose + 15 mM fructose) media for 6 hours. Statistical significance was determined using a One-Way ANOVA followed by a Tukey's test. Means followed by the same letter are not significantly different ($p<0.05$) according to Tukey's test. N=5. Box plot legend: median (midline), box (25th–75th percentile), whiskers (extrema).

Chapter 4: Discussion

4.1 Impact of individual nutrient components on hepatocytes

4.1.1 Development of steatosis in NAFLD

Adherence to the Western dietary pattern is associated with hepatic lipid accumulation, as the excessive intake of fatty acids and sugars contribute to the development of steatosis[47] – the first stage of NAFLD. To investigate the impact of nutrient components individually and combined on the development of a NAFLD model, cells were treated with media supplemented with a palmitic and oleic acid mixture (PA/OA), glucose, fructose, and a Western diet (WD)-like media (PA/OA + glucose + fructose). Cells were then analyzed based on the level of steatosis present through Oil Red O and triglyceride measurements to determine the feasibility of the model, and to discern how each nutrient component contributed to its development.

Following treatment, high-fat and WD-treated cells displayed an increase in the accumulation of lipid droplets and triglycerides (**Fig. 3.1.1-1 & 3.1.2-1**). This indicated that these treatments were able to induce steatosis, effectively establishing the model of NAFLD. In contrast, both high-fructose and glucose conditions were unable to cause steatosis on their own; however, morphological changes were observed following treatment. Both the fructose and glucose groups presented with intracellular swellings, which was observed in the WD treatment, but not in the PA/OA treatment (**Fig. 3.1.1-2**). Additionally, in regard to lipid droplets, the WD group exhibited increased lipid droplet accumulation compared to control, glucose, and fructose treatments.

The results presented here suggest that the high-fat and WD treatments cause an imbalance in the regulatory processes of triglyceride and lipid droplet formation. This is supported by work done in animal models of NAFLD, where short-term exposure to high-fat and the WD caused significantly steatotic livers in rodents[9,150]. Additionally, in pre-steatotic models, short-term exposure to a WD displayed an increase in the number and frequency of lipid droplets, further supporting this work. *In vitro* studies in HepG2 cells have also found that the increased exposure of cells to media supplemented with fatty acids, such as oleate and palmitate, significantly induce steatosis[227,254,255].

As many studies have stated that increased sugar intake, specifically of fructose, causes lipid accumulation in animal models and HepG2 cells[33–36,234,256], the results in this study, although unexpected, revealed that fructose and glucose were unable to cause steatosis on their own. However, due to the increase in lipid droplet formation in the WD treatment, the sugars may be contributing to this change rather than triglyceride accumulation[257]; and overall, the treatment duration used may limit the ability of fructose and glucose to cause steatosis, indicating that dietary fat is important in establishing steatosis in early NAFLD[258]. Additionally, the majority of previous studies have treated cells for time periods ranging from 24–48 hours and have induced glucose uptake with insulin[227,234,259]. As such, the longer time frame of treatment, paired with insulin induction, may play a role in the development of steatosis in sugar treatments, which was not observed in this study. Evidence also points to a greater activation of *de novo* lipogenesis (DNL) in hyperinsulinemic obese patients, as it has been proposed that DNL is more significant after longer time periods of sustained nutrient intake and energy imbalances[260]. While it can be concluded that high fats are contributing to steatosis development through triglyceride accumulation in early NAFLD, at this point in time, the sugar treatments may not yet be significantly activating lipogenic pathways, which is supported by the unchanged expression of DNL genes observed (*FASN, ACACA, SCD1*; **Fig. 3.2.2-2**).

Collectively, these results indicate that with consumption of the WD, the majority of fat accumulation seen in hepatocytes during early stages of NAFLD are attributable to the excessive intake of fatty acids. While increased sugar intake plays a larger role in the induction of DNL during hyperinsulinemic states[73], overall, in the case of basal insulin levels, glucose and fructose consumption alone are not sufficient to cause steatosis. However, although inconclusive, these sugars may cause morphological changes in the cells, and may account for the increased accumulation of lipid droplets in the WD, which was not observed in the PA/OA treatment. These results also support the notion that while the quantity of macronutrients have negative effects on hepatocytes, the quality of nutrients consumed may be of more importance as their individual effects may work in tandem to contribute to the detrimental outcomes often seen in WD-induced NAFLD.

4.2   Signaling pathways in early NAFLD

4.2.1 *SREBP* expression

Sterol regulatory element binding proteins (SREBPs) are an important family of transcription factors that are involved in the maintenance of lipogenesis in the liver[4,97]. These proteins are highly implicated in NAFLD pathogenesis; and, the expression of these genes were examined in this study using qRT-PCR analysis. Although unexpected, no changes were observed in the expression of *SREBP-1c* and *SREBP-2* isoforms across all treatment groups (**Fig. 3.2.1-2**); however, there was a decrease in the expression of *SREBP-1a* observed in both the PA/OA and WD treatments when compared to fructose alone (**Fig. 3.2.1-1**). This change in *SREBP-1a* expression was significantly decreased in the PA/OA group compared to control, suggesting that the fructose supplement in the WD treatment may account for its slightly higher expression in this group. It can also be speculated that *SREBP-1a* mRNA expression is decreased in these treatments as a result of high protein levels of mature n-SREBP-1a; however, protein levels were not investigated in this study and additional research is needed to further characterize this effect.

It is widely accepted that the expression of SREBPs are regulated by nutritional changes, as well as through the nuclear receptor, LXRα[110]. However, no changes in *LXRα* gene expression were observed across all treatment groups (**Fig. 3.2.2-3A**), indicating that *SREBP-1a* expression was changed in response to nutrient excess. While SREBP-1c is preferentially activated by increased carbohydrates and increased insulin levels, SREBP-1a and -2 are activated in response to sterols[99]. Many studies have examined the ability of fatty acid saturation to activate or inhibit SREBP activity and have found that PA treatment alone in HepG2 cells significantly enhances the expression of *SREBP-1c*[261,140] and *SREBP-2*[259]; while Chen et al. found this expression can be subsequently downregulated after administration of PA/OA treatment[261]. Although *SREBP-1a* was not investigated in the previous study, it has been reported that unsaturated fatty acids can directly inhibit both *SREBP-1c* and *-1a* isoforms[137,138]. This suggests that the oleic acid content in the fatty acid mixture is acting to inhibit the PA-induced upregulation of these genes, accounting for the decreased expression of *SREBP-1a* observed in high-fat and WD cells in this study.

Additionally, since *SREBP-1a* possesses a longer transactivation domain compared to *SREBP-1c* and *-2*, the *-1a* isoform is the most potent activator of all SREBP target genes in both fatty acid and cholesterol biosynthetic pathways[124]. While this study did not observe significant changes in expression of the majority of SREBP target genes (*FASN, ACACA, SCD1, G6PD, HMGCR*; **Fig. 3.2.2-2**), it is speculated that over time, fructose may contribute to activation of the *-1a* transcript and its target genes in the WD treatment[135], resulting in inappropriate activation of lipogenic and cholesterolgenic genes. However, this warrants further research to characterize the underlying mechanism of action.

While the majority of NAFLD studies have focused on the SREBP-1c isoform[107–109,115,116,119–122,130–132,135,139,143], few have examined the effects of SREBP-1a[101,125]. This is likely due to the fact that induction of SREBP-1c is greatly dependent on insulin spikes after feeding, especially in the obese and T2DM phenotypes[116]. As such, the activation of all SREBP isoforms in the context of lean NAFLD have not been well studied, especially under non-hyperinsulinemic conditions. Together, this study sheds light on the activation of these pathways and suggests that the *SREBP-1a* isoform should not be ignored as it may be of more importance in the early stages of NAFLD. While evidence has shown that fructose-rich diets are strong activators of SREBP-1c and lipogenesis[133–135], this was not observed in this study; however, it may have the ability to alter *SREBP-1a* expression. Although this model did not capture later stages of the disease, this data suggests that the fructose component of the diet under basal insulin levels may cause activation of *SREBP-1a*. This activation may have implications on lipogenic pathways in the WD treatment, and subsequently, on the development of steatosis.

4.2.2 Insulin signaling pathways and inflammation

Inflammation and the dysregulation of insulin signaling, specifically the PI3K and MAPK pathways, are a known contributor to NAFLD pathogenesis[262]. As such, *TNFα, IRS1, PI3K*, and *KRAS* transcript levels were analyzed in this study using qRT-PCR. No changes in expression were observed in all four genes (**Fig. 3.2.2-3B-E**), indicating that these pathways were not yet dysregulated in the early stages of NAFLD.

It was important to classify whether the dysregulation of these pathways was occurring in early stages of NAFLD, specifically through non-hyperinsulinemic and nutrient-excess feedback

systems. These pathways are activated by IRS1/2, which is often stimulated by insulin, revealing its important role in the regulation of carbohydrate and lipid metabolism[146]. However, evidence has shown that insulin-independent feedback also contributes to the dysregulation of these pathways in metabolic diseases, such as NAFLD, as lipids and inflammatory mediators can phosphorylate IRS1/2 at the same sites as insulin, and at additional sites[147]. In support of the results in this study, rats fed a high-fructose diet exhibited no changes in *IRS1* levels[263]. Interestingly, the PI3K pathway can influence the proteolytic processing of SREBP-1[264], and both PI3K and KRAS can effect lipogenesis through activation of SREBP-1, especially in HCC – the end stage of NAFLD[265,266]. Studies have revealed that SREBP-1 expression is significantly higher in HCC as well[267]. This work, paired with my results, indicate that dysregulated insulin signaling and activation of SREBP-1 may be increasingly significant in later stages of NAFLD.

Monounsaturated fatty acids (MUFAs), such as oleic acid, are known to promote metabolic health when consumed in moderation[11]. In contrast, saturated fatty acids (SFA), like palmitic acid, contribute to weight gain and inflammation, and successfully induce insulin resistance[268,269]. Oleic acid has been shown to prevent SFA-induced inflammation as it can reduce the levels of inflammatory cytokines such as TNFα[268], which remained unchanged across all treatment groups in this study (**Fig. 3.2.2-3E**). However, there was a ~1.2-fold increase in *TNFα* expression in both the Western diet and fructose treatments, which was not significant (**Fig. 3.2.2-3E**). Importantly, the absence of this cytokine further establishes the early NAFLD model in this study as inflammation is a key component of steatosis progression to NASH[72,221].

Taken together, these results reveal that the insulin signaling pathways are not yet dysregulated in early stages of NAFLD. Moreover, it is unclear whether the absence of inflammation in these cells was due to the protective action of OA, or if the slight increases seen may be attributable to the fructose component in the WD treatment; however, it is likely that inflammation is not yet present in the current NAFLD model system.

4.2.3 *LDLR* expression

The dysregulation of cholesterol metabolism has been linked to NAFLD, along with progression to more severe stages of the disease such as NASH[153,154]. Cholesterol homeostasis relies heavily on the SREBP target gene, LDLR, to regulate cholesterol at the cellular level.

While many SREBP target genes were investigated in this study using qRT-PCR, changes were only observed in *LDLR* gene expression. Significantly, upon glucose treatment, cells exhibited a decrease in *LDLR* expression compared to both the control and WD-treated cells (**Figure 3.2.2-1**).

Compared to triglyceride metabolism, cholesterol metabolism has not been studied as extensively in NAFLD, especially in the context of carbohydrate metabolism[270]; however, it is now understood that the metabolism of glucose can interact with cholesterol absorption and synthesis. In healthy individuals following a meal, increased insulin levels promote the uptake of glucose into the liver[271], which is stored as glycogen. However, in insulin-resistant or hyperinsulinemic states, gluconeogenesis cannot be inactivated, causing an increase in glucose production. As the liver cannot store the excess glucose, it is shuttled toward glycolysis, providing pyruvate, the precursor for acetyl-CoA formation, which can then be converted into either FFAs or cholesterol[272]. Although LDLR protein levels were not examined in this study, my work, combined with the work of previous studies, show that under non-hyperinsulinemic conditions, a decrease in the *LDLR* may contribute to reduced cholesterol uptake to counter the potential increase in its synthesis. This would be expected due to its mechanism of action and regulation by SREBPs. Interestingly, in non-diabetic men, high plasma glucose levels are associated with lowered cholesterol absorption and increased synthesis[270,273]. Additionally, MetS subjects fed a diet composed of rye bread and pasta – which has been associated with a decreased postprandial insulin response[274,275] – displayed a positive correlation to cholesterol synthesis, while inhibiting cholesterol absorption[163]. Collectively, this suggests that when exposed to high levels of glucose/carbohydrates in non-hyperinsulinemic states, this may cause an increase in the synthesis of cholesterol paired with a decrease in its uptake through changes in the LDLR feedback system. However, future studies should incorporate protein analysis, as well as measures of cholesterol for further clarification.

The *LDLR* is a key target gene of SREBPs, more specifically for SREBP-2; although SREBP-1a has the ability to activate all SREBP genes, including *LDLR*[162]. Perhaps *SREBP-1a*, as discussed in the previous section, may be acting on the *LDLR* in the WD treatment. In many mouse models of NAFLD and NASH, the expression of LDLR in hepatocytes is enhanced, resulting from an increase in SREBP-2 activation[199,216,276]. Additionally, in mice fed a

methionine- and choline-deficient diet – a diet that causes steatohepatitis and induces low serum insulin levels – there was no upregulation of the LDLR in hepatocytes[276]. Together with my results, these studies demonstrate the role that both hyperinsulinemia and excessive nutrient consumption play in the dysregulation of hepatic cholesterol homeostasis. With hepatic cholesterol stores already increased in NAFLD livers[153,154], hyperinsulinemia can cause prolonged, non-physiological expression of LDLR, resulting in further cholesterol uptake into cells[276]. While the results of this study are inconclusive, it can be speculated that insulin is unlikely the only mediator of dysregulated cholesterol metabolism in early NAFLD, as excess nutrient components are shown to alter *LDLR* expression as well. My work also points to a potential mechanism at which the level of cholesterol metabolism may become dysregulated in response to excess nutrient consumption.

While the majority of previous studies were done in NASH models, this suggests that dysregulation of the LDLR becomes more apparent in later stages of the disease, especially under hyperinsulinemic conditions. In the context of this research, during the early stages of NAFLD and in response to dietary insults, the expression of *LDLR* in the WD treatment is not downregulated as seen in glucose-treated cells. The excess glucose may be shuttled towards cholesterol synthesis, effectively downregulating *LDLR* expression to avoid further uptake and synthesis of cholesterol. If glucose is causing an increase in intracellular cholesterol, this effect may also be apparent in the WD treatment; however, the same effect was not observed in that *LDLR* expression levels were unchanged. Perhaps in lean NAFLD progression, failure to downregulate the *LDLR* may be a potential mechanism that leads to increased uptake and accumulation of free cholesterol, causing significant damage to cells in this disease.

4.2.4 *PLIN2* expression

An increase in lipid droplet formation can significantly contribute to steatosis as they play a large role in hepatic lipid metabolism[167,277]. Perilipin 2 (PLIN2), a lipid droplet surface binding protein, has been highly implicated in NAFLD pathogenesis as it can promote triglyceride accumulation, while inhibiting fatty acid oxidation[177,178]. To determine if *PLIN2* expression was influenced by nutrient components in the early stages of NAFLD, qRT-PCR analysis was used. It was found that with exposure to the high-fat and WD treatments, the

expression of *PLIN2* was significantly increased compared to all other treatment groups (**Fig. 3.2.3-1**).

Similar to the model in this study, other studies with HepG2 cells using treatments of PA/OA[278], and fructose and glucose[256], found that PLIN2 expression was increased and was stated to be "the most comprehensive marker of lipid accumulation"[256]. Perilipin expression is common in many steatosis models, and specifically, PLIN2 is the most upregulated perilipin in rodents and humans with NAFLD[167]. The enhanced *PLIN2* expression in this study is further supported by obese mice models, where a high-fat diet induced increases in *PLIN2* mRNA in the presence of steatosis[277]. While protein levels of PLIN2 were not investigated in this study, it seems that transcription of *PLIN2* is more important in earlier stages of NAFLD. This is supported by studies in which prolonged WD-like treatment (48 hours) in HepG2 cells displayed no changes in *PLIN2* mRNA levels; however, PLIN2 protein levels were significantly increased[256]. Additionally, after 30 weeks of WD feeding, there were no significant changes in hepatic *PLIN2* mRNA levels in mice[181]; and upon further observation of obese and insulin resistant animals, PLIN2 was involved in hepatic inflammation and fibrosis[181], which are hallmarks of NAFLD progression to NASH. Collectively with my work, these results suggest that the increase in *PLIN2* gene expression is important during the early stages of steatosis development, and is less important once steatosis is already present, most likely due to early lipid droplet formation.

As triglycerides accumulate within hepatocytes during steatosis, these triglycerides are stored in lipid droplets. When there is an imbalance in lipid droplet formation and mobilization, this can further accentuate lipid accumulation in NAFLD[277]. As shown in my study, cells treated with both PA/OA and WD media displayed an increased accumulation of lipid droplets (**Fig. 3.1.1-1**) and triglycerides (**Fig. 3.1.2-1**), which was correlated with the increased expression of *PLIN2*. Due to the increased significance in which the WD treatment accumulated neutral lipid droplets compared to control, which I presume is caused by the sugar components, this may account for the larger fold-change in *PLIN2* gene expression observed when compared to the PA/OA group. This suggests that *PLIN2* expression is strongly enhanced by dietary FFAs, and to a lesser extent by dietary sugars, to accommodate for increased lipid droplets in both conditions. While the mechanism behind lipid droplet formation in this study was not investigated, I can

speculate how this may be occurring as excess triglyceride storage in lipid droplets tends to occur through these three mechanisms: (1) increased triglyceride synthesis paired with lipid droplet growth/biogenesis; (2) decreased lipid droplet catabolism with decreased fatty acid oxidation; and (3) impaired secretion of triglycerides or VLDLs[167]. Overall, the increased expression of *PLIN2* in both the PA/OA and WD treatments, paired with the observed increase in triglyceride accumulation under non-hyperinsulinemic conditions, may shed light on the role of *PLIN2* in early steatosis development.

Lipid droplets are also important in protecting cells from lipotoxicity; however, an increase in lipid droplet formation favours the increased storage of lipotoxic lipids, exacerbating their effects on hepatocytes as hepatic lipid stores can incorporate FFAs from various sources[277]. Additionally, changes in glycerophospholipid ratios, which is commonly observed in NAFLD and NASH patients[280], causes increased package defects in lipid droplet monolayers, which results in the formation of unstable lipid droplets[281]. This can contribute to a decrease in VLDL secretion and stabilization, causing hepatic lipid accumulation, and consequently, lipotoxicity[282]. These package defects may be further exacerbated by an increased flux of FFAs from the diet, as neutral lipids in the lipid droplet core can intercalate into the monolayer, causing hydrophobic patches on the lipid droplet surface[277]. Although lipid droplet composition was not studied in this work, it is interesting that the expression of PLIN2 is important for establishing and stabilizing lipid droplet compartments[278]. As an increased flux of FFAs are entering the endoplasmic reticulum (ER) – where lipid droplet formation occurs – to be processed, perhaps *PLIN2* expression is increased to not only prevent the formation of lipotoxic species, but to also aid in the stabilization of defective lipid droplets in NAFLD and steatosis development.

This does not, however, explain the increase in SREBPs that is commonly observed in this disease. Interestingly, a PLIN2 deletion in WD-fed mice exhibited significant decreases in all SREBP isoform mRNA levels[283,284]. These decreases in SREBP expression were also evident in control diet-fed PLIN2-null mice, further supporting the notion that PLIN2 may contribute to the regulation of lipid metabolism in the absence of obesity[284]. From these results, an increase in SREBP mRNA levels would be expected along with *PLIN2*; however, I observed the opposite effect in that *SREBP-1a* expression was decreased in the PA/OA and WD treatments. This may indicate that induction of SREBP transcription by PLIN2 may occur at later stages in the disease,

as this effect was not present in my cell model, or that this activation may be insulin-dependent. Additionally, SREBP activation has been shown to affect glycerophospholipid synthesis in non-mammalian organisms[285–287], pointing to SREBPs as important regulators in membrane lipid biogenesis[141,287,288]. Perhaps SREBPs are activated by PLIN2 in order to further stabilize the lipid droplets, which also becomes maladaptive in that more lipids are produced through DNL.

Although inconclusive, I speculate that in the early stages of NAFLD, an increase in *PLIN2* mRNA may be a crucial event in the development of steatosis. While I have shown that during times of nutrient excess, the activation of *PLIN2* is correlated with increased triglyceride and lipid droplet accumulation, I propose that the formation of lipid droplets occurs to protect cells from lipotoxicity, which may be maladaptive. This may also lead to the degradation and decreased secretion of VLDLs, causing hepatic lipid accumulation. Overall, this work points to the important role of PLIN2 in NAFLD and provides a potential marker of early steatosis development before metabolic comorbidities complicate this disease.

4.3 Impact of nutrient components on lipid metabolism and cell number

4.3.1 Changes in lipid metabolism

Dysregulated hepatic lipid metabolism significantly contributes to the development of steatosis, and consequently NAFLD, resulting from the imbalance between FFA uptake, synthesis, export, and degradation[41–43]. To evaluate changes in metabolism, an MTT assay was conducted to determine how individual nutrient components may effect metabolic processes in hepatocytes. I found that the activity of cells treated with PA/OA media displayed a significant increase in activity compared to all treatment groups (**Fig. 3.3.1-1**). While the WD treatment seemed to be increased compared to control- and glucose-treated cells, this increase in activity was significant when compared to cells treated with fructose only (**Fig. 3.3.1-1**).

In the MTT reaction, the tetrazolium salt is reduced to form formazan crystals, which is heavily dependent on metabolically active cells[252]. The measured OD values are accepted as the representation of formazan concentration and therefore the capacity of cells to reduce MTT[252]. Many studies have wrongfully applied the MTT assay to measure mitochondrial activity[252,289], as other studies have shown the localization of the reduced formazan crystals in various intracellular organelles such as in the ER and cytosolic lipid droplets[289,290]. It has been assumed

that MTT is reduced in the mitochondria, allowing this assay to be a suitable indicator of mitochondrial function and activity. This is concerning given that evidence shows the majority of MTT is reduced in the cytoplasm by NADPH and dehydrogenases associated with the ER[291]. Interestingly, a study done by Stockert et al. found that MTT formazan tends to accumulate in the cytoplasm first, with none of this product appearing in the lysosomes or the mitochondria[289], suggesting MTT reduction is unlikely in these organelles. Additionally, following treatment with oil to form lipid droplets, the MTT formazan product was increasingly abundant within the lipid droplets compared to untreated cells[289]. A similar effect may be occurring in this study as the only treatments associated with increased triglyceride and lipid droplet formation (PA/OA and Western diet) displayed increases in formazan levels. This supports the notion that an increase in lipid droplet formation within the ER may be associated with the increased MTT signal observed.

While it is assumed that MTT reduction occurs through the activity of mitochondrial dehydrogenases in living cells[292], previous studies have found that HepG2 treatment with PA causes a significant decrease and changes in oxidative phosphorylation (OXPHOS) enzyme activity, while this activity remains unchanged in OA-treated cells after 24 hours[293,294]. Along with my work, these results further suggest that this diet-induced increase in MTT reduction may not be a result of mitochondrial OXPHOS activity, but may be from another source. Since MTT is cationic, following its uptake into cells, it is likely to bind to anionic sites[289], such as the phosphate groups associated with the ER (membrane phospholipids, ribosomal RNA). Consequently, this would result in a quick and easy reduction of MTT by ER dehydrogenases[289], and suggests that the increased amount of formazan observed in my study may be a result of enhanced ER activity in lipid metabolism. While increased lipid droplet accumulation was evident in this study, this offers further support for the idea that these droplets may also be large reservoirs for formazan produced from the MTT reaction.

During the early stages of NAFLD, there is a compensatory increase in mitochondrial activity, and this activity is altered to protect hepatocytes from the harmful effects caused by lipid storage[189], which becomes maladaptive as this results in the increased production and accumulation of ROS[189,199]. This is supported by my work as increases in lipid droplet accumulation with a concomitant increase in *PLIN2* expression were observed, along with

increased activity in PA/OA and WD cells. Although it is unclear whether this increased activity is occurring in the mitochondria or ER, I cannot dismiss the possibility that in the early stages of NAFLD, steatosis may be a protective mechanism in order to prevent further liver damage in NAFLD progression[44], and that this effect may be due to compensatory mechanisms in the mitochondria. Equally compelling is the idea that mitochondrial activity may not yet be compensating for the increase in lipid droplet formation in this acute culture system.

While sugars can contribute to lipotoxic species, my results show that at this point in time, the FFAs in the PA/OA treatment are contributing to the increased activity observed. This activity may be manifesting as changes in ER lipid metabolism and homeostasis, which has the potential to lead to lipotoxic species and ER stress[295]; as the formation of lipid droplets in the ER serve as a convenient space to sequester toxic lipids and proteins that accumulate within the ER network[296]. While the source of increased activity remains to be resolved, I can speculate that in early stages of NAFLD under basal insulin levels, lipid droplet formation is an important process in the maintenance of ER homeostasis and to protect against lipotoxic species. It is interesting to note that these changes are observed in the absence of hyperinsulinemia, illuminating the detrimental effects of individual dietary components on liver lipid metabolism. This notion further supports the idea that lipid droplet formation is a key event in the development of steatosis, although it may be maladaptive; as over time, constant insults from oxidative stress and increased lipid droplet formation can lead to NAFLD progression.

4.3.2 Cell number

The metabolically demanding process of cell division requires large amounts of energy to occur[297], and the decision to undergo this process is mediated by the cell's metabolic status and availability of nutrients. While metabolism changes significantly during the cell cycle, it has been found that metabolism can also regulate cell cycle progression. Cell number was analyzed in this study under each nutrient condition, and interestingly, there was a significant decrease in cell number observed in the PA/OA and WD treatments compared to cells treated with glucose and fructose (**Fig. 3.3.2-1**). This decrease was also significantly different from that of the control group when compared to the PA/OA treatment.

A commitment to enter the cell cycle is successful when sufficient nutrients are available[297]. In this study, both sugar treatments displayed the highest cell number counts, and as expected, these macromolecules undergo glycolytic metabolism, thereby promoting proliferation. Proliferating cells prefer to use glycolysis for macromolecule biosynthesis through the pentose phosphate and serine biosynthesis pathways[298], while non-proliferating cells use mitochondrial OXPHOS[299]. However, expression of the rate-limiting enzyme of the pentose phosphate pathway, *G6PD*, remained unchanged, suggesting glucose and fructose were not shuttled toward this pathway (**Fig. 3.2.2-2E**).

In line with my work, studies have shown that HepG2 incubation with OA and PA significantly inhibit cell growth[300]. Others have shown that inhibition of cell growth in HepG2 cells is not induced by lipid peroxidation, but by changes in fatty acid metabolism[301], as speculated in the previous section. While it is widely accepted that PA can induce apoptosis and trigger ER stress in HepG2 cells[228,236], OA is anti-apoptotic in nature and seems to be more important for the accumulation and formation of triglycerides[204,227,236,302,303]. While MUFAs are known to promote metabolic health[11,15,16], this offers further support for the observed increase in triglycerides and lipid droplets in this cell model as a defense system against the pro-apoptotic effects caused by large amounts of FFAs in cells[228,303], which is likely attributable to the SFA intake in the WD. Taken together, this work suggests that lipotoxic intermediates may be present in both the PA/OA and WD treatments, effectively halting the cell cycle and causing a lower cell count. However, lipotoxic intermediates were not investigated, therefore it is equally important to consider that changes in fatty acid metabolism may be altering cell cycle progression in these treatments; which may be of more importance in this model considering our MTT assay may suggest increased lipid metabolism in the ER.

It has been speculated that the presence of lipid droplets is incompatible with cell proliferation, as their accumulation is associated with liver regenerative processes and not cell division[304]. This notion is supported by my results in that both groups exhibiting increased triglyceride and lipid droplet accumulation (PA/OA and WD) displayed decreases in cell number. Additionally, in obese/diabetic mouse models, animals exhibit impaired cell cycle progression in hepatocytes following liver regeneration[304,305], as steatosis and lipid droplet accumulation can reduce proliferation and negatively regulate cell division in

hepatocytes[304,306,307]; a mechanism of action in my study. Interestingly, these steatotic effects on the cell cycle remain with no changes in serum concentrations of insulin[306,307], which is pro-proliferative in nature. Together, along with my results, this supports the idea that regardless of insulin concentrations, high-fat content within the liver may affect the cell cycle, and possibly lead to decreased cell proliferation. Although previous studies investigated cell cycle effects in obese models, my work demonstrates that this phenomenon may also be present in the onset of NAFLD, before metabolic comorbidities arise.

Overall, it is speculated that a dysregulation in lipid metabolism is greatly influencing cell division and proliferation in early stages of NAFLD. This work highlights that high fat content can disrupt cell number even in the absence of hyperinsulinemia, although it may be occurring through various unknown mechanisms. This is concerning given that these effects may occur in otherwise healthy individuals in response to dietary insults, revealing the threat posed by increased intake and habitual consumption of the WD to cellular processes.

4.4   Induction of ROS in lipid accumulation

4.4.1 Sources of ROS

The presence of oxidative stress and the overproduction of ROS throughout the stages of NAFLD has been described as central factors involved in its pathogenesis[189]. To determine how excess nutrients can affect ROS production and if ROS is involved in the early stages of NAFLD, assays were used to measure the amount of ROS in the cells. A DCFDA assay was used to measure total ROS levels, followed by MitoSOX™ to determine if the source of ROS was mitochondrial, and finally an antioxidant assay to assess if changes were occurring at the antioxidant level. It was found that total ROS levels were increased in the PA/OA and WD cells compared to all other treatments (**Fig. 3.4.3-2**), with no changes observed in both the MitoSOX™ (**Fig. 3.4.2-2**) and antioxidant assay (**Fig. 3.4.1-1**).

The mitochondria are considered as the "most quantitatively relevant ROS generators" in the cell[42,192,193] and have been recognized as the most important source of ROS in NAFLD pathogenesis[192–194]. One way in which the mitochondria deal with increases in FFAs is by activating mitochondrial β-oxidation to prevent further accumulation of lipids within the liver[195]. However, no changes in the gene expression of enzymes involved in the β-oxidation pathway

were observed, indicating that this compensatory mechanism was not yet activated in the cells (**Fig. 3.2.3-1**). Further, no changes in mitochondrial superoxide were detected, suggesting that the mitochondria may be resilient to changes in lipid metabolism during the early stages of NAFLD. This is supported by *in vivo* work where mice fed a high-fat diet for 4 weeks exhibited decreased activation of β-oxidation which was recovered after 8 weeks of feeding[308]. Others have shown that following both short- and long-term exposure to a high-fat diet, rodent livers do not present with drastic changes in mitochondrial bioenergetics[309]; and fluctuations in β-oxidation following palmitate treatment have also been observed[310,311]. Additionally, peroxisomal β-oxidation cannot be dismissed as during this process, electrons are not delivered to the electron transport chain (ETC), but are sent directly to oxygen, forming H_2O_2[42,44]. Peroxisomal β-oxidation in diet-induced obese mice has also been associated with inflammation, the hallmark of NASH, as well as increased expression of HCC genes[312]. While peroxisomes are a large source of cytoplasmic ROS and may be contributing to the effect observed in this cell model, the results in previous studies suggest that peroxisomal β-oxidation is increasingly significant in the progression of NAFLD[313], and therefore may be less apparent in this early NAFLD cell model.

While superoxide production is known to markedly increase in the presence of FFAs[314], this study did not observe significant changes in superoxide levels, which may be attributable to the shorter duration of treatment with FFAs, as the majority of studies used treatment regimens of 12–24 hours[293,294,314–316]. In HepG2 cells, palmitate has been associated with increases in ROS products such as H_2O_2[302], lipid peroxidation by-products[293,294,314], and ER stress[316], while oleic acid is shown to ameliorate these effects[293,316]. Additionally, these FFAs can incorporate into the inner mitochondrial membrane, causing increased membrane fluidity and increased electron leakage[42]. Through their incorporation into the mitochondrial membrane, these FFAs cause imbalances between the ETC and β-oxidation, further promoting superoxide production[42]. This study cannot dismiss mitochondrial superoxide completely in NAFLD progression; however, we can conclude that this source of ROS is not yet predominant in early stages of steatosis, and may be more apparent in later stages of this disease. While superoxide was not significantly increased in this study, we did observe an increase in total ROS products, suggesting that in early stages of NAFLD, ROS may be sourced from other organelles such as the ER or peroxisomes. Equally

compelling is that H_2O_2, most commonly measured through DCFDA assays, may be the predominant ROS species present in early NAFLD.

In regard to both sugar treatments alone, this study did not observe changes in total ROS products under basal insulin conditions. This contrasts previous studies as increases in ROS production were observed in response to fructose treatments administered under hyperinsulinemia[317], and under high glucose concentrations (25 mM)[294]. As such, my work reveals that this effect is not apparent under basal insulin levels at this point in time. This may have been due to the lower concentration of sugars used, as well as the shorter treatment duration. As such, it is reasonable to assume that under basal insulin levels in early steatosis development, the sugars are not yet contributing to the increased ROS in the WD treatment. Instead, this phenomenon is likely due to the high-fat component in the media, suggesting that FFAs may be initiating the first diet-induced insults in this disease in the context of ROS production.

The results in this study support the presence of an alternative source of ROS by providing evidence for the absence of significant mitochondrial superoxide levels in the beginning stages of NAFLD. While mitochondrial dysfunction in NAFLD has been viewed as the result of systemic decline and not a causative factor[42], this further adds to the idea that diet-induced ROS may originate elsewhere. Although this study did not investigate ER stress markers, this major source of ROS is reported to be upregulated in NAFLD and may be common to all stages of the disease, as it is prominent in the development of simple steatosis[209,318] and NASH[42]. Additionally, through ER-mitochondrial cross-talk during situations of oxidative stress, later stages of NAFLD may present with mitochondrial ROS products as a result. Importantly, the ER serves as the central communicator between all organelles, and it would be reasonable to believe that dysregulated ER activity and communication to other organelles would result in their dysfunction as well.

In regard to antioxidant levels, this study did not observe any changes in total antioxidant capacity of the cells, suggesting that antioxidant levels have not yet adapted to the increase in ROS at this stage in disease development. There tend to be discrepancies in the literature on antioxidant levels in NAFLD; however, the consensus is that antioxidants are generally

decreased in most NAFLD/NASH patients[42]. Due to the low-quality WD that lacks essential vitamins to counteract ROS products[5], it is possible that the available antioxidant mechanisms are not yet exhausted, or have not been activated. Additionally, this assay did not take into account individual antioxidant markers, therefore we cannot conclude whether dietary components cause changes in individual antioxidants as these effects may be masked in the assay. Future studies should be aimed at the nutrient-induced activation or inactivation of individual antioxidant markers that are commonly implicated in NAFLD.

Overall, these results point to the contribution of increased FFAs to the induction of ROS. Although the source of ROS is inconclusive, this study shows that total ROS levels are increased in early NAFLD under basal insulin conditions, and are not significantly sourced from the mitochondria. This work is meaningful in that it demonstrates the presence of ROS in beginning stages of this disease, providing a ripe environment for the deterioration of metabolic health, and illuminating the role of ROS throughout NAFLD disease progression; however, other sources of ROS must be considered for further clarification in future studies.

4.5 Limitations and Future Work

This study was unique in that it revealed the important role of individual dietary components on steatosis development in early NAFLD under basal insulin conditions. While some of these findings expand on current research in the field, it also adds significant knowledge to the underrepresented lean NAFLD population and the non-hyperinsulinemic side of the story. However, this study can only provide insight on the activity of one cell type during NAFLD pathogenesis. While I have shown that my cell culture model mirrors the characteristics observed in NAFLD, including key outcomes such as increased triglyceride and lipid droplet accumulation, changes in lipid metabolism, and increased ROS production, this study is not without its limitations. First, this study was carried out in a two-dimensional cell culture model and therefore does not account for the complexity of NAFLD at the organ level. This disease is complicated by many comorbidities such as insulin resistance, high blood pressure, hypertriglyceridemia, and impaired glucose tolerance, indicating the presence of multi-organ cross-talk involved in NAFLD, which was not captured in this study. Additionally, this tissue culture system only investigates hepatocytes, which is one of many major cell types in the liver; and there are various non-parenchymal cells that play a role in inflammatory processes during

the progression of NAFLD[225,319]. Together, these cell types form a functional hepatic unit that regulate key processes in physiological and pathological conditions[319]; and without them, this system does not recapitulate the behaviour and microenvironment of these cells *in vivo*. In future studies, co-culturing of hepatic stellate cells and hepatocytes may be useful for identifying the action of inflammatory cytokines in the progression of simple steatosis to NASH[225]. Additionally, to corroborate if the findings in this study are applicable to human NAFLD models, it will be important to validate these observations in primary human hepatocytes, which most resemble hepatocytes *in vivo*[225], along with diet-induced animal models of this disease.

It is also important to note that although the HepG2 cell line is commonly used in NAFLD models[225], its tumour phenotype often complicates its direct applicability to human NAFLD. During the immortalization process, this cell line exhibits altered metabolic function[225], which is often limited compared to primary hepatocytes[226]. While HepG2 cells retain features of normal hepatocytes, they most closely resemble tumour cells in hepatoblastoma[320]. In contrast to normal hepatocytes, the HepG2 smooth ER is poorly developed and these cells have less mitochondria[320], with the former having implications on the storage of proteins and lipids, and the latter effecting cellular metabolic activity. Given that HepG2 cells possess an intermediate phenotype between tumorigenic and normal hepatocytes, they still provide insight on hepatocyte functioning in disease states; however, I cannot directly apply my findings to the *in vivo* situation in NAFLD.

Although this study only sampled at one time point (6 hours) to examine the early development of steatosis, and hence NAFLD, this disease is multi-faceted and is characterized by a myriad of insults occurring at different times. As such, this may limit my study as my results only provide a snapshot of this disease at this point in time, and I cannot conclude if the events observed mark the beginning of disease onset; or if earlier/later time points may provide more information as specific key features of NAFLD were not yet present in this cell model (*e.g.,* changes in β-oxidation, mitochondrial stress, etc.).

This work is also limited by the absence of protein analysis, as it is difficult to draw conclusions from mRNA expression data alone. While this study provides evidence for mRNA-level changes, this does not always correlate to changes at the protein level. Therefore, I can only

speculate what may be occurring at this point in time. Regarding SREBP signaling, INSIGs, which are important in the regulation of SREBP processing, are of particular importance for protein analysis as their activity under hyperinsulinemic and basal insulin conditions would be an interesting area of study. This work would complement the current findings and provide a more complete picture on the activity of these genes. Additionally, examining gene expression and protein levels at different time points would allow for the characterization of NAFLD progression.

While free cholesterol accumulation and deposition within lipid droplets is increasingly being recognized as an important characteristic of NAFLD[154], cholesterol levels were not measured in this study. Future studies should be aimed at measuring and staining cholesterol in these cells to determine its accumulation and localization, respectively. Further, studying the role of VLDL production and secretion in steatosis would be relevant as it can promote steatosis and/or hypertriglyceridemia, and is linked to many of the biological mechanisms discussed in NAFLD progression.

While this work identified that ROS is present early in disease progression and may be a driver of NAFLD, studying the effects of diet on ROS presence at earlier time points, as well as on the pathways investigated in this study, may reveal how NAFLD progression may occur. Further, measuring ROS products presents a challenge as they are highly reactive molecules with short half-lives[321]. Both MitoSOX™ and the DCFDA assay present limitations as they can exhibit nonspecific oxidation of their products from atmospheric oxygen, or from other products within cells. Although useful for measuring total ROS levels, the DCFDA assay does not always directly react with H_2O_2 to produce fluorescence[321], therefore I cannot definitively conclude that the DCFDA output is from H_2O_2 alone. In regard to MitoSOX™, this product is advantageous for the localization of superoxide; however, it is difficult to quantify, as with the majority of fluorescent probes[321]. While the assays used in this study provide knowledge on the presence of ROS, they are not completely reliable, therefore I cannot conclude which ROS product is present or most abundant. This can be addressed by detecting ROS formation through Western blot analysis by examining markers of ER stress that are involved in the UPR, such as PERK, ATF6, and IRE1. Investigation of ROS-induced damage to nucleic acids, lipids, and proteins, as well as determining the type of ROS present through the use of more specific and accurate probes will

provide invaluable evidence on where the ROS has evolved from. Other major sources of ROS such as NADPH oxidases and peroxisomes should be measured to further characterize the diet-induced effects of ROS on early NAFLD development and progression.

Finally, lipid droplet biology paired with ER membrane dynamics in the context of lean NAFLD and steatosis development will be an intriguing avenue of research as it has heavy implications on early NAFLD and disease progression. The involvement of PLIN2 in disease onset through multiple mechanisms triggered by dietary insults, such as through the ER, SREBPs, and ROS would aid in understanding the complexity of steatosis development and provide a new area of drug targeting research for this burdensome disease.

4.6   Conclusion

This study was governed by the hypothesis that with induction of the NAFLD phenotype through Western diet-like culture media, this would cause steatosis with significant alterations in hepatic functioning, specifically through lipogenic signaling pathways, and through reactive oxygen species. This hypothesis is supported by the findings outlined below.

Overall, this work revealed that in the early stages of NAFLD, the high-fat component of the media promoted the majority of pathological conditions observed in this disease, as these effects from the PA/OA treatment alone also manifested in the Western diet group. These phenotypes included increased triglyceride and lipid droplet accumulation, increased activity and ROS production, and decreases in cell number. Moreover, this study also observed changes in mRNA expression of genes involved in important cellular signaling pathways.

The first objective aimed to establish a cell culture model of NAFLD in order to investigate the pathogenic mechanisms involved in the early stages of its development. The changes in lipid accumulation observed were attributable to the increased FFA component in the media[227,254,255], most likely as a result of an imbalance between triglyceride use and synthesis causing lipid droplet formation. However, the greater increase in neutral lipids observed in the Western diet treatment may be due to the ability of the sugar components to activate DNL; although this may be more relevant in hyperinsulinemic states[73]. Overall, early steatosis development in NAFLD is likely caused by an increased flux of FFAs in the diet under

physiological insulin levels as DNL remained unchanged, indicating that sugars are not yet contributing to hepatic lipid accumulation.

Attention was then focused on the mechanisms behind steatosis development, as the second objective investigated the alteration of signaling pathways under lipid accumulation and basal insulin levels. It was found that the expression of *SREBP-1a* was reduced in both the PA/OA and Western diet treatments compared to fructose. As such, it is speculated that this reduction in *SREBP-1a* expression may be due to the protective effects of OA[137,138,261], while fructose may be acting to slightly increase its expression in the Western diet treatment[133–135]. Since *SREBP-1a* is a potent activator of all SREBP target genes, it was also theorized that this was able to override the ability of Western diet cells to downregulate the *LDLR*, as observed in the glucose-treated cells. It is likely that the excess glucose is shuttled toward cholesterol biosynthetic pathways[272], and cells are therefore exhibiting the correct response in downregulating *LDLR* to prevent further cholesterol synthesis and uptake into hepatocytes. As such, the addition of fructose in the Western diet media may be causing dysregulation in cholesterol metabolism at the level of *LDLR*, which is linked to NAFLD pathogenesis[154] (**Fig. 4.6.1-1**).

Lastly, the expression of *PLIN2* was significantly increased as a result of the high-fat component in the media[257], which was correlated with the accumulation of triglycerides and lipid droplets observed. It is speculated that this increase in *PLIN2* mRNA serves as a protective mechanism in the development of steatosis, and therefore NAFLD. This would ensure stabilization of lipid droplets, along with the sequestration of triglycerides and FFAs[278], effectively protecting cells from lipotoxicity. However, over time, this response may be maladaptive as the lipid droplets may exhibit package defects and harbour increased amounts of lipotoxic lipids[277], culminating in phenomena such as insulin resistance, mitochondrial dysfunction, and inflammation[186] (**Fig. 4.6.1-1**).
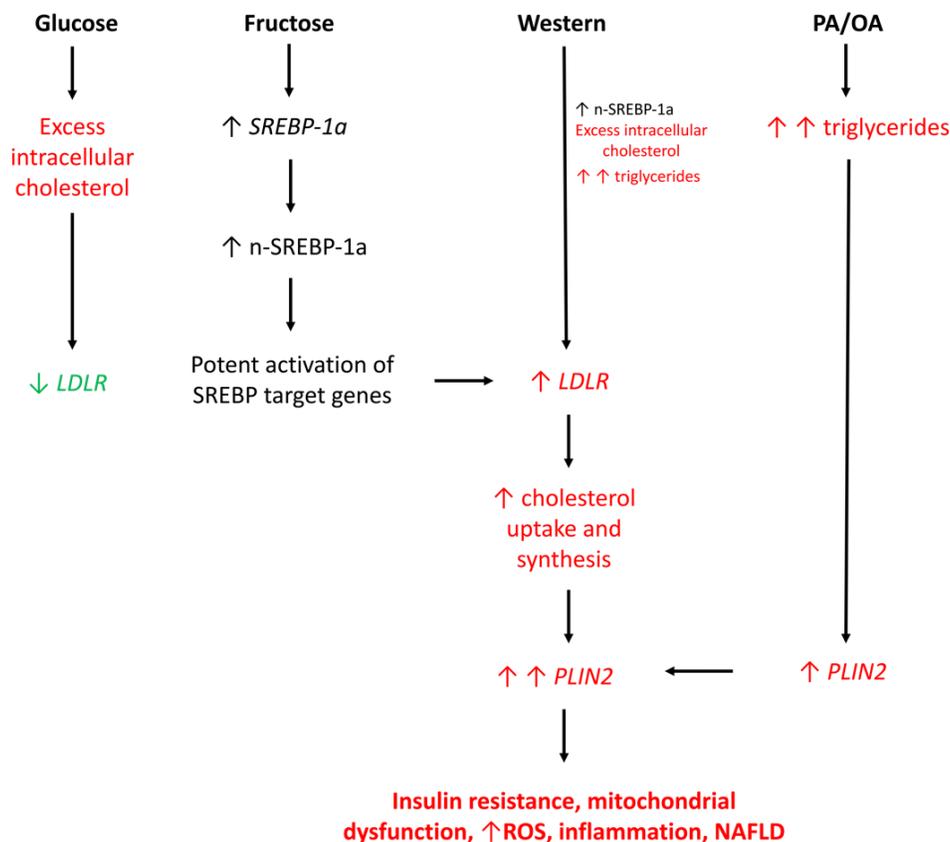
Figure 4.6.1-1. Proposed mechanism of action in early NAFLD induced by each individual dietary component in excess under basal insulin levels. Free fatty acids (PA/OA) in the Western diet treatment cause an increase in triglyceride levels, resulting in their storage in lipid droplets, and consequently an increase in *PLIN2* expression. The excess glucose may be converted into cholesterol, causing in increase in intracellular cholesterol, followed by the appropriate decrease in *LDLR* expression to avoid further uptake and synthesis of cholesterol. Fructose in the diet may cause increased *SREBP-1a* expression, which may translate to an increase in n-SREBP-1a. Since SREBP-1a is a potent activator of all SREBP target genes, this slight activation in the fructose treatment may contribute to the inability of the Western diet treatment to downregulate the *LDLR* as observed in the glucose-treated cells, possibly leading to an increase in its expression. As a result, there would be an increase in cholesterol uptake and synthesis, further increasing *PLIN2* expression, which eventually culminates in NAFLD and other cellular abnormalities. PA/OA: palmitic acid/oleic acid; *SREBP-1a*: sterol regulatory element binding protein 1a; n-SREBP-1a: nuclear SREBP-1a; *LDLR*: low-density lipoprotein receptor; *PLIN2*: perilipin 2; ROS: reactive oxygen species; NAFLD: non-alcoholic fatty liver disease.

Finally, the third objective aimed to discern the effects of different nutrient components on ROS in NAFLD development. As a result of lipid accumulation, the PA/OA and Western diet cells exhibited increased activity, with a concomitant decrease in cell number. While it is likely that the increase in activity was due to changes in OXPHOS, treatment with PA/OA often causes inhibition of this process[294]. This leads to the conclusion that this activity may be caused by an increase in lipid metabolism within the ER, the major hub of lipid homeostasis and the site of lipid droplet formation[277]. With an increase in lipid droplets and ROS production, this creates an unfavourable environment for cell division[300], which may contribute to the decreased cell number observed.

This work is significant in that it provides evidence of ROS from the onset of steatosis, and therefore NAFLD, in an otherwise healthy model. Again, this increase in ROS was attributed to the high-fat component of the media in the Western diet; however, this work revealed that this ROS was not mitochondrial in nature, suggesting it is originating from another source in the development of steatosis. Since many signaling pathways like β-oxidation and insulin signaling were not yet effected by nutrient components under basal insulin levels, these results are meaningful in that it reveals ROS to be both a contributing factor and driver of dysregulated signaling mechanisms in later stages of NAFLD. Moreover, this study is unique in that it illuminates the differential effects of dietary components on hepatocytes individually and combined; and this model is one of few that exist in the current literature. While it is common knowledge that excessive calories are detrimental to human health, this research reveals how the quality of one's diet is equally concerning and should not be overlooked.

Overall, it is proposed that steatosis development in the onset of NAFLD is influenced by the interaction between PLIN2 and lipid droplet formation, ER stress, and subsequently ROS. Interestingly, the activity and increased expression of PLIN2 has been shown to lead to oxidative stress, as the presence of ROS in the form of H_2O_2 can upregulate the expression of *PLIN2* in HepG2 cells[283]. This is interesting to note, as H_2O_2 is the major ROS species produced from the ER lumen[322] – the area in which lipid droplet and occasionally VLDL formation occurs[277]. As such, it is likely that the high-fat and Western diet cells in this study may be presenting with ER stress due to the increased accumulation of lipid droplets and *PLIN2* expression, followed by package defects. To support this lipid droplet/VLDL formation and secretion, the liver will

continuously synthesize large amounts of phospholipids. The membranes of these droplets are similar in composition to the ER, which mainly consists of glycerophospholipids[277]. Interestingly, the activity of SREBP-1 isoforms can upregulate the expression of genes involved in glycerophospholipid metabolism[285]; and perhaps the reason for changes in glycerophospholipid ratios in NAFLD patients is a response to the increasing stiffness of the membrane from SFAs[280].

In regard to the ER membrane, which is highly sensitive to miniscule changes in its membrane cholesterol content[285], it can activate the UPR independently of misfolded/unfolded proteins due to a lipid saturated membrane[204] – an effect that has been linked to palmitate exposure[323]. While SFAs cause stiffening of the ER membrane, MUFAs have an opposite effect[324]. Since MUFAs alleviate this stress, DNL may be activated to produce oleic acid – the end product of this process; and an altered ER environment can also cause SCAP dissociation from INSIG, resulting in SREBP activation[285]. Therefore, it is possible that an altered ER environment may lead to increased activation of SREBPs and subsequently, DNL, providing further support for ROS as a driver of this disease and steatosis development.

Taken together, it is proposed that through increased FFA and sugar intake associated with WD consumption, this may cause an increase in both *PLIN2* expression and ER stress. These two processes will feed back on each other as more lipid droplets form, causing package defects and the secretion of lipotoxic lipids. These package defects, paired with ER membrane changes and increased ER stress may cause the activation of SREBP isoforms, specifically *SREBP-1a* in this model. This may then lead to the increased activation of *LDLR* and DNL, resulting in an increase in both FFA and cholesterol uptake and synthesis – two processes which further promote ER stress. The ER stress will be continually producing ROS, which culminates in steatosis, effectively establishing lean NAFLD and eventually leading to insulin resistance, inflammation, and mitochondrial dysfunction with disease progression (**Fig. 4.6.1-2**). This proposed mechanism of action will be a fascinating avenue of research for future studies.

Collectively, this work has revealed the differential effects of individual dietary components in the Western diet on hepatocytes in the context of NAFLD, providing invaluable evidence on the dangers of Western diet consumption, regardless of BMI. This study has

demonstrated that in early stages of steatosis and NAFLD development, each nutrient component may act in different ways within the Western diet to modify metabolic functioning of cells, specifically through the alteration of cellular signaling pathways, lipid processing genes, and the induction of ROS. These results strongly support the idea that diet quality may be more important than diet quantity, especially in otherwise healthy lean individuals, where excessive intake of these nutrients lead to the onset and progressive deterioration of liver functioning. Although the present study has only provided a glance at the mechanisms of early disease development, these events are likely to cause long-term detrimental effects to hepatic metabolism and overall health. As such, increased intake of these nutrients pose a great risk to all individuals, as habitual consumption of this diet can cause steatosis development before metabolic comorbidities and visible phenotypes arise. Often an asymptomatic disease, especially in the lean population, this research serves to educate individuals on the detrimental effects of this diet, in hopes that better dietary and lifestyle choices are made in order to preserve metabolic health, and therefore prevent the onset of NAFLD.
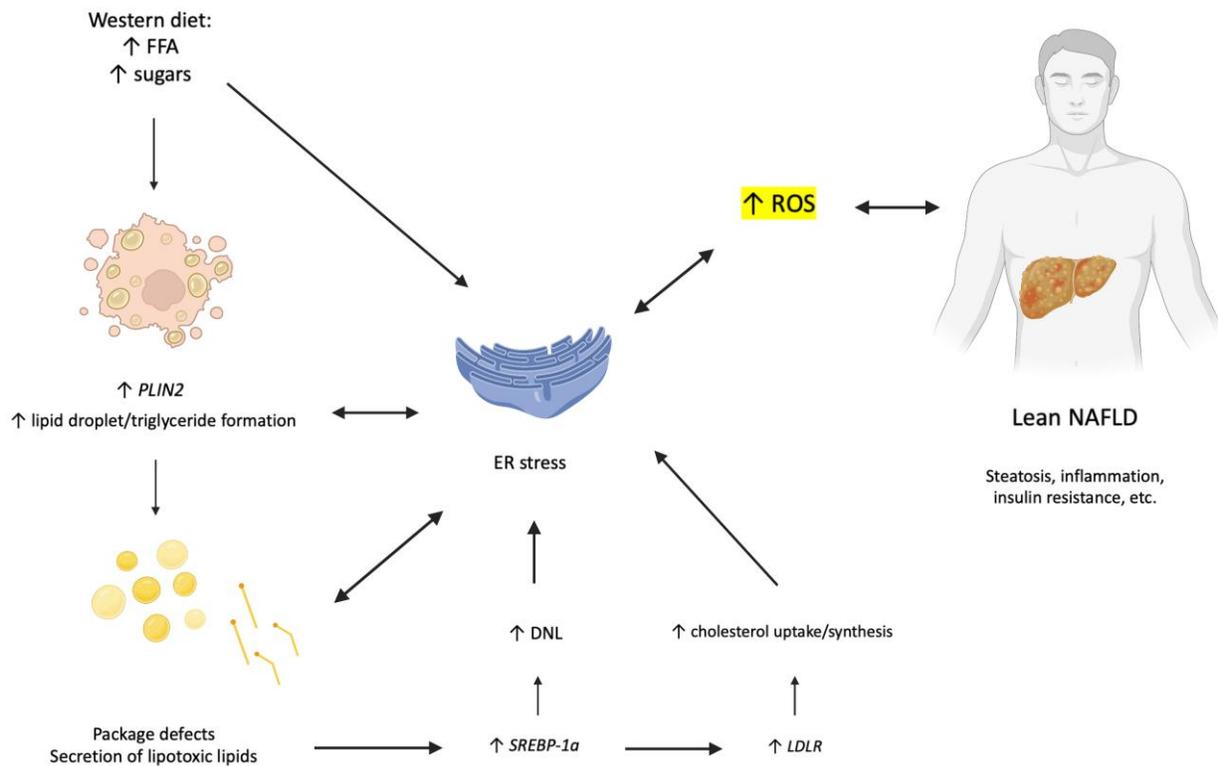
Figure 4.6.1-2. Proposed mechanism of steatosis and onset of lean NAFLD. Through Western diet consumption, this causes an increase in *PLIN2* expression, followed by the formation of triglycerides and their sequestration in lipid droplets. An increased flux of FFAs will cause defectively packaged lipid droplets, resulting in the secretion of lipotoxic lipids. To compensate for the package defects, this may cause an increase in SREBPs, specifically *SREBP-1a* expression, to activate *de novo* lipogenesis to repair both the ER and lipid droplet membranes. This would cause activation of SREBP target genes, such as *LDLR*, which would result in enhanced cholesterol uptake and synthesis. All of these events would disrupt ER homeostasis, leading to ER stress, and consequently, increased production of ROS. This culminates in the establishment of steatosis and lean NAFLD, followed by inflammation, and other metabolic abnormalities such as insulin resistance, causing disease progression. FFA: free fatty acids; *PLIN2*: perilipin 2; *SREBP-1a*: sterol regulatory element binding protein 1a; *LDLR*: low density lipoprotein receptor; DNL: *de novo* lipogenesis; ER: endoplasmic reticulum; ROS: reactive oxygen species; NAFLD: non-alcoholic fatty liver disease.

References

1. Kopp W. How western diet and lifestyle drive the pandemic of obesity and civilization diseases. *Diabetes, Metab Syndr Obes Targets Ther*. 2019;12:2221–2236.

2. Zhao J, Li Z, Gao Q, et al. A review of statistical methods for dietary pattern analysis. *Nutr J*. 2021;20(1):37.

3. Schulze MB, Martínez-González MA, Fung TT, et al. Food based dietary patterns and chronic disease prevention. *BMJ*. 2018;361:k2396.

4. Cordain L, Eaton SB, Sebastian A, et al. Origins and evolution of the Western diet: health implications for the 21st century. *Am J Clin Nutr*. 2005;81(2):341–354.

5. Malesza IJ, Malesza M, Walkowiak J, et al. High-fat, Western-Style Diet, Systemic Inflammation, and Gut Microbiota: A Narrative Review. *Cells*. 2021;10(11):3164.

6. Azzam A. Is the world converging to a "Western diet"? *Public Health Nutr*. 2021;24(2):309–317.

7. Gasbarrini A, Piscaglia AC. A natural diet versus modern Western diets? A new approach to prevent "well-being syndromes". *Dig Dis Sci*. 2005;50(1):1–6.

8. National Research Council (US) Committee on Diet and Health. Diet and Health: Implications for Reducing Chronic Disease Risk. *Washington (DC): National Academies Press (US)*. 1989.

9. Inoue KI, Yamagishi H, Jojima T, et al. Development of Non-alcoholic Steatohepatitis and Nodular Regenerative Hyperplasia in C57BL/6J Mice Fed a Fructose-containing Western Diet. *Anticancer Res*. 2022;42(1):609–617.

10. Marriott BP, Cole N, Lee E. National estimates of dietary fructose intake increased from 1977 to 2004 in the United States. *J Nutr*. 2009;139(6):1228S–1235S.

11. Ravaut G, Légiot A, Bergeron KF, et al. Monounsaturated Fatty Acids in Obesity-Related Inflammation. *Int J Mol Sci*. 2020;22(1):330.

12. Myles IA. Fast food fever: reviewing the impacts of the Western diet on immunity. *Nutr J*. 2014;13:61.

13. Agatston AS. The end of the diet debates? All fats and carbs are not created equal. *Cleve Clin J Med*. 2005;72(1):946–950.

14. Gammone MA, Riccioni G, Parrinello G, et al. Omega-3 Polyunsaturated Fatty Acids: Benefits and Endpoints in Sport. *Nutrients*. 2018;11(1):46.

15. Wang Z, Zhao Y. Gut microbiota derived metabolites in cardiovascular health and disease. *Protein Cell*. 2018;9(5):416–431.

16. De Filippis F, Pellegrini N, Vannini L, et al. High-level adherence to a Mediterranean diet beneficially impacts the gut microbiota and associated metabolome. *Gut*. 2016;65(11):1812–1821.

17. Trichopoulou A, Katsouyanni K, Gnardellis C. The traditional Greek diet. *Eur J Clin Nutr*. 1993;47 Suppl 1:S76–81.

18. Widmer RJ, Flammer AJ, Lerman LO, et al. The Mediterranean diet, its components, and cardiovascular disease. *Am J Med*. 2015;128(3):229–238.

19. Cesari F, Sofi F, Lova RM, et al. Aging process, adherence to Mediterranean diet and nutritional status in a large cohort of nonagenarians: Effects on endothelial progenitor cells. *Nutr Metab Cardiovasc Dis*. 2018;28(1):84–90.

20. De Pergola G, D'Alessandro A. Influence of Mediterranean Diet on Blood Pressure. *Nutrients*. 2018;10(11):1700.

21. Esposito K, Maiorino MI, Bellastella G, et al. Mediterranean diet for type 2 diabetes: cardiometabolic benefits. *Endocrine*. 2017;56(1):27–32.

22. Tuttolomondo A, Simonetta I, Daidone M, et al. Metabolic and Vascular Effect of the Mediterranean Diet. *Int J Mol Sci*. 2019;20(19):4716.

23. Osadnik K, Osadnik T, Lonnie M, et al. Metabolically healthy obese and metabolic syndrome of the lean: the importance of diet quality. Analysis of MAGNETIC cohort. *Nutr J*. 2020;19(1):19.

24. Kalra A, Yetiskul E, Wehrle CJ, et al. Physiology, Liver. *In: StatPearls [Internet].Treasure Island (FL): StatPearls Publishing*. 2022.

25. Parry SA, Hodson L. Influence of dietary macronutrients on liver fat accumulation and metabolism. *J Investig Med*. 2017;65(8):1102–1115.

26. Green CJ, Hodson L. The influence of dietary fat on liver fat accumulation. *Nutrients*. 2014;6(11):5018–5033.

27. Yki-Järvinen H. Liver fat in the pathogenesis of insulin resistance and type 2 diabetes. *Dig Dis*. 2010;28(1):203–209.

28. Puri P, Baillie RA, Wiest MM, et al. A lipidomic analysis of nonalcoholic fatty liver disease. *Hepatology*. 2007;46(4):1081–1090.

29. Puri P, Wiest, MM, Cheung O, et al. The plasma lipidomic signature of nonalcoholic steatohepatitis. *Hepatology*. 2009;50(6):1827–1838.

30. Leamy AK, Egnatchik RA, Young JD. Molecular mechanisms and the role of saturated fatty acids in the progression of non-alcoholic fatty liver disease. *Prog Lipid Res*. 2013;52(1):165–174.

31. Tariq Z, Green CJ, Hodson L. Are oxidative stress mechanisms the common denominator in the progression from hepatic steatosis towards non-alcoholic steatohepatitis (NASH)? *Liver Int*. 2014;34(&):e180–190.

32. Hodson L, Fielding BA. Stearoyl-CoA desaturase: rogue or innocent bystander? *Prog Lipid Res*. 2013;52(1):15–42.

33. Ishimoto T, Lanaspa MA, Rivard CJ, et al. High-fat and high-sucrose (western) diet induces steatohepatitis that is dependent on fructokinase. *Hepatology*. 2013;58(5):1632–1643.

34. Ackerman Z, Oron-Herman M, Grozovski M, et al. Fructose-induced fatty liver disease: hepatic effects of blood pressure and plasma triglyceride reduction. *Hypertension*. 2005;45(5):1012–1018.

35. Roncal-Jimenez CA, Lanaspa MA, Rivard C, et al. Sucrose induces fatty liver and pancreatic inflammation in male breeder rats independent of excess energy intake. *Metabolism*. 2011;60(9):1259–1270.

36. Collison KS, Maqbool ZM, Inglis AL, et al. Effect of dietary monosodium glutamate on HFCS-induced hepatic steatosis: expression profiles in the liver and visceral fat. *Obesity (Silver Spring)*. 2010;18(6):1122–1134.

37. Ouyang X, Cirillo P, Sautin Y, et al. Fructose consumption as a risk factor for non-alcoholic fatty liver disease. *J Hepatol*. 2008;48(6):993–999.

38. Lanaspa MA, Cicerchi C, Garcia G, et al. Counteracting roles of AMP deaminase and AMP kinase in the development of fatty liver. *PLoS One*. 2012;7(11):e48801.

39. Lanaspa MA, Sanchez-Lozada LG, Cicerchi C, et al. Uric acid stimulates fructokinase and accelerates fructose metabolism in the development of fatty liver. *PLoS One*. 2012;7(10):e47948.

40. Lanaspa MA, Sanchez-Lozada LG, Choi YJ, et al. Uric acid induces hepatic steatosis by generation of mitochondrial oxidative stress: potential role in fructose-dependent and -independent fatty liver. *J Biol Chem*. 2012;287(48):40732–40744.

41. Alves-Bezerra M, Cohen DE. Triglyceride Metabolism in the Liver. *Compr Physiol*. 2017;8(1):1–8.

42. Chen Z, Tian R, She Z, et al. Role of oxidative stress in the pathogenesis of nonalcoholic fatty liver disease. *Free Radic Biol Med*. 2020;152:116–141.

43. Nguyen P, Leray V, Serisier S, et al. Liver lipid metabolism. *J Anim Physiol Anim Nutr (Berl)*. 2008;92(3):272–283.

44. Masarone M, Rosato V, Dallio M, et al. Role of Oxidative Stress in Pathophysiology of Nonalcoholic Fatty Liver Disease. *Oxid Med Cell Longev*. 2018;2018:9547613.

45. Browning JD, Szczepaniak LS, Dobbins R, et al. Prevalence of hepatic steatosis in an urban population in the United States: impact of ethnicity. *Hepatology*. 2004;40(6):1387–1395.

46. Chen Z, Yu Y, Cai J, et al. Emerging Molecular Targets for Treatment of Nonalcoholic Fatty Liver Disease. *Trends Endocrinol Metab*. 2019;30(12):903–914.

47. Ipsen DH, Lykkesfeldt J, Tveden-Nyborg P. Molecular mechanisms of hepatic lipid accumulation in non-alcoholic fatty liver disease. *Cell Mol Life Sci*. 2018;75(18):3313–3327.

48. Rao MS, Reddy JK. Peroxisomal beta-oxidation and steatohepatitis. *Semin Liver Dis*. 2001;21(1):43–55.

49. von Loeffelholz C, Döcke S, Lock JF, et al. Increased lipogenesis in spite of upregulated hepatic 5'AMP-activated protein kinase in human non-alcoholic fatty liver. *Hepatol Res*. 2017;47(9):890–901.

50. Han HS, Kang G, Kim JS, et al. Regulation of glucose metabolism from a liver-centric perspective. *Exp Mol Med*. 2016;48(3):e218.

51. Jang C, Hui S, Lu W, et al. The Small Intestine Converts Dietary Fructose into Glucose and Organic Acids. *Cell Metab*. 2018;27(2):351–361.e3.

52. Softic S, Cohen De, Kahn CR. Role of Dietary Fructose and Hepatic De Novo Lipogenesis in Fatty Liver Disease. *Dig Dis Sci*. 2016;61(5):1282–1293.

53. Geidl-Flueck B, Gerber PA. Insights into the Hexose Liver Metabolism-Glucose versus Fructose. *Nutrients*. 2017;9(9)1026.

54. Towle HC, Kaytor EN, Shih HM. Regulation of the expression of lipogenic enzyme genes by carbohydrate. *Annu Rev Nutr*. 1997;17:403–433.

55. Johnston RD, Stephenson MC, Crossland H. No difference between high-fructose and high-glucose diets on liver triacylglycerol or biochemistry in healthy overweight men. *Gastroenterology*. 2013;145(5):1016–1025.e2.

56. Lê KA, Ith M, Kreis R, et al. Fructose overconsumption causes dyslipidemia and ectopic lipid deposition in healthy subjects with and without a family history of type 2 diabetes. *Am J Clin Nutr*. 2009;89(6):1760–1765.

57. Ngo Sock ET, Lê KA, Ith M, et al. Effects of a short-term overfeeding with fructose or glucose in healthy young males. *Br J Nutr*. 2012;103(7):939–943.

58. Sobrecases H, Lê KA, Bortolotti M, et al. Effects of short-term overfeeding with fructose, fat and fructose plus fat on plasma and hepatic lipids in healthy men. *Diabetes Metab*. 2010;36(3):244–246.

59. Hudgins LC, Parker TS, Levine DM, et al. A dual sugar challenge test for lipogenic sensitivity to dietary fructose. *J Clin Endocrinol Metab*. 2011;96(3):861–868.

60. Chong MFF, Fielding BA, Frayn KN. Mechanisms for the acute effect of fructose on postprandial lipemia. *Am J Clin Nutr*. 2007;85(6):1511–1520.

61. Diraison F, Moulin Ph, Beylot M. Contribution of hepatic de novo lipogenesis and reesterification of plasma non esterified fatty acids to plasma triglyceride synthesis during non-alcoholic fatty liver disease. *Diabetes Metab*. 2003;29(5):478–485.

62. Timlin MT, Parks EJ. Temporal pattern of de novo lipogenesis in the postprandial state in healthy men. *Am J Clin Nutr*. 2005;81(1):35–42.

63. Parks EJ, Krauss RM, Christiansen MP, et al. Effects of a low-fat, high-carbohydrate diet on VLDL-triglyceride assembly, production, and clearance. *K Clin Invest*. 1999;104(8):1087–1096.

64. Hellerstein MK. De novo lipogenesis in humans: metabolic and regulatory aspects. *Eur J Clin Nutr*. 1999;53 Suppl 1:S53–65.

65. Marques-Lopes I, Ansorena D, Astiasaran I, et al. Postprandial de novo lipogenesis and metabolic changes induced by a high-carbohydrate, low-fat meal in lean and overweight men. *Am J Clin Nutr*. 2001;73(2):253–261.

66. Della Torre S. Non-alcoholic Fatty Liver Disease as a Canonical Example of Metabolic Inflammatory-Based Liver Disease Showing a Sex-Specific Prevalence: Relevance of Estrogen Signaling. *Front Endocrinol (Lausanne)*. 2020;11:572490.

67. Eslam M, Newsome PN, Sarin SK, et al. A new definition for metabolic dysfunction-associated fatty liver disese: An international expert consensus statement. *J Hepatol*. 2020;73(1):202–209.

68. Pham DG, Zhang C, Yin C. Using zebrafish to model liver diseases–Where do we stand? *Curr Pathobiol Rep*. 2017;5(2):207–221.

69. Dihingia A, Bordoloi J, Dutta P, et al. Hexane-Isopropanolic Extract of Tungrymbai, a North-East Indian fermented soybean food prevents hepatic steatosis via regulating AMPK-mediated SREBP/FAS/ACC/HMGCR and PPARα/CPT1A/UCP2 pathways. *Sci Rep*. 2018;8(1):10021.

70. Ruissen MM, Mak AL, Beuers U, et al. Non-alcoholic fatty liver disease: a multidisciplinary approach towards a cardiometabolic liver disease. *Eur J Endocrinol*. 2020;183(3):R57–R73.

71. Younossi Z, Anstee QM, Marietti M, et al. Global burden of NAFLD and NASH: trends, predictions, risk factors and prevention. *Nat Rev Gastroenterol Hepatol*. 2018;15(1):11–20.

72. EASL-EASD-EASO. Clinical Practice Guidelines for the management of non-alcoholic fatty liver disease. *J Hepatol*. 2016;64(6):1388–1402.

73. Arab JP, Arrese M, Trauner M. Recent Insights into the Pathogenesis of Nonalcoholic Fatty Liver Disease. *Annu Rev Pathol*. 2018;13:321–350.

74. Ye Q, Zou B, Yeo YH, et al. Global prevalence, incidence, and outcomes of non-obese or lean non-alcoholic fatty liver disease: a systematic review and meta-analysis. *Lancet Gastroenterol Hepatol* 2020;5(8):739–752.

75. Sinn DH, Kang D, Cho SO, et al. Lean non-alcoholic fatty liver disease and development of diabetes: a cohort study. *Eur J Endocrinol*. 2019;181(2):185–192.

76. Wang AY, Dhaliwal J, Mouzaki M. Lean non-alcoholic fatty liver disease. *Clin Nutr*. 2019;38(3):975–981.

77. Albhaisi A, Chowdhury A, Sanyal AJ. Non-alcoholic fatty liver disease in lean individuals. *JHEP Rep*. 2019;1(4):329–341.

78. Kuchay MS, Martínez-Montoro JI, Choudhary NS, et al. Non-Alcoholic Fatty Liver Disease in Lean and Non-Obese Individuals: Current and Future Challenges. *Biomedicines*. 2021;9(1):1346.

79. Ahadi M, Molooghi K, Masoudifar N, et al. A review of non-alcoholic fatty liver disease in non-obese and lean individuals. *J Gastroenterol Hepatol*. 2021;36(6):1497–1507.

80. Kim SS, Cho HJ, Kim HJ, et al. Nonalcoholic fatty liver disease as a sentinel marker for the development of diabetes mellitus in non-obese subjects. *Dig Liver Dis*. 2018;50(4):370–377.

81. Sung KC, Seo DC, Lee SJ, et al. Non alcoholic fatty liver disease and risk of incident diabetes in subjects who are not obese. *Nutr Metab Cardiovasc Dis*. 2019;29(5):489–495.

82. Gonzalez-Cantero J, Matin-Rodriguez JL, Gonzalez-Cantero A, et al. Insulin resistance in lean and overweight non-diabetic Caucasian adults: Study of its relationship with liver triglyceride content, waist circumference and BMI. *PLoS One*. 2018;13(2):e0192663.

83. Alberti KG, Zimmet P, Shaw J, et al. The metabolic syndrome—a new worldwide definition. *Lancet*. 2005;366(9491):1059–1062.

84. Feng RN, Du SS, Wang C, et al. Lean-non-alcoholic fatty liver disease increases risk for metabolic disorders in a normal weight Chinese population. *World J Gastroenterol*. 2014;20(47):17932–17940.

85. Ha Y, Seo N, Shim JH, et al. Intimate association of visceral obesity with non-alcoholic fatty liver disease in healthy Asians: A case-control study. *J Gastroenterol Hepatol*. 2015;30(11):1666–1672.

86. Petta S, Amato MC, Di Marco V, et al. Visceral adiposity index is associated with significant fibrosis in patients with non-alcoholic fatty liver disease. *Aliment Pharmacol Ther*. 2012;35(2):238–247.

87. Kumar R, Rastogi A, Sharma MK, et al. Clinicopathological characteristics and metabolic profiles of non-alcoholic fatty liver disease in Indian patients with normal body mass index: Do they differ from obese or overweight non-alcoholic fatty liver disease? *Indian J Endocrinol Metab*. 2013;17(4):665–671.

88. Assy N, Nasser G, Kamayse I, et al. Soft drink consumption linked with fatty liver in the absence of traditional risk factors. *Can J Gastroenterol*. 2008;22(1):811–816.

89. Shi Y, Wang Q, Sun Y, et al. The Prevalence of Lean/Nonobese Nonalcoholic Fatty Liver Disease: A Systematic Review and Meta-Analysis. *J Clin Gastroenterol*. 2020;54(4):378–387.

90. Wei JL, Leung JCF, Loong TCW, et al. Prevalence and Severity of Nonalcoholic Fatty Liver Disease in Non-Obese Patients: A Population Study Using Proton-Magnetic Resonance Spectroscopy. *Am J Gastroenterol*. 2015;110(9):1306–1314.

91. Golabi P, Paik J, Fukui N, et al. Patients With Lean Nonalcoholic Fatty Liver Disease Are Metabolically Abnormal and Have a Higher Risk for Mortality. *Clin Diabetes*. 2019;37(1):65–72.

92. Johnson NA, Sachinwalla T, Walton DW, et al. Aerobic exercise training reduces hepatic and visceral lipids in obese individuals without weight loss. *Hepatology*. 2009;50(4):1105–1112.

93. Bae JC, Suh S, Park SE, et al. Regular exercise is associated with a reduction in the risk of NAFLD and decreased liver enzymes in individuals with NAFLD independent of obesity in Korean adults. *PLoS One*. 2012;7(10):e46819.

94. Kistler KD, Brunt EM, Clark JM, et al. Physical activity recommendations, exercise intensity, and histological severity of nonalcoholic fatty liver disease. *Am J Gastroenterol*. 2011;106(3):460–468.

95. Armstrong MJ, Gaunt P, Aithal GP, et al. Liraglutide safety and efficacy in patients with non-alcoholic Steatohepatitis (LEAN): a multi centre, double-blind, randomised, placebo-controlled phase 2 study. *Lancet*. 2016;387(10019):679–690.

96. Younossi ZM, Koenig AB, Abdelatif D, et al. Global epidemiology of nonalcoholic fatty liver disease–Meta-analytic assessment of prevalence, incidence, and outcomes. *Hepatology*. 2016;64(1):73–84.

97. Zhang X, Zhan Y, Lin W, et al. Smurf1 aggravates non-alcoholic fatty liver disease by stabilizing SREBP-1c in an E3 activity-independent manner. *FASEB J*. 2020;34(6):7631–7643.

98. Horie T, Nishino T, Baba O, et al. MicroRNA-33 regulates sterol regulatory element-binding protein 1 expression in mice. *Nat Commun*. 2013;4:2883.

99. Ferré P, Foufelle F. SREBP-1c transcription factor and lipid homeostasis: clinical perspective. *Horm Res*. 2007;68(2):72–82.

100. Shimano H. Sterol regulatory element-binding protein-1 as a dominant transcription factor for gene regulation of lipogenic enzymes in the liver. *Trends Cardiovasc Med*. 2000;10(7):275–278.

101. Shimomura I, Shimano H, Horton JD, et al. Differential expression of exons 1a and 1c in mRNAs for sterol regulatory element binding protein-1 in human and mouse organs and cultured cells. *J Clin Invest*. 1997;99(5):838–845.

102. Eberlé D, Hegarty B, Bossard P, et al. SREBP transcription factors: master regulators of lipid homeostasis. *Biochimie*. 2004;86(11):839–848.

103. Dong XY, Tang SQ. Insulin-induced gene: a new regulator in lipid metabolism. *Peptides*. 2010;31(11):2145–2150.

104. Rome S, Lecomte V, Meugnier E, et al. Microarray analyses of SREBP-1a and SREBP-1c target genes identify new regulatory pathways in muscle. *Physiol Genomics*. 2008;34(3):327–337.

105. Dong X, Tan P, Cai Z, et al. Regulation of FADS2 transcription by SREBP-1 and PPAR-α influences LC-PUFA biosynthesis in fish. *Sci Rep*. 2017;7:40024.

106. Fernández-Alvarez A, Alvarez MS, Cucarella C, et al. Characterization of the human insulin-induced gene 2 (INSIG2) promoter: the role of Ets-binding motifs. *J Biol Chem*. 2010;285(16):11765–11774.

107. Ferré P, Phan F, Foufelle F. SREBP-1c and lipogenesis in the liver: an update. *Biochem J*. 2021;478(20):3723–3739.

108. Azzout-Marniche D, Bécard D, Guichard C, et al. Insulin effects on sterol regulatory-element-binding protein-1c (SREBP-1c) transcriptional activity in rat hepatocytes. *Biochem J*. 2000;350 Pt 2(Pt2):389–393.

109. Repa JJ, Liang G, Ou J, et al. Regulation of mouse sterol regulatory element-binding protein-1c gene (SREBP-1c) by oxysterol receptors, LXRalpha and LXRbeta. *Genes Dev*. 2000;14(22):2819–2830.

110. Schultz JR, Tu H, Luk A, et al. Role of LXRs in control of lipogenesis. *Genes Dev*. 2000;14(22):2831–2838.

111. Laffitte BA, Chao LC, Li J, et al. Activation of liver X receptor improves glucose tolerance through coordinate regulation of glucose metabolism in liver and adipose tissue. *Proc Natl Acad USA*. 2003;100(9):5419–5424.

112. Tobin KA, Ulven SM, Schuster GU, et al. Liver X receptors as insulin-mediating factors in fatty acid and cholesterol biosynthesis. *J Biol Chem*. 2022;277(12):10691–10697.

113. Shimano H. Sterol regulatory element-binding protein family as global regulators of lipid synthetic genes in energy metabolism. *Vitam Horm*. 2002;65:167–194.

114. Shimano H, Sato R. SREBP-regulated lipid metabolism: convergent physiology – divergent pathophysiology. *Nat Rev Endocrinol*. 2017;13(12):710–730.

115. Matsuzaka T, Shimano H, Yahagi N, et al. Insulin-independent induction of sterol regulatory element-binding protein-1c expression in the livers of streptozotocin-treated mice. *Diabetes*. 2004;53(3):560–569.

116. Haas JT, Miao J, Chanda D, et al. Hepatic insulin signaling is required for obesity-dependent expression of SREBP-1c mRNA but not for feeding-dependent expression. *Cell Metab*. 2012;15(6):873–884.

117. Auguet T, Berlanga A, Guiu-Jurado E, et al. Altered fatty acid metabolism-related gene expression in liver from morbidly obese women with non-alcoholic fatty liver disease. *Int J Mol Sci*. 2004;15(12):22173–22187.

118. Yang ZX, Shen W, Sun H. Effects of nuclear receptor FXR on the regulation of liver lipid metabolism in patients with non-alcoholic fatty liver disease. *Hepatol Int*. 2010;4(4):741–748.

119. Pettinelli P, Videla LA. Up-regulation of PPAR-gamma mRNA expression in the liver of obese patients: an additional reinforcing lipogenic mechanism to SREBP-1c induction. *J Clin Endocrinol Metab*. 2011;96(5):1424–1430.

120. Kammoun HL, Chabanon H, Hainault I, et al. GRP78 expression inhibits insulin and ER stress-induced SREBP-1c activation and reduces hepatic steatosis in mice. *J Clin Invest*. 2009;119(5):1201–1215.

121. Shimomura I, Matsuda M, Hammer RE, et al. Decreased IRS-2 and increased SREBP-1c lead to mixed insulin resistance and sensitivity in livers of lipodystrophic and ob/ob mice. *Mol Cell*. 2000;6(1):77–86.

122. Shimomura I, Bashmakov Y, Ikemoto S, et al. Insulin selectively increases SREBP-1c mRNA in the livers of rats with streptozotocin-induced diabetes. *Proc Natl Acad Sci USA*. 1999;96(24):13656–13661.

123. Horton JD, Shah NA, Warrington JA, et al. Combined analysis of oligonucleotide microarray data from transgenic and knockout mice identifies direct SREBP target genes. *Proc Natl Acad Sci USA*. 2003;100(21):12027–12032.

124. Horton JD, Goldstein JL, Brown MS. SREBPs: activators of the complete program of cholesterol and fatty acid synthesis in the liver. *J Clin Invest*. 2002;109(9):1125–1131.

125. Shimano H, Horton JD, Hammer RE, et al. Overproduction of cholesterol and fatty acids causes massive liver enlargement in transgenic mice expressing truncated SREBP-1a. *J Clin Invest*. 1996;98(7):1575–1584.

126. Horton JD, Shimomura I, Brown MS, et al. Activation of cholesterol synthesis in preference to fatty acid synthesis in liver and adipose tissue of transgenic mice overproducing sterol regulatory element-binding protein-2. *J Clin Invest*. 1998;101(11):2331–2339.

127. Yahagi N, Shimano H, Hasty AH, et al. Absence of sterol regulatory element-binding protein-1 (SREBP-1) ameliorates fatty livers but not obesity or insulin resistance in Lep(ob)/Lep(ob) mice. *J Biol Chem*. 2002;277(22):19353–19357.

128. Moon YA, Liang G, Xie X, et al. The Scap/SREBP pathway is essential for developing diabetic fatty liver and carbohydrate-induced hypertriglyceridemia in animals. *Cell Metab*. 2012;15(2):240–246.

129. Espenshade PJ, Hughes AL. Regulation of sterol synthesis in eukaryotes. *Annu Rev Genet*. 2007;41:401–427.

130. Foretz M, Pacot C, Dugail I, et al. ADD1/SREBP-1c is required in the activation of hepatic lipogenic gene expression by glucose. *Mol Cell Biol*. 1999;19(5):3760–3768.

131. Deng X, Cagen LM, Wilcox HG, et al. Regulation of the rat SREBP-1c promoter in primary rat hepatocytes. *Biochem Biophys Res Commun*. 2002; 290(1):256–262.

132. Bécard D, Hainault I, Azzout-Marniche D, et al. Adenovirus-mediated overexpression of sterol regulatory element binding protein-1c mimics insulin effects on hepatic gene expression and glucose homeostasis in diabetic mice. *Diabetes*. 2001;50(11):2425–2430.

133. Nagai Y, Yonemitsu S, Erion DM, et al. The role of peroxisome proliferator-activated receptor gamma coactivator-1 beta in the pathogenesis of fructose-induced insulin resistance. *Cell Metab*. 2009;9(3):252–264.

134. Nagai Y, Nishio Y, Nakamura T, et al. Amelioration of high fructose-induced metabolic derangements by activation of PPARalpha. *Am J Physiol Endocrinol Metab*. 2002;282(5):E1180–1190.

135. Zhang C, Chen X, Zhu RM, et al. Endoplasmic reticulum stress is involved in hepatic SREBP-1c activation and lipid accumulation in fructose-fed mice. *Toxicol Lett*. 2012;212(3):229–240.

136. Basciano H, Federico L, Adeli K. Fructose, insulin resistance, and metabolic dyslipidemia. *Nutr Metab (Lond)*. 2005; 2(1):5.

137. Jump DB. Dietary polyunsaturated fatty acids and regulation of gene transcription. *Curr Opin Lipidol*. 2002;13(2):155–164.

138. Xu J, Teran-Garcia M, Park JH, et al. Polyunsaturated fatty acids suppress hepatic sterol regulatory element-binding protein-1 expression by accelerating transcript decay. *J Biol Chem*. 2001;276(13):9800–9807.

139. Nakakuki M, Kawano H, Notsu T, et al. A novel processing system of sterol regulatory element-binding protein-1c regulated by polyunsaturated fatty acid. *J Biochem*. 2014;155(5):301–313.

140. Hannah VC, Ou J, Luong A, et al. Unsaturated fatty acids down-regulate srebp isoforms 1a and 1c by two mechanisms in HEK-293 cells. *J Biol Chem*. 2001;276(6):4365–4372.

141. Seegmiller AC, Dobrosotskaya I, Goldstein JL, et al. The SREBP pathway in Drosophila: regulation by palmitate, not sterols. *Dev Cell*. 2002;2(2):229–238.

142. Dorotea D, Koya D, Ha H. Recent Insights Into SREBP as a Direct Mediator of Kidney Fibrosis via Lipid-Independent Pathways. *Front Pharmacol*. 202011:265.

143. Matsuzaka T, Shimano H. Insulin-dependent and -independent regulation of sterol regulatory element-binding protein-1c. *J Diabetes Investig*. 2013;4(5):411 – 412.

144. Brown MS, Goldstein JL. Selective versus total insulin resistance: a pathogenic paradox. *Cell Metab*. 2008;7(2):95–96.

145. Copps KD, White MF. Regulation of insulin sensitivity by serine/threonine phosphorylation of insulin receptor substrate proteins IRS1 and IRS2. *Diabetologia*. 2012;55(1):2565–2582.

146. White MF. Insulin signaling in health and disease. *Science*. 2003;302(5651):1710–1711.

147. Tanti JF, Jager J. Cellular mechanisms of insulin resistance: role of stress-regulated serine kinases and insulin receptor substrates (IRS) serine phosphorylation. *Curr Opin Pharmacol*. 2009;9(6):753–762.

148. Michael MD, Kulkarni RN, Postic C, et al. Loss of insulin signaling in hepatocytes leads to severe insulin resistance and progressive hepatic dysfunction. *Mol Cell*. 2000;6(1):87–97.

149. Hong T, Chen Y, Li X, et al. The Role and Mechanism of Oxidative Stress and Nuclear Receptors in the Development of NAFLD. *Oxid Med Cell Longev*. 2021;2021:6889533.

150. St-Amand R, Ngo Sock ET, Quinn S, et al. Two weeks of western diet disrupts liver molecular markers of cholesterol metabolism in rats. *Lipids Health Dis*. 2020;19(1):192.

151. Cali AM, Zern TL, Taksali SE, et al. Intrahepatic fat accumulation and alterations in lipoprotein composition in obese adolescents: a perfect proatherogenic state. *Diabetes Care*. 2007;30(12):3093–3098.

152. Wieckowska A, Papouchado BG, Li Z, et al. Increased hepatic and circulating interleukin-6 levels in human nonalcoholic steatohepatitis. *Am J Gastroenterol*. 2008;103(6):1372–1379.

153. Musso G, Gambino R, Cassader M. Cholesterol metabolism and the pathogenesis of non-alcoholic steatohepatitis. *Prog Lipid Res*. 2013;52(1):175–191.

154. Zhang Y, Ma KL, Ruan XZ, et al. Dysregulation of the Low-Density Lipoprotein Receptor Pathway Is Involved in Lipid Disorder-Mediated Organ Injury. *Int J Biol Sci*. 2016;12(5):569–579.

155. Arguello G, Balboa E, Arrese M, et al. Recent insights on the role of cholesterol in non-alcoholic fatty liver disease. *Biochim Biophys Acta*. 2015;1852(9):1765–1778.

156. Min HK, Kapoor A, Fuchs M, et al. Increased hepatic synthesis and dysregulation of cholesterol metabolism is associated with the severity of nonalcoholic fatty liver disease. *Cell Metab*. 2012;15(5):665–674.

157. Magri-Tomaz L, Melbouci L, Mercier J, et al. Two weeks of high-fat feeding disturb lipid and cholesterol molecular markers. *Cell Biochem Funct*. 2018;36(7):387–393.

158. Paquette A, Shinoda M, Lhoret RR, et al. Time course of liver lipid infiltration in ovariectomized rats: impact of a high-fat diet. *Maturitas*. 2007;58(2):182–190.

159. Gauthier MS, Favier R, Lavoie JM. Time course of the development of non-alcoholic hepatic steatosis in response to high-fat diet-induced obesity in rats. *Br J Nutr*. 2006;95(2):273–281.

160. Catapano AL. The low density lipoprotein receptor: structure, function and pharmacological modulation. *Pharmacol Ther*. 1989;43(2):187–219.

161. Soutar AK, Knight BL. Structure and regulation of the LDL-receptor and its gene. *Br Med Bull*. 1990;46(4):891–916.

162. Horton JD, Shimano H, Hamilton RL, et al. Disruption of LDL receptor gene in transgenic SREBP-1a mice unmasks hyperlipidemia resulting from production of lipid-rich VLDL. *J Clin Invest*. 1999;103(7):1067–1076.

163. Hallikainen M, Toppinen L, Mykkänen H, et al. Interaction between cholesterol and glucose metabolism during dietary carbohydrate modification in subjects with the metabolic syndrome. *Am J Clin Nutr*. 2006;84(6):1385–1392.

164. Pihlajamäki J, Gylling H, Miettinen TA, et al. Insulin resistance is associated with increased cholesterol synthesis and decreased cholesterol absorption in normoglycemic men. *J Lipid Res*. 2004;45(3):507–512.

165. Ma KL, Ruan XZ, Powis SH, et al. Inflammatory stress exacerbates lipid accumulation in hepatic cells and fatty livers of apolipoprotein E knockout mice. *Hepatology*. 2008;48(3):770–781.

166. Chen Y, Ruan XZ, Li Q, et al. Inflammatory cytokines disrupt LDL-receptor feedback regulation and cause statin resistance: a comparative study in human hepatic cells and mesangial cells. *Am J Physiol Renal Physiol*. 2007;293(3):F680–687.

167. Gluchowki NL, Becuwe M, Walther TC, et al. Lipid droplets and liver disease: from basic biology to clinical implications. *Nat Rev Gastroenterol Hepatol*. 2017;14(6):343–355.

168. Carr RM, Ahima RS. Pathophysiology of lipid droplet proteins in liver diseases. *Exp Cell Res* 2016;340(2):187–192.

169. Okumura T. Role of lipid droplet proteins in liver steatosis. *J Physiol Biochem*. 2011;67(4):629–636.

170. Sztalryd C, Brasaemle DL. The perilipin family of lipid droplet proteins: Gatekeepers of intracellular lipolysis. *Biochim Biophys Acta Mol Cell Biol Lipids*. 2017;1862(10 Pt B):1221–1232.

171. Hsieh K, Lee YK, Londos C, et al. Perilipin family members preferentially sequester to either triacylglycerol-specific or cholesteryl-ester-specific intracellular lipid storage droplets. *J Cell Sci*. 2012;125(Pt 17):4067–4076.

172. Straub BK, Stoeffel P, Heid H, et al. Differential pattern of lipid droplet-associated proteins and de novo perilipin expression in hepatocyte steatogenesis. *Hepatology*. 2008;47(6):1936–1946.

173. Nocetti D, Espinosa A, Pino-De la Fuente F, et al. Lipid droplets are both highly oxidized and Plin2-covered in hepatocytes of diet-induced obese mice. *Appl Physiol Nutr Metab*. 2020;45(12):1368–1376.

174. Heid HW, Moll R, Schwerlich I, et al. Adipophilin is a specific marker of lipid accumulation in diverse cell types and diseases. *Cell Tissue Res*. 1998;294(2):309–321.

175. Wang X, Reape TJ, Li X, et al. Induced expression of adipophilin mRNA in human macrophages stimulated with oxidized low-density lipoprotein and in atherosclerotic lesions. *FEBS Lett*. 1999;462(1-2):145-150.

176. Varela GM, Antwi DA, Dhir R, et al. Inhibition of ADRP prevents diet-induced insulin resistance. *Am J Physiol Gastrointest Liver Physiol*. 2008;295(3):G621–628.

177. Magnusson B, Asp L, Boström P, et al. Adipocyte differentiation-related protein promotes fatty acid storage in cytosolic triglycerides and inhibits secretion of very low-density lipoproteins. *Arterioscler Thromb Vasc Biol*. 2006;26(7):1566–1571.

178. Imai Y, Varela GM, Jackson MB, et al. Reduction of hepatosteatosis and lipid levels by an adipose differentiation-related protein antisense oligonucleotide. *Gastroenterology*. 2007;132(5):1947–1954.

179. Smagris E, BasuRay S, Li J, et al. Pnpla3I148M knockin mice accumulate PNPLA3 on lipid droplets and develop hepatic steatosis. *Hepatology*. 2015;61(1):108–118.

180. Chang, BHJ Li L, Paul A, et al. Protection against fatty liver but normal adipogenesis in mice lacking adipose differentiation-related protein. *Mol Cell Biol*. 2006;26(3):1063–1076.

181. Orlicky DJ, Libby AE, Bales ES, et al. Perilipin-2 promotes obesity and progressive fatty liver disease in mice through mechanistically distinct hepatocyte and extra-hepatocyte actions. *J Physiol*. 2019;597(6):1565–1584.

182. Najt CP, Senthivinayagam S, Alijazi MB, et al. Liver-specific loss of Perilipin 2 alleviates diet-induced hepatic steatosis, inflammation, and fibrosis. *Am J Physiol Gastrointest Liver Physiol*. 2016;310(9):G726–738.

183. Fabbrini E, Mohammed BS, Magkos F, et al. Alterations in adipose tissue and hepatic lipid kinetics in obese men and women with nonalcoholic fatty liver disease. Gastroenterology. 2008;134(2):424–431.

184. Najt CP, Devarajan M, Mashek DG. Perilipins at a glance. *J Cell Sci*. 2022;135(5):jcs259201.

185. Paul A, Chang BHJ, Li L, et al. Deficiency of adipose differentiation-related protein impairs foam cell formation and protects against atherosclerosis. *Circ Res*. 2008;102(12):1492–1501.

186. Carr RM, Dhir R, Mahadev K, et al. Perilipin Staining Distinguishes Between Steatosis and Nonalcoholic Steatohepatitis in Adults and Children. *Clin Gastroenterol Hepatol*. 2017;15(1):145–147.

187. Imai Y, Boyle S, Varela GM, et al. Effects of Perilipin 2 antisense oligonucleotide treatment on hepatic lipid metabolism and gene expression. *Physiol Genomics*. 2012;44(22):1125–1131.

188. Welte MA, Gould AP. Lipid droplet functions beyond energy storage. *Biochim Biophys Acta Mol Cell Biol Lipids*. 2017;1862(10 Pt B):1260–1272.

189. Gonzalez A, Huerta-Salgado C, Orozco-Aguilar J, et al. Role of Oxidative Stress in Hepatic and Extrahepatic Dysfunctions during Nonalcoholic Fatty Liver Disease (NAFLD). *Oxid Med Cell Longev*. 2020;2020:1617805.

190. Forrester SJ, Kikuchi DS, Hernandes MS, et al. Reactive Oxygen Species in Metabolic and Inflammatory Signaling. *Circ Res*. 2018;122(6):877–902.

191. Crosas-Molist E, Fabregat I. Role of NADPH oxidases in the redox biology of liver fibrosis. *Redox Biol*. 2015;6:106–111.

192. Mansouri A, Gattolliat CH, Asselah T. Mitochondrial Dysfunction and Signaling in Chronic Liver Diseases. *Gastroenterology*. 2018;155(3):629–647.

193. Begriche K, Massart J, Robin MA, et al. Mitochondrial adaptations and dysfunctions in nonalcoholic fatty liver disease. *Hepatology*. 2013;58(4):1497–1507.

194. Simões ICM, Fontes A, Pinton P, et al. Mitochondria in non-alcoholic fatty liver disease. *Int J Biochem Cell Biol*. 2018;95:93–99.

195. Sunny NE, Bril F, Cusi K. Mitochondrial Adaptation in Nonalcoholic Fatty Liver Disease: Novel Mechanisms and Treatment Strategies. *Trends Endocrinol Metab*. 2017;28(4):250–260.

196. Tahara EB, Navarete FD, Kowaltowski AJ. Tissue-, substrate-, and site-specific characteristics of mitochondrial reactive oxygen species generation. *Free Radic Biol Med*. 2009;46(9):1283–1297.

197. Chönfeld P, Wojtczak L. Fatty acids as modulators of the cellular production of reactive oxygen species. *Free Radic Biol Med*. 2008;45(3):231–241.

198. Stillwell W, Jenski LJ, Crump FT, et al. Effect of docosahexaenoic acid on mouse mitochondrial membrane properties. *Lipids*. 1997;32(5):497–506.

199. Donnelly KL, Smith CI, Schwarzenberg SJ, et al. Sources of fatty acids stored in liver and secreted via lipoproteins in patients with nonalcoholic fatty liver disease. *J Clin Invest*. 2005;115(5):1343–1351.

200. Ahsraf NU, Sheikh TA. Endoplasmic reticulum stress and Oxidative stress in the pathogenesis of Non-alcoholic fatty liver disease. *Free Radic Res*. 2015;49(12):1405–1418.

201. Malhi H, Kaufman RJ. Endoplasmic reticulum stress in liver disease. *J Hepatol*. 2011;54(4):795–809.

202. Rutkowski DT, Wu J, Back SH, et al. UPR pathways combine to prevent hepatic steatosis caused by ER stress-mediated suppression of transcriptional master regulators. *Dev Cell*. 2008;15(6):829–840.

203. Malhotra JD, Kaufman RJ. The endoplasmic reticulum and the unfolded protein response. *Semin Cell Dev Biol*. 2007;18(6):716–731.

204. Mota M, Banini BA, Cazanave SC, et al. Molecular mechanisms of lipotoxicity and glucotoxicity in nonalcoholic fatty liver disease. *Metabolism*. 2016;65(8):1049–1061.

205. Volmer R, van der Ploeg K, Ron D. Membrane lipid saturation activates endoplasmic reticulum unfolded protein response transducers through their transmembrane domains. *Proc Natl Acad Sci USA*. 2013;110(12):4628–4633.

206. Puri P, Mirshahi F, Cheung O, et al. Activation and dysregulation of the unfolded protein response in nonalcoholic fatty liver disease. *Gastroenterology*. 2008;134(2):568–576.

207. Du D, Shi YH, Le GW. Oxidative stress induced by high-glucose diet in liver of C57BL/6J mice and its underlying mechanism. *Mol Biol Rep*. 2010;37(8):3833–3839.

208. Maslak E, Buczek E, Szumny A, et al. Individual CLA Isomers, c9t11 and t10c12, Prevent Excess Liver Glycogen Storage and Inhibit Lipogenic Genes Expression Induced by High-Fructose Diet in Rats. *Biomed Res Int*. 2015;2015;535982.

209. Zhang Y, Yang X, Shi H, et al. Effect of α-linolenic acid on endoplasmic reticulum stress-mediated apoptosis of palmitic acid lipotoxicity in primary rat hepatocytes. *Lipids Health Dis*. 2011;10:122.

210. Bachar E, Ariav Y, Ketzinel-Gilad M, et al. Glucose amplifies fatty acid-induced endoplasmic reticulum stress in pancreatic beta-cells via activation of mTORC1. *PLoS One*. 2009;4(3):e4954.

211. Deniaud A, Sharaf el dein O, Maillier E, et al. Endoplasmic reticulum stress induces calcium-dependent permeability transition, mitochondrial outer membrane permeabilization and apoptosis. *Oncogene*. 2008;27(3):285–299.

212. Wei Y, Wang D, Gentile CL, et al. Reduced endoplasmic reticulum luminal calcium links saturated fatty acid-mediated endoplasmic reticulum stress and cell death in liver cells. *Mol Cell Biochem*. 2009;331(1–2):31–40.

213. Griffiths EJ, Rutter GA. Mitochondrial calcium as a key regulator of mitochondrial ATP production in mammalian cells. *Biochem Biophys Acta*. 2009;1787(11):1324–1333.

214. Yin X, Zheng F, Pan Q, et al. Glucose fluctuation increased hepatocyte apoptosis under lipotoxicity and the involvement of mitochondrial permeability transition opening. *J Mol Endocrinol*. 2015;55(3):169–181.

215. DeFronzo RA. Insulin resistance, lipotoxicity, type 2 diabetes and atherosclerosis: the missing links. The Claude Bernard Lecture 2009. *Diabetologia*. 2010;53(7):1270–1287.

216. Musso G, Cassader M, Paschetta E, et al. Bioactive Lipid Species and Metabolic Pathways in Progression and Resolution of Nonalcoholic Steatohepatitis. *Gastroenterology*. 2018;155(2):282–302.e8.

217. Abu Bakar MH, Kian Kai C, Wan Hassan WN, et al. Mitochondrial dysfunction as a central event for mechanisms underlying insulin resistance: the roles of long chain fatty acids. *Diabetes Metab Res Rev*. 2015;31(5):453–475.

218. VanWagner LB, Armstrong MS. Lean NAFLD: A not so benign condition? *Hepatol Commun*. 2018;2(1):5–8.

219. Maier S, Wieland A, Cree-Green M, et al. Lean NAFLD: an underrecognized and challenging disorder in medicine. *Rev Endocr Metab Disord*. 2021;22(2):351–366.

220. Janorkar AV, King KR, Megeed Z, et al. Development of an in vitro cell culture model of hepatic steatosis using hepatocyte-derived reporter cells. *Biotechnol Bioeng*. 2009;102(5):1466–1474.

221. Kanuri G, Bergheim I. In vitro and in vivo models of non-alcoholic fatty liver disease (NAFLD). *Int J Mol Sci*. 2013;14(6):11963–11980.

222. Jahn D, Kircher S, Hermanns HM, et al. Animal models of NAFLD from a hematologists point of view. *Biochim Biophys Acta Mol Casis Dis*. 2019;1865(5):943–953.

223. Xu R, Pan J, Zhou W, et al. Recent advances in lean NAFLD. *Biomed Pharmacother*. 2022;153:113331.

224. Lopez YO, Garufi G, Seyhan AA. Altered levels of circulating cytokines and microRNAs in lean and obese individuals with prediabetes and type 2 diabetes. *Mol Biosyst*. 2016;13(1):106–121.

225. Soret PA, Magusto J, Housset C, et al. In Vitro and In Vivo Models of Non-Alcoholic Fatty Liver Disease: A Critical Appraisal. *J Clin Med*. 2020;10(1):36.

226. Donato MT, Tolosa L, Gómez-Lechón MJ. Culture and Functional Characterization of Human Hepatoma HepG2 Cells. *Methods Mol Biol*. 2015;1250:77–93.

227. Ricchi M, Odoardi MR, Carulli L, et al. Differential effect of oleic and palmitic acid on lipid accumulation and apoptosis in cultured hepatocytes. *J Gastroenterol Hepatol*. 2009;25(5):830–840.

228. Ritz P, Krempf M, Cloarec D, et al. Comparative continuous-indirect-calorimetry study of two carbohydrates with different glycemic indices. *Am J Clin Nutr*. 1991;54(5):855–859.

229. Listenberger LL, Ory DS, Schaffer JE. Palmitate-induced apoptosis can occur through a ceramide-independent pathway. *J Biol Chem*. 2001;276(18):14890–14895.

230. Stoianov AM, Robson DL, Hetherington AM, et al. Elongation Factor 1A-1 Is a Mediator of Hepatocyte Lipotoxicity Partly through Its Canonical Function in Protein Synthesis. *PLoS One*. 2015;10(6):e0131269.

231. Hetherington AM, Sawyez CG, Zilberman E, et al. Differential Lipotoxic Effects of Palmitate and Oleate in Activated Human Hepatic Stellate Cells and Epithelial Hepatoma Cells. *Cell Physiol Biochem*. 2016;39(4):1648–1662.

232. Wilson RB, Chen YJ, Sutherland BG, et al. The marine compound and elongation factor 1A1 inhibitor, didemnin B, provides benefit in western diet-induced non-alcoholic fatty liver disease. *Pharmacol Res*. 2020;161:105208.

233. Belfort R, Harrison SA, Brown K, et al. A placebo-controlled trial of pioglitazone in subjects with nonalcoholic steatohepatitis. *N Engl J Med*. 2006;255(22):2297–2307.

234. Zhao L, Guo X, Wang O, et al. Fructose and glucose combined with free fatty acids induce metabolic disorders in HepG2 cell: A new model to study the impacts of high-fructose/sucrose and high-fat diets in vitro. *Mol Nutr Food Res*. 2016;60(4):909–921.

235. Hui H, Huang D, McArthur D, et al. Direct spectrophotometric determination of serum fructose in pancreatic cancer patients. *Pancreas*. 2009;38(6):706–712.

236. Eynaudi A, Díaz-Castro F, Bórquez JC, et al. Differential Effects of Oleic and Palmitic Acids on Lipid Droplet-Mitochondria Interaction in the Hepatic Cell Line HepG2. *Front Nutr*. 2021;8:775382.

237. Fam TK, Klymchenko AS, Collot M. Recent Advances in Fluorescent Probes for Lipid Droplets. *Materials (Basel)*. 2018;11(9):1768.

238. Piccolis M, Bond LM, Kampmann M, et al. Probing the Global Cellular Responses to Lipotoxicity Caused by Saturated Fatty Acids. *Mol Cell*. 2019;74(1):32–44.e8.

239. Chen M, Chen LM, Chai KX. Androgen regulation of prostasin gene expression is mediated by sterol-regulatory element-binding proteins and SLUG. *Prostate*. 2006;66(9):911–920.

240. Xu W, Lu X, Liu J, et al. Identification of PAFAH1B3 as Candidate Prognosis Marker and Potential Therapeutic Target for Hepatocellular Carcinoma. *Front Oncol*. 2021;11:700700.

241. Mbikay M, Sirois F, Simoes S, et al. Quercetin-3-glucoside increases low-density lipoprotein receptor (LDLR) expression, attenuates proprotein convertase subtilisin/kexin 9 (PCSK9) secretion, and stimulates LDL uptake by Huh7 human hepatocytes in culture. *FEBS Open Bio*. 2014;4:755–762.

242. Li Q, Zhang H, Zou J, et al. Bisphenol A induces cholesterol biosynthesis in HepG2 cells via SREBP-2/HMGCR signaling pathway. *J Toxicol Sci*. 2019; 44(7):481–491.

243. Kim MS, Sweeney TR, Shigenaga JK, et al. Tumor necrosis factor and interleukin 1 decrease RXRalpha, PPARalpha, PPARgamma, LXRalpha, and the coactivators SRC-1, PGC-1alpha, and PGC-1beta in liver cells. *Metabolism*. 56(2):267–279.

244. Wang G, Pan J, Zhang L, et al. Long non-coding RNA CRNDE sponges miR-384 to promote proliferation and metastasis of pancreatic cancer cells through upregulating IRS1. *Cell Prolif*. 2017;50(6):e12389.

245. Wang Y, Qiu W, Liu N, et al. Forkhead box K1 regulates the malignant behaviour of gastric cancer by inhibiting autophagy. *Ann Transl Med*. 2020;8(4):107.

246. Nakayama T, Funakoshi-Tago M, Tamura H. Coffee reduces KRAS expression in Caco-2 human colon carcinoma cells via regulation of miRNAs. *Oncol Lett*. 2017;14(1):1109–1114.

247. Patrick S, Gowda P, Lathoria K, et al. YAP1-mediated regulation of mitochondrial dynamics in IDH1 mutant gliomas. *J Cell Sci*. 2021;134(22):jcs259188.

248. Taylor SC, Nadeua K, Abbasi M, et al. The Ultimate qPCR Experiment: Producing Publication Quality, Reproducible Data the First Time. *Trends Biotechnol*. 2019;37(7):761–774.

249. Pfaffl MW. A new mathematical model for relative quantification in real-time RT-PCR. *Nucleic Acids Res*. 2001;29(9):e45.

250. Vandesompele J, De Preter K, Pattyn F, et al. Accurate normalization of real-time quantitative RT-PCR data by geometric averaging of multiple internal control genes. *Genome Biol*. 2002;3(7):RESEARCH0034.

251. Schott MB, Weller SG, Schulze RJ, et al. Lipid droplet size directs lipolysis and lipophagy catabolism in hepatocytes. *J Cell Biol*. 2019;218(1):3320–3335.

252. Ghasemi M, Turnbull T, Sebastian S, et al. The MTT Assay: Utility, Limitations, Pitfalls, and Interpretation in Bulk and Single-Cell Analysis. *Int J Mol Sci*. 2021;22(23):12827.

253. Ramírez-Zacarías JL, Castro-Muñozledo F, Kuri-Harcuch W. Quantitation of adipose conversion and triglycerides by staining intracytoplasmic lipids with Oil red O. *Histochemistry*. 1992;97(6):493–497.

254. Siculella L, Tocci R, Rochira A, et al. Lipid accumulation stimulates the cap-independent translation of SREBP-1a mRNA by promoting hnRNP A1 binding to its 5'-UTR in a cellular model of hepatic steatosis. *Biochim Biophys Acta*. 2016;1861(5):471–481.

255. Izdebska M, Piatkowska-Chmiel I, Korolczuk A, et al. The beneficial effects of resveratrol on steatosis and mitochondrial oxidative stress in HepG2 cells. *Can J Physiol Pharmacol*. 2017;95(12)L1442–1453.

256. Hoang NA, Richter F, Schubert M, et al. Differential capability of metabolic substrates to promote hepatocellular lipid accumulation. *Eur J Nutr*. 2019;58(8):3023–3034.

257. Cydylo MA, Davis AT, Kavanagh K. Fatty liver promotes fibrosis in monkeys consuming high fructose. *Obesity (Silver Spring)*. 2017;25(2):290–293.

258. Park M, Yoo JH, Lee YS, et al. *Lonicera caerulea* Extract Attenuates Non-Alcoholic Fatty Liver Disease in Free Fatty Acid-Induced HepG2 Hepatocytes and in High Fat Diet-Fed Mice. *Nutrients*. 2019;11(3):494.

259. Wu L, Guo T, Deng R, et al. Apigenin Ameliorates Insulin Resistance and Lipid Accumulation by Endoplasmic Reticulum Stress and SREBP-1c/SREBP-2 Pathway in Palmitate-Induced HepG2 Cells and High-Fat Diet-Fed Mice. *J Pharmacol Exp Ther*. 2021; 377(1):146–156.

260. McDevitt RM, Bott SJ, Harding M, et al. De novo lipogenesis during controlled overfeeding with sucrose or glucose in lean and obese women. *Am J Clin Nutr*. 2001;74(6):737–746.

261. Chen X, Li L, Liu X, et al. Oleic acid protects saturated fatty acid mediated lipotoxicity in hepatocytes and rat of non-alcoholic steatohepatitis. *Life Sci*. 2018; 203:291–304.

262. Matsuda S, Kobayashi M, Kitagishi Y. Roles for PI3K/AKT/PTEN Pathway in Cell Signaling of Nonalcoholic Fatty Liver Disease. *ISRN Endocrinol*. 2013;2013:472432.

263. Yang JY, Zhang TT, Dong Z, et al. Dietary Supplementation with Exogenous Sea-Cucumber-Derived Ceramides and Glucosylceramides Alleviates Insulin Resistance in High-Fructose-Diet-Fed Rats by Upregulating the IRS/PI3K/Akt Signaling Pathway. *J Agric Food Chem.*. 2021;69(32):9178–9187.

264. Sun EJ, Wankell M, Palamuthusingam P, et al. Targeting the PI3K/Akt/mTOR Pathway in Hepatocellular Carcinoma. *Biomedicines*. 2021;9(11):1639.

265. Sunami Y. NASH, Fibrosis and Hepatoccellular Carcinoma: Lipid Synthesis and Glutamine/Acetate Signaling. *Int J Mol Sci*. 2020;21(18):6799.

266. Ricoult SJH, Yecies JL, Ben-Sahra I, et al. Oncogenic PI3K and K-Ras stimulate de novo lipid synthesis through mTORC1 and SREBP. *Oncogene*. 2016;35(1):1250–1260.

267. Li C, Yang W, Zhang J, et al. SREBP-1 has a prognostic role and contributes to invasion and metastasis in human hepatocellular carcinoma. *Int J Mol Sci*. 2014;15(5):7124–7138.

268. Piccinin E, Cariello M, De Santis S, et al. Role of Oleic Acid in the Gut-Liver Axis: From Diet to the Regulation of Its Synthesis via Stearoyl-CoA Desaturase 1 (SCD1). *Nutrients*. 2019;11(10):2283.

269. Lundman P, Boquist S, Samnegård A, et al. A high-fat meal is accompanied by increased plasma interleukin-6 concentrations. *Nutr Metab Cardiovasc Dis*. 2007;17(3):195–202.

270. Strandberg TE, Tilvis RS, Pitkala KH, et al. Cholesterol and glucose metabolism and recurrent cardiovascular events among the elderly: a prospective study. *J Am Coll Cardiol*. 2006;48(4):708–714.

271. Chen L, Chen XW, Huang X, et al. Regulation of glucose and lipid metabolism in health and disease. *Sci China Life Sci*. 2019;62(11):1420–1458.

272. Hylemon PB, Zhou H, Pandak WM, et al. Bile acids as regulatory molecules. *J Lipid Res*. 2009;50(8):1509–1520.

273. Strandberg TE, Salomaa V, Vanhanen H, et al. Associations of fasting blood glucose with cholesterol absorption and synthesis in nondiabetic middle-aged men. *Diabetes*. 1996;45(6):755–761.

274. Juntunen KS, Laaksonen DE, Autio K, et al. Structural differences between rye and wheat breads but not total fiber content may explain the lower postprandial insulin response to rye bread. *Am J Clin Nutr*. 2003;78(5):957–964.

275. Laaksonen DE, Toppinen LK, Juntunen KS, et al. Dietary carbohydrate modification enhances insulin secretion in persons with the metabolic syndrome. *Am J Clin Nutr*. 2005;82(6):1218–1227.

276. Van Rooyen DM, Larter CZ, Haigh WG, et al. Hepatic free cholesterol accumulates in obese, diabetic mice and causes nonalcoholic steatohepatitis. *Gastroenterology*. 2011;141(4):1393–1403.

277. Seebacher F, Zeigerer A, Kory N, et al. Hepatic lipid droplet homeostasis and fatty liver disease. *Semin Cell Dev Biol*. 2020;108:72–81.

278. Kim MS, Lee KT, Iseli TJ, et al. Compound K modulates fatty acid-induced lipid droplet formation and expression of proteins involved in lipid metabolism in hepatocytes. *Liver Int*. 2013;33(1):1583–1593.

279. Pontes-da-Silva RM, de Souza Marinho T, de Macedo Cardoso LE, et al. Obese mice weight loss role on nonalcoholic fatty liver disease and endoplasmic reticulum stress treated by a GLP-1 receptor agonist. *Int J Obese (Lond)*. 2022;46(1):21–29.

280. Li Z, Agellon LB, Allen TM, et al. The ratio of phosphatidylcholine to phosphatidylethanolamine influences membrane integrity and steatohepatitis. *Cell Metab*. 2006;3(5):321–331.

281. Krahmer N, Guo Y, Wilfling F, et al. Phosphatidylcholine synthesis for lipid droplet expansion is mediated by localized activation of CTP:phosphocholine cytidylyltransferase. *Cell Metab*. 2011;14(4):504–515.

282. Verkade HJ, Fast DG, Rusiñol AE, et al. Impaired biosynthesis of phosphatidylcholine causes a decrease in the number of very low density lipoprotein particles in the Golgi but not in the endoplasmic reticulum of rat liver. *J Biol Chem*. 1993;268(33):24990–24996.

283. Jin Y, Tan Y, Chen L, et al. Reactive Oxygen Species Induces Lipid Droplet Accumulation in HepG2 Cells by Increasing Perilipin 2 Expression. *Int J Mol Sci*. 2018;19(11):3445.

284. Libby AE, Bales E, Orlicky DJ, et al. Perilipin-2 Deletion Impairs Hepatic Lipid Accumulation by Interfering with Sterol Regulatory Element-binding Protein (SREBP) Activation and Altering the Hepatic Lipidome. *J Biol Chem*. 2016;291(46):24231–24246.

285. Jacquemyn J, Cascalho A, Goodchild RE. The ins and outs of endoplasmic reticulum-controlled lipid biosynthesis. *EMBO Rep*. 2017;18(11):1905–1921.

286. Walker AK, Jacobs RL, Watts JL, et al. A conserved SREBP-1/phosphatidylcholine feedback circuit regulates lipogenesis in metazoans. *Cell*. 2011;147(4):840–852.

287. Dobrosotskaya IY, Seegmiller AC, Brown MS, et al. Regulation of SREBP processing and membrane lipid production by phospholipids in Drosophila. *Science*. 2002;296(5569):879–883.

288. Sanchez-Alvarez M, Finger F, del Mar Arias-Garcia M, et al. Signaling networks converge on TORC1-SREBP activity to promote endoplasmic reticulum homeostasis. *PLoS One*. 2014;9(7):e101164.

289. Stockert JC, Blázquez-Castro A, Cañete M, et al. MTT assay for cell viability: Intracellular localization of the formazan product is in lipid droplets. *Acta Histochem*. 2012;114(8):785–796.

290. Diaz G, Melis M, Musin A, et al. Localization of MTT formazan in lipid droplets. An alternative hypothesis about the nature of formazan granules and aggregates. *Eur J Histochem*. 2007;51(3):213–218.

291. Berridge MV, Herst PM, Tan AS. Tetrazolium dyes as tools in cell biology: new insights into their cellular reduction. *Biotechnol Annu Rev*. 2005;11:127–152.

292. Śliwka L, Wiktorska K, Suchocki P, et al. The Comparison of MTT and CVS Assays for the Assessment of Anticancer Agent Interactions. *PLoS One*. 2016;11(5):e0155772.

293. García-Ruiz I, Solís-Muñoz P, Fernández-Moreira D, et al. In vitro treatment of HepG2 cells with saturated fatty acids reproduces mitochondrial dysfunction found in nonalcoholic steatohepatitis. *Dis Model Mech*. 2015;8(2):183–191.

294. Alnahdi A, John A, Raza H. Augmentation of Glucotoxicity, Oxidative Stress, Apoptosis and Mitochondrial Dysfunction in HepG2 cells by Palmitic Acid. *Nutrients*. 2019;11(9):1979.

295. Mendez-Sanchez N, Cruz-Ramon VS, Ramirez-Perez OL, et al. New Aspects of Lipotoxicity in Nonalcoholic Steatohepatitis. *Int J Mol Sci*. 2018;19(7):2034.

296. Henne WM, Reese ML, Goodman JM. The assembly of lipid droplets and their roles in challenged cells. *EMBO J*. 2018;37(12):e98947.

297. Kalucka J, Missiaen R, Georgiadou M, et al. Metabolic control of the cell cycle. *Cell Cycle*. 2015;14(21):3379–3388.

298. Lemons JMS, Feng XJ, Bennett BD, et al. Quiescent fibroblasts exhibit high metabolic activity. *PLoS Biol*. 2010;8(10):e1000514.

299. Lunt SY, Vander Heiden MG. Aerobic glycolysis: meeting the metabolic requirements of cell proliferation. *Annu Rev Cell Dev Biol*. 2011;27:441–464.

300. Lystad E, Høstmark AT, Kiserud C, et al. Influence of fatty acids and bovine serum albumin on the growth of human hepatoma and immortalized human kidney epithelial cells. *In Vitro Cell Dev Biol Anim*. 1994;30A(9):568–573.

301. Igarashi M, Miyazawa T. The growth inhibitory effect of conjugated linoleic acid on a human hepatoma cell line, HepG2, is induced by a change in fatty acid metabolism, but not the facilitation of lipid peroxidation in the cells. *Biochim Piophys Acta*. 2001;1530(2–3):162–171.

302. Paramitha PN, Zakaria R, Maryani A, et al. Raman Study on Lipid Droplets in Hepatic Cells Co-Cultured with Fatty Acids. *Int J Mol Sci*. 2021;22(14):7378.

303. Listenberger LL, Han X, Lewis SE, et al. Triglyceride accumulation protects against fatty acid-induced lipotoxicity. *Proc Natl Acad Sci USA*. 2003;100(6):3077–3082.

304. Caldez MJ, Bjorklund M, Kaldis P. Cell cycle regulation in NAFLD: when imbalanced metabolism limits cell division. *Hepatol Int*. 2020;14(4):463–474.

305. Selzner M, Clavien PA. Failure of regeneration of the steatotic rat liver: disruption at two different levels in the regeneration pathway. *Hepatology*. 2000;31(1):35–42.

306. Hamano M, Ezaki H, Kiso S, et al. Lipid overloading during liver regeneration causes delayed hepatocyte DNA replication by increasing ER stress in mice with simple hepatic steatosis. *J Gastroenterol*. 2014;49(2):305–316.

307. DeAngelis RA, Markiewski MM, Taub R, et al. A high-fat diet impairs liver regeneration in C57BL/6 mice through overexpression of the NF-kappaB inhibitor, IkappaBalpha. *Hepatology*. 2005;42(5):1148–1157.

308. Kakimoto PA, Chausse B, Caldeira da Silva CC, et al. Resilient hepatic mitochondrial function and lack of iNOS dependence in diet-induced insulin resistance. *PLoS One*. 2019;14(2):e0211733.

309. Cardoso AR, Kakimoto PA, Kowaltowski AJ. Diet-senstive sources of reactive oxygen species in liver mitochondria: role of very long chain acyl-CoA dehydrogenases. *PLoS One*. 2013;8(10):e77088.

310. Rizki G, Arnaboldi L, Gabrielli B, et al. Mice fed a lipogenic methionine-choline-deficient diet develop hypermetabolism coincident with hepatic suppression of SCD-1. *J Lipid Res*. 2006;47(10):2280–2290.

311. Serviddio G, Giudetti AM, Bellanti F, et al. Oxidation of hepatic carnitine palmitoyl transferase-I (CPT-I) impairs fatty acid beta-oxidation in rats fed a methionine-choline deficient diet. *PLoS One*. 2011;6(9):e24084.

312. Moreno-Fernandez ME, Giles DA, Stankiewicz TE, et al. Peroxisomal β-oxidation regulates whole body metabolism, inflammatory visor, and pathogenesis of nonalcoholic fatty liver disease. *JCI Insight*. 2018;3(6):e93626.

313. Ding L, Sun W, Balaz M, et al. Peroxisomal β-oxidation acts as a sensor for intracellular fatty acids and regulates lipolysis. *Nat Metab*. 2021;3(12):1648–1661.

314. Liu J, Yang P, Zuo G, et al. Long-chain fatty acid activates hepatocytes through CD36 mediated oxidative stress. *Lipids Health Dis*. 2018;17(1):153.

315. Malik SA, Acharya JD, Mehendale NK, et al. Pterostilbene reverses palmitic acid mediated insulin resistance in HepG2 cells by reducing oxidative stress and triglyceride accumulation. *Free Radic Res*. 2019;53(7):815–827.

316. Zeng X, Zhu M, Liu X, et al. Oleic acid ameliorates palmitic acid induced hepatocellular lipotoxicity by inhibition of ER stress and pyroptosis. *Nutr Metab (Lond)*. 2020;17:11.

317. Castro MC, Francini F, Gagliardino JJ, et al. Lipoic acid prevents fructose-induced changes in liver carbohydrate metabolism: role of oxidative stress. *Biochim Biophys Acta*. 2014;1840(3)1145–1151.

318. Guo B, Li Z. Endoplasmic reticulum stress in hepatic steatosis and inflammatory bowel diseases. *Front Genet*. 2014;5:242.

319. Malik R, Selden C, Hodgson H. The role of non-parenchymal cells in liver growth. *Semin Cell Dev Biol*. 2002;13(6):425–431.

320. Arzumanian VA, Kiseleva OI, Poverennaya EV. The Curious Case of the HepG2 Cell Line: 40 Years of Expertise. *Int J Mol Sci*. 2021;22(23):13135.

321. Griendling KK, Touyz RM, Zweier JL, et al. Measurement of Reactive Oxygen Species, Reactive Nitrogen Species, and Redox-Dependent Signaling in the Cardiovascular System: A Scientific Statement From the American Heart Association. *Circ Res*. 2016;119(5):e39–75.

322. Cao SS, Kaufman RJ. Endoplasmic reticulum stress and oxidative stress in cell fate decision and human disease. *Antioxid Redox Signal*. 2014;21(3):396–413.

323. Borradaile NM, Han X, Harp JD, et al. Disruption of endoplasmic reticulum structure and integrity in lipotoxic cell death. *J Lipid Res*. 2006;47(12):2726–2737.

324. Shen Y, Zhao Z, Zhang L, et al. Metabolic activity induces membrane phase separation in endoplasmic reticulum. *Proc Natl Acad Sci USA*. 2017;114(51):13394–13399.

Appendices

Appendix A. Nile Red quantification and fluorescence microscopy data

Nile Red quantification

Cells were stained with Nile Red dye to quantify lipid droplet accumulation after treatment with various concentrations of fatty acid combinations and glucose from 0–48 hours. Cells were plated in 96-well culture dishes at 60,000 cells/well and grew for 3 days prior to treatment and use in this experiment. Following the manufacturer's instructions, 100 μL Nile Red Staining Solution was added to each well after treatment. Cells were then incubated at 37°C in the dark for 15 minutes. Fluorescence was then read at 550/640 nm using the GloMax®-Multi Detection System (Promega). The fat treatments used were similar to those described in Chapter 2.2.1, however additional treatment durations (0, 12, 24, 48 hours) and concentrations (control; 1 mM and 2 mM PA, 1 mM and 2 mM OA, 1 mM and 2 mM PA/OA) were used. The glucose treatments were made from 30 mM glucose stock solutions that were diluted in cell culture grade water and incorporated into the media to reach the desired final concentrations (12.5 mM and 20 mM). The control treatments for glucose consisted of cell culture grade water and media only.

Upon staining and quantification of Nile Red fluorescence using a microplate reader, no significant changes in fat accumulation were found among all fatty acid treatments of 1 mM (**Table A-1**) and 2 mM (**Table A-2**) at each time point (0, 12, 24, and 48 hours) compared to control. Similarly, no significant changes in lipid droplet accumulation were observed among both glucose treatments of 12.5 mM (**Table A-3**) and 20 mM (**Table A-4**) at 0, 12, 24, and 48 hours compared to control. These results further show the inaccuracy and non-specific labeling of Nile Red compared to Oil Red O as lipid droplet accumulation was expected in the 1 mM PA/OA treatment. The results also showed considerable variation. One common trend observed among all treatments, with the 2 mM PA treatment being the only exception, was a progressive increase in lipid droplets up to 24 hours, followed by a decrease in fluorescence at 48 hours.

Table A-1. Nile Red fluorescence (nm) of lipid droplets in cells treated with 1 mM of various fatty acid combinations.

	Fluorescence (nm)			
	Control	PA	OA	PA/OA
Time (h)				
0	155.180 ± 42.308	126.227 ± 38.116	145.793 ± 49.631	120.259 ± 21.121
12	175.041 ± 54.666	135.959 ± 29.371	252.119 ± 53.487	189.719 ± 36.360
24	192.055 ± 67.135	214.481 ± 54.986	302.621 ± 69.319	251.286 ± 65.591
48	137.491 ± 31.065	134.746 ± 35.809	194.229 ± 35.198	196.716 ± 29.098

Note: Cells were treated with control, 1 mM PA, 1 mM OA, and 1 mM PA/OA media for 0, 12, 24, and 48 hours. Values are presented as mean ± SEM. Statistical significance was determined using a Two-Way ANOVA. N=6.

Table A-2. Nile Red fluorescence (nm) of lipid droplets in cells treated with 2 mM of various fatty acid combinations.

	Fluorescence (nm)			
	Control	PA	OA	PA/OA
Time (h)				
0	154.676 ± 56.337	164.881 ± 44.870	132.501 ± 20.559	132.450 ± 40.409
12	241.899 ± 106.307	140.791 ± 34.139	200.019 ± 43.096	189.962 ± 47.438
24	243.513 ± 106.397	307.715 ± 131.079	275.950 ± 83.449	359.468 ± 122.995
48	207.038 ± 81.789	180.782 ± 58.576	195.932 ± 30.020	226.507 ± 33.092

Note: Cells were treated with control, 2 mM PA, 2 mM OA, and 2 mM PA/OA media for 0, 12, 24, and 48 hours. Values are presented as mean ± SEM. Statistical significance was determined using a Two-Way ANOVA. N=6.

Table A-3. Nile Red fluorescence (nm) of lipid droplets in cells treated with 12.5 mM of glucose.

	Fluorescence (nm)	
	Control	Glucose
Time (h)		
0	99.586 ± 27.464	159.574 ± 36.836
12	259.458 ± 64.246	258.040 ± 45.602
24	338.115 ± 72.680	266.945 ± 45.039
48	154.751 ± 19.595	173.654 ± 28.432

Note: Cells were treated with control and 12.5 mM glucose media for 0, 12, 24, and 48 hours. Values are presented as mean ± SEM. Statistical significance was determined using a Two-Way ANOVA. N=6.

Table A-4. Nile Red fluorescence (nm) of lipid droplets in cells treated with 20 mM of glucose.

	Fluorescence (nm)	
	Control	Glucose
Time (h)		
0	115.520 ± 37.588	165.593 ± 34.454
12	224.760 ± 62.894	231.453 ± 71.050
24	381.956 ± 95.292	318.483 ± 58.742
48	164.214 ± 31.393	174.157 ± 19.687

Note: Cells were treated with control and 20 mM glucose media for 0, 12, 24, and 48 hours. Values are presented as mean ± SEM. Statistical significance was determined using a Two-Way ANOVA. N=6.

Nile Red fluorescence microscopy

Based on the trend observed from the quantitative Nile Red data, two treatments from the 24-hour time point (1 mM OA and 12.5 mM glucose) were used for fluorescence microscopy. Cells were grown on coverslips at 400,000 cells, treated with 1 mM OA and 12.5 mM glucose for 24 hours, then stained with Nile Red. Following staining, cells were fixed with 4% paraformaldehyde for 5 minutes, followed by 3 PBS washes. Coverslips were then mounted onto microscope slides using DAPI/Antifade Solution (Sigma-Aldrich S7113) and imaged using a Zeiss Upright AxioImagerZ1 fluorescent microscope (Biotron Integrated Microscopy Facility, Western University).

There appeared to be an increase in lipid droplets in the OA treatment compared to control, as observed from the quantitative data, although this change was not significant (**Fig. A-1**). In regard to glucose, the amount of lipid droplets stained compared to control did not differ as fluorescence appeared to be comparable (**Fig. A-2**). Although the quantitative data suggested a slight decrease in fluorescence in the 24-hour 12.5 mM glucose treatment compared to control, this may have been due to an increase in cell number in the control group as the cell density appeared to be higher (**Fig. A-2**).
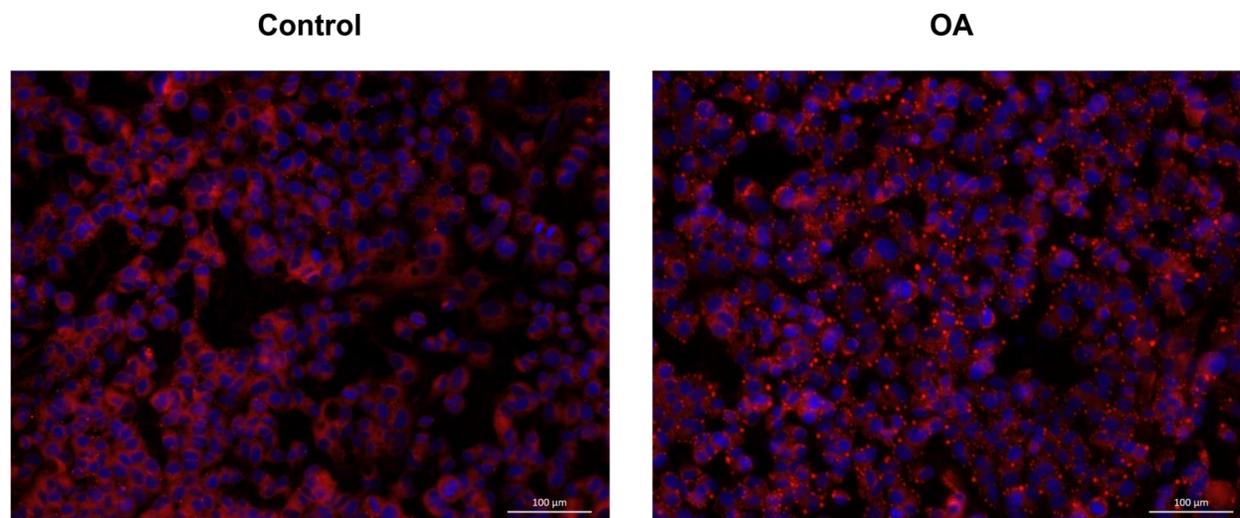
Control **OA**

Figure A-1. Lipid droplet staining appeared to increase in cells treated with OA. Fluorescence microscopy images of cells stained with Nile Red dye after 24 hours of treatment with control and 1 mM OA. Cells were counterstained with DAPI and images were taken at 20X using a Zeiss Upright AxioImagerZ1 fluorescent microscope. Scale bar = 100 μm.
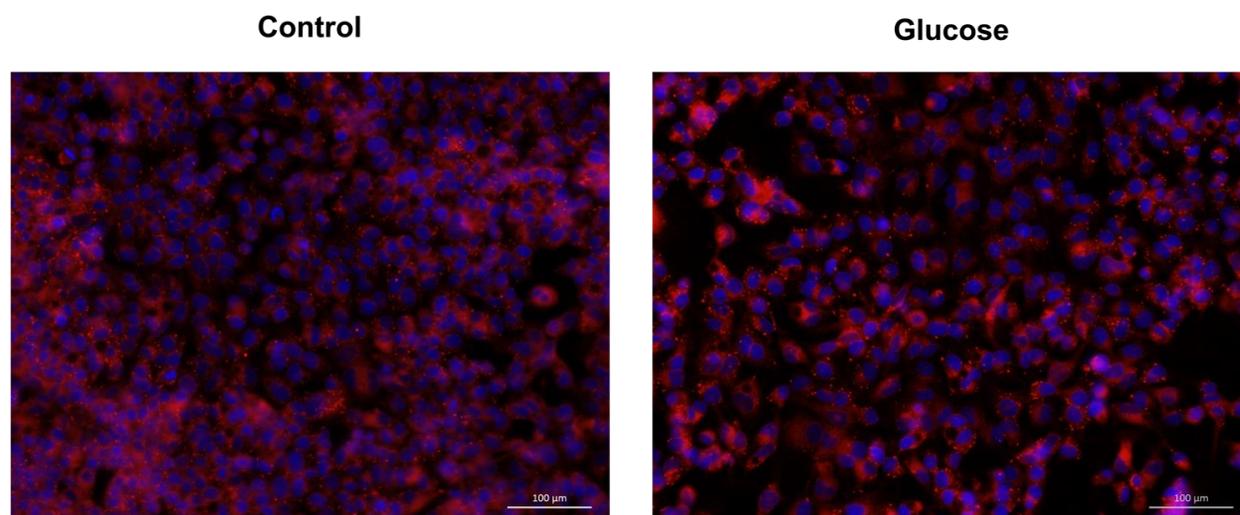
Control **Glucose**

Figure A-2. Lipid droplet staining appeared unchanged in cells treated with glucose. Fluorescence microscopy images of cells stained with Nile Red dye after 24 hours of treatment with control and 12.5 mM glucose. Cells were counterstained with DAPI and images were taken at 20X using a Zeiss Upright AxioImagerZ1 fluorescent microscope. Scale bar = 100 μm.

Appendix B. Expression of reference genes

Expression of the three reference genes used in this study (*RPLP0*, *ACTB*, *PSMB6*) did not differ between the treatments (**Table B-1**).

Table B-1. Quantitation cycle (C_q) values for the reference genes used in this study.

	C_q values				
	Control	Glucose	Fructose	PA/OA	Western
RPLP0	22.068 ± 0.487	21.458 ± 0.250	22.137 ± 0.351	21.878 ± 0.370	21.859 ± 0.273
ACTB	22.737 ± 0.815	21.890 ± 0.163	22.832 ± 1.050	22.524 ± 0.373	22.516 ± 0.861
PSMB6	24.623 ± 0.325	24.141 ± 0.202	24.674 ± 0.541	24.507 ± 0.335	24.146 ± 0.416

Note: Cells were treated with control, 12.5 mM glucose, 15 mM fructose, 1 mM PA/OA, and Western diet (1 mM PA/OA + 12.5 mM glucose + 15 mM fructose) media for 6 hours. C_q values were measured using the CFX Connect Real-Time PCR Detection System (Bio-Rad Laboratories). Values are presented as geomean ± SEM. N=4.

Appendix C. Antioxidant assay standard curve

The standard curve for the antioxidant assay was calculated through the preparation of Trolox standards as per the manufacturer's instructions (**Fig. C-1**). Trolox is an antioxidant like vitamin E and has the capability to reduce oxidative stress. Samples were plated in duplicate, and absorbance was measured using a microplate reader at 750 nm. The linear regression of the standard curve was used to calculate the concentration of antioxidants in each sample.
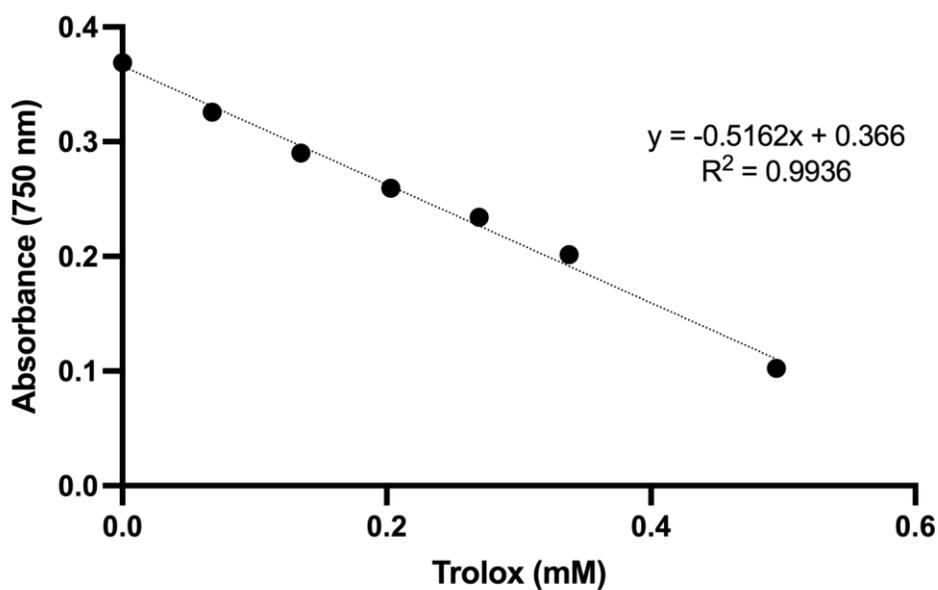

Figure C-1. Standard curve of Trolox standards. Absorbance (750 nm) of Trolox antioxidant capacity (mM) and linear regression of the standard curve used in this study to calculate antioxidant concentrations.

Curriculum Vitae

NAME   Celina Valvano

EDUCATION

2015–2019   **University of Western Ontario**
                        Bachelor of Science
                        Double Major in Biology and Medical Sciences

2020–2022   **University of Western Ontario**
                        Master of Science
                        Biology, Collaborative Specialization in Developmental Biology

MERITS/HONORS/SCHOLARSHIPS/AWARDS

2015   **Western Scholar's Elective Student**
                        University of Western Ontario

2015   **The Western Scholarship of Excellence**
                        University of Western Ontario

2018–2020   **Dean's Honor List**
                        University of Western Ontario

2020   **Laura Bassi Scholarship**
                        The Editing Press

2020–2022   **Western Graduate Research Scholarship**
                        University of Western Ontario

2021–2022   **Ontario Graduate Scholarship**
                        Canadian Graduate Scholarships, University of Western Ontario

2022   **Western Certificate in University Teaching and Learning**
                        University of Western Ontario

TEACHING EXPERIENCE

2020	**Biology for Sciences I (Year 1 Undergraduate), University of Western Ontario** Teaching Assistant
2021, 2022	**Scientific Methods in Biology (Year 2 Undergraduate); Advanced Cell Biology (Year 3 Undergraduate), University of Western Ontario** Teaching Assistant

PUBLICATIONS

Valvano C, Regnault T, Kelly G. The molecular mechanisms behind non-alcoholic fatty liver disease: a closer look at individual nutrient components in the Western diet. *Manuscript in Preparation (To be published, 2022).*

Valvano C, Regnault T, Kelly G. Effects of Western diet-like culture conditions and oxidative stress on signaling pathways in non-alcoholic fatty liver disease. *Manuscript in Preparation (To be published, 2022).*

RESEARCH PRESENTATIONS

Valvano C, Regnault T, Kelly G. Western diet-like culture conditions and oxidative stress on a cell model of lean non-alcoholic fatty liver disease (Invited Talk). Recruitment Event, International Max Planck Research School for Molecular Organ Biology, Virtual, March 10, 2022.

Valvano C, Regnault T, Kelly G. Effects of a Western-like diet on lean non-alcoholic fatty liver disease (Platform Talk). Biology Graduate Research Forum, Department of Biology, University of Western Ontario, Virtual, November 5, 2021.